Behaviour of clay stabilised with fly ash and alkali activated fly ash

Submitted by Canan Turan to the University of Exeter as a thesis for the degree of Doctor of Philosophy in Engineering

October 2022

I certify that all material in this thesis which is not my own work has been identified and that any material that has previously been submitted and approved for the award of a degree by this or any other University has been acknowledged.

Signature: *C. Turan*

Abstract

Addition of cement to the soil is a common method to improve the geotechnical properties of soils in construction. However, it is generally known that 8% of the total CO_2 emissions is from the Portland cement production. In order to reduce the usage of cement and its environmental impact, waste materials, such as fly ash, have become popular in geotechnical applications. Also, using waste materials can decrease the environmental threat caused by the disposal of huge quantities of these waste materials. Some types of fly ash lack adequate cementitious properties, therefore, they can be mixed with other additives such as lime or alkali activators to improve the mechanical properties of soils. Alkali activated waste materials are found comparable to cement in terms of strength performance. Therefore, they have the potential to replace cement in soil stabilisation. However, a current gap is noticed in detailed investigations of soils stabilised with fly ash and alkali activated fly ash. For soils stabilised with fly ash, triaxial and consolidation analyses are limited, while for soils stabilised with alkali activated fly ash, inconsistency is observed between the alkali ratios of sodium silicate/sodium hydroxide.

In this research, the effects of class C fly ash, class F fly ash, and alkali activated fly ash, as stabilising agents, were studied in stabilising clay soil. The thesis investigated the role of different fly ash and alkali activated fly ash contents on the physical, mechanical, and chemical behaviour of the stabilised soil. The experimental programme included compaction, unconfined compressive strength, one-dimensional consolidation, and consolidated-undrained triaxial tests as well as scanning electron microscopy and X-Ray diffraction analysis on the control and stabilised samples at 1 day, 7 days, and 28 days of curing times. This research contributes to this context in 2 phases. In the first phase, the effects of class C and class F fly ash were compared considering the mechanical and microstructural behaviour of the stabilised soil. The results showed that the strength parameters of stabilised soil improved and swelling and compression indices decreased with the addition of fly ash and with the increase of curing time. A higher permeability was observed at 1 day of curing and the permeability decreased with the curing time. It was observed that class C fly ash can be used

as a soil stabilisation agent whereas class F fly ash need to be mixed with different additives such as alkali activators to stabilise the soil.

In the second phase, class F fly ash was used with alkali activators (sodium silicate and sodium hydroxide) as a soil stabilising agent. For the alkali activated class F fly ash, a rigorous dosage method using parameters such as alkali dosage and silica modulus was applied to determine soil mix proportions and produce replicable samples. After the designation of the optimal parameters, mechanical tests, microstructural and mineralogical analysis were carried out. The results showed that the strength improvement of stabilised soil was considerable when the fly ash was activated. The recommended optimal strength parameters were alkali dosages of 12% and silica modulus of 1.25. The addition of either alkali activated fly ash or fly ash to the soil led to a decrease of compression and swelling indices, while yield stress increased. Stress-strain behaviour of soil was modified from ductile to brittle strain-softening response with the addition of alkali activated fly ash and curing time, whereas stress-strain behaviour had ductile response at all curing times with the addition of non-activated fly ash. X-Ray diffraction analysis indicated a decrease in the peak intensities of illite and kaolinite, while scanning electron microscopy analysis showed a modification with the addition of alkali activated fly ash.

Acknowledgements

I would like to express my greatest gratitude and thanks to my supervisors, Professor Akbar Javadi and Dr Raffaele Vinai, for their help and encouragement throughout this thesis. Their guidance, beneficial assessments and suggestions, and constructive comments were crucial for the production of this document. They will always be a role model for me in my future academic life. I also would like to thank Professor Akbar Javadi once again. He has helped not only as my supervisor for this thesis but also given me plenty of opportunities to communicate the research outcomes in many ways.

The financial support provided by the Turkish Ministry of National Education (MoNE) during this thesis is gratefully acknowledged.

I also want to thank the European Union Horizon 2020 research and innovation program and Geores Project under the Marie Sklodowska-Curie grant agreement, No. 778120 for supporting me to communicate many experts in the field.

A special thanks goes to laboratory assistants Jordi Castan Guillen and Julian Yates for their help in my experimental work. They have always provided me with the best working environment possible during hard covid times and supported me with any technical issues.

I would like to thank all my friends for the calls and conversations, their support throughout this research has been invaluable.

Finally, and most importantly, I would like to express my deepest thanks to my family for their patience, support, and encouragement throughout the completion of my thesis.

Dissemination

Published journal papers

- (Journal 1) - Turan, C., Javadi, A. A., & Vinai, R. (2022a). Effects of Class C and Class F Fly Ash on Mechanical and Microstructural Behaviour of Clay Soil – A Comparative Study, *Materials, 15,* 1845. https://doi.org/10.3390/ma15051845.
- (Journal 2) - Turan, C., Javadi, A. A., Vinai, R., & Russo, G. (2022b). Effects of Fly Ash Inclusion and Alkali Activation on Physical, Mechanical, and Chemical Properties of Clay, *Materials, 15,* 4628. https://doi.org/10.3390/ma15134628.
- (Journal 3) - Turan, C., Javadi, A. A., & Vinai, R. & Beig Zali, R. (2022c). Geotechnical characteristics of fine-grained soils stabilized with fly ash, a review, *Sustainability, 14,* 16710. https://doi.org/10.3390/su142416710.

Currently under-review journal paper

- (Journal 4) - Turan, C., Javadi, A. A., & Vinai, R. (n.a). Consolidation and strength behaviour of soils stabilised with alkali activated fly ash (under preparation for journal submission).

Conference papers

- Turan, C., Javadi, A., Vinai, R., Cuisinier, O., Russo, G., & Consoli, N. C. (2019, June 10-12). *Mechanical Properties of Calcareous Fly Ash Stabilized Soil,* EUROCOALASH conference, Dundee, Scotland.
- Turan, C., Javadi, A., Vinai, R., Shariatmadari, N., & Farmani, R. (2020, October 19-21). *Use of class C fly ash for stabilisation of fine-grained soils.* In proceedings of the EUNSAT conference, Lisbon, Portugal.

Contents

List of Figures

Chapter 2 Literature Review

Chapter 3 Methodology

Chapter 4 Results and Discussions

List of Tables

Chapter 2 Literature Review

Chapter 3 Methodology

Chapter 4 Results and Discussions

Abbreviations

ASTM	American Society for Testing Materials
Al_2O_3	Aluminium oxide
BS	British Standard
CAH	Calcium aluminate hydrate
CASH	Calcium aluminium silicate hydrate
CBR	California Bearing Ratio
CCP	Coal combustion products
CEC	Cation exchange capacity
CSH	Calcium silicate hydrate
CSL	Critical state line
CU	Consolidated-undrained
C_3A	Tri-calcium aluminate
C_2S	Di-calcium silicate
DDL	Diffuse double layer
E	Elastic modulus
F	Class F fly ash
F+AA	Class F fly ash + alkali activators
FBA	Furnace bottom ash
FHWA	US Federal Highway Administration
LL	Liquid limit
M+	Alkali Dosages
MDD	Maximum dry density
NASH	Sodium aluminosilicate hydrate
NOR	Naturally Occurring Radionuclide
NORM	Naturally Occurring Radioactive Materials
NP	Non-plastic
OMC	Optimum moisture content
PFA	Pulverised fuel ash

PI	Plasticity index
PL	Plastic limit
SEM	Scanning Electron Microscopy
SH	Sodium hydroxide
SiO_2	Silicon oxide
SM	Silica Modulus
SS	Sodium silicate
UCS	Unconfined Compressive Strength
UKQAA	United Kingdom Quality Ash Association
USEPA	U.S Environmental Protection Agency
USGS	United States Geological Survey
WWCCPN	World-Wide Coal Combustion Products Network
XRD	X-Ray Diffraction
XRF	X-Ray Fluorescence

Nomenclature

c'	Effective cohesion
φ'	Effective angle of shearing resistance
q	Deviatoric stress
C_s	Swelling index
C_c	Compression index
m_v	Volume compressibility
c_v	Coefficient of consolidation
k	Permeability
σ'_c	Effective confining pressure
σ'_1	Major effective principal stress
σ'_3	Minor effective principal stress
M	Gradient of critical state line
ε_a	Axial strain
Δu	Excess pore water pressure
σ_y	Yield stress

Chapter 1 Introduction

Fine-grained soils generally have low strength and high compressibility and are often found on many construction sites (Zhang et al, 2013; Turan et al, 2020). Chemical stabilisation with cement is a method widely used to improve the strength and compressibility characteristics of this type of soil (Phummiphan et al, 2016; Dungca and Codilla, 2018; Parhi et al, 2018). However, producing 1 tonne of Portland cement releases approximately 0.7 – 1.1 tonne of carbon dioxide (Corrêa-Silva et al, 2018; Ghadir and Ranjbar, 2018; Ridtirud et al, 2018; Wong et al, 2019). Therefore, to reduce the environmental impacts due to the use of cementitious binders, fly ash, an industrial by-product, has been used by many researchers working on soil stabilisation. Fly ash has high aluminosilicate content and can react effectively with alkali activators to produce geopolymers. Geopolymers, a novel class of materials, can be defined as aluminosilicate cementitious materials, they can have good to excellent mechanical properties and are considered environmentally friendly when compared to Portland cement. The disposal of large amounts of fly ash in stockpiles results in damage to the environment because of the emission of the toxic trace elements present in fly ash. However, such trace elements could be trapped and immobilised by the geopolymerisation process. Therefore, using fly ash to produce geopolymer also brings a ‘new green solution’ due to the immobilisation of trace elements within geopolymer bonding (Van Deventer et al, 2006; Zhuang et al, 2016; Wong et al, 2019).

In recent years, there has been increasing interest in development of new cementitious binders to replace Portland cement in soil stabilisation. Using fly ash and alkali activated fly ash as alternative soil stabilisation agents can provide

immense advantages in terms of reducing environmental impact, reducing waste and encouraging circular economy. However, there has been limited studies on some aspects of behaviour of soils stabilised with fly ash and alkali activated fly ash. In the first phase of the research, it was noticed that although many studies have been conducted to analyse the Atterberg limits, compaction behaviour, unconfined compressive strength and swelling parameters, limited study has been conducted using triaxial and oedometer tests in soils stabilised with fly ash. Also, there is no study found in the context of comparison of class C and class F fly ash in these tests. Therefore, broader mechanical properties of soils stabilised with class C and class F fly ash such as stress-strain, shear, critical state, and consolidation parameters need to be analysed to understand the soil behaviour fully. In the second phase of the thesis, many studies were found on soils stabilised with alkali activated fly ash with the ratios of sodium silicate/sodium hydroxide (SS/SH) and alkali activator solution/fly ash using mainly unconfined compressive strength (UCS) and California Bearing Ratio (CBR) tests. However, using the ratio of SS/SH caused an inconsistency in the soil stabilisation studies. This is because SS and SH solutions produced for the usage of alkali activated binders can be commercially available with various chemical compositions. Therefore, there is a need to investigate the actual chemical compositions of the alkali activators used in the field of soil stabilisation. Dosage parameters, alkali dosages (M+) and silica modulus (SM), described in the geopolymer cement technology can be used to cover this knowledge gap. Also, based on the literature, UCS and CBR tests have been commonly applied on soils stabilised with alkali activated fly ash. However, there is limited research on detailed mechanical (triaxial and consolidation), microstructural, and mineralogical

behaviour of the stabilised soil and the tests and analyses have been carried out with the basic dosage concentrations of SS/SH. Detailed investigation of the stabilised soil conducting triaxial and consolidation tests, scanning electron microscopy and X-Ray diffraction with the dosages of M+ and SM is necessary to eliminate this gap.

Based on the above considerations, this thesis investigates the mechanical, microstructural, and mineralogical behaviour of soil stabilised with fly ash and soil stabilised with alkali activated fly ash with the dosages of M+ and SM. It analyses the mechanical behaviour of stabilised soil through a range of soil mechanics tests, such as compaction, unconfined compressive strength, one-dimensional consolidation (oedometer), and consolidated-undrained triaxial tests, as well as microstructural and mineralogical analyses by conducting scanning electron microscopy and X-ray diffraction.

1.1 Aim, objectives, and research areas

The primary aim of the thesis is to study the behaviour of clay soils when stabilised with class C fly ash, class F fly ash, or alkali activated class F fly ash, through compaction, UCS, triaxial, and consolidation tests as well as SEM and XRD analysis. The thesis covers two main research areas and the correlated objectives as follows:

- Stabilisation of a clay soil with class C and class F fly ash;
  - To investigate and compare the effects of class C and class F fly ash on the compaction characteristics of clay soil.

- To evaluate compressive strength on soils stabilised with class C and class F fly ash to observe the effects of fly ashes and to find optimal dosages for further tests.
- To obtain the effects of fly ash on the stress-strain behaviour, shear strength, critical state, and consolidation parameters by undertaking triaxial and one-dimensional consolidation tests on soils stabilised with class C and class F fly ash.
- To observe the microstructural modifications of soils stabilised with class C and class F fly ash by conducting scanning electron microscopy analysis.
- To investigate the effects of curing time on the behaviour of soils stabilised with class C and class F fly ash to observe and compare the long-time performance (28 days) for each test described above.

❖ Stabilisation of a clay soil with alkali activated class F fly ash;

- To systematically examine the effects of silica modulus (SM) and alkali dosages (M+) on the compaction and compressive strength behaviour of soil stabilised with alkali activators, proposing a novel approach in terms of mix design, to find the optimal strength of the stabilised soil based on SM and M+, and to use the optimal dosages for further tests.
- To determine the effects of alkali activated fly ash on the stress-strain, pore pressure-strain, shear strength, critical state, and consolidation behaviour of clay soil by applying triaxial and consolidation tests.

- To examine the effects of alkali activated fly ash on the microstructural and mineralogical behaviour of clay soil from scanning electron microscopy and X-Ray diffraction analysis.
- To observe the effects of curing time for soils stabilised with alkali activated fly ash.
- To compare the above parameters of soils stabilised with alkali activated fly ash with soils stabilised with class F fly ash to highlight the effects of alkali activators.

1.2 Thesis overview

This thesis consists of 5 chapters. Following this chapter, chapter 2 provides a detailed review of coal fly ash, geopolymer and geopolymerisation, an overview of previous studies on behaviour of soils stabilised with class C fly ash, class F fly ash and alkali activated fly ash, highlighting the current gaps in this area. Chapter 2 has been used for drafting the literature review sections of journal papers 2 and 3. Chapter 3 describes the materials, sample preparations for soils stabilised with class C fly ash, class F fly ash and alkali activated fly ash, and the testing methods and procedures. Chapter 4 covers the results and discussions of the thesis. The chapter has been used for drafting the results and discussions sections of journal papers 1, 2, and 4.

- Section 4.1 discusses and compares soils stabilised with class C and class F fly ash through a program of experiments including compaction, unconfined compressive strength (UCS), consolidated-undrained (CU) triaxial, and one-dimensional consolidation tests, and scanning electron microscopy (SEM) analysis considering the effects of curing times. This

section was used for drafting the results and discussions sections of Turan et al (2022a).

  - Journal 1: **Turan, C.,** Javadi, A. A., & Vinai, R. (2022a). Effects of Class C and Class F Fly Ash on Mechanical and Microstructural Behaviour of Clay Soil – A Comparative Study, *Materials, 15,* 1845. https://doi.org/10.3390/ma15051845.

- Section 4.2 discusses the compaction and compressive strength behaviour of soils stabilised with alkali activated fly ash. A novel mix design for soils stabilised with alkali activated fly ash is proposed. A range of alkali dosages and silica modulus is used to find the optimal compressive strength parameters in soils stabilised with alkali activated fly ash. The effects of M+, SM, curing times, and fly ash dosages on the UCS of the samples are discussed in detail. A comparison is made with the results obtained with soils stabilised with class F fly ash to assess the effects of alkali activation on the mechanical properties of the stabilised samples. After obtaining the optimal dosages of M+ and SM, the consolidation, stress-strain, pore pressure-strain, shear strength, and critical state parameters of soils stabilised with alkali activated fly ash and fly ash are studied. This section also investigates the microstructural and mineralogical behaviour of soils stabilised with alkali activated class F fly ash and class F fly ash through scanning electron microscopy and X Ray Diffraction analysis. This section has been used for drafting the results and discussions sections of Turan et al (2022b) and Turan et al (n.a).

- Journal 2: **Turan, C.,** Javadi, A. A., Vinai, R., & Russo, G. (2022b). Effects of Fly Ash Inclusion and Alkali Activation on Physical, Mechanical, and Chemical Properties of Clay, *Materials, 15,* 4628. https://doi.org/10.3390/ma15134628.

- Journal 4: **Turan, C.,** Javadi, A. A., & Vinai, R. (n.a). Consolidation and strength behaviour of clay stabilised with fly ash and alkali activated fly ash (under preparation for journal submission).

Chapter 5 draws conclusions from the thesis and makes some recommendations for future work. The original contributions to the knowledge are also described.

Chapter 2 Literature Review

This chapter initially reviews the classification, physical, geotechnical, chemical, and mineralogical properties, health concerns (environmental impact and potential impact to health), availability, and cost of fly ash. It then focuses on the literature on consistency limits, compaction, California bearing ratio, unconfined compressive strength, shear strength, swelling, and consolidation characteristics of fly ash stabilised fine-grained soils, and highlights the practical aspects of using fly ash in geotechnical applications. Furthermore, the literature review includes alkali activated fly ash stabilised soil, detailed description of geopolymers and geopolymerisation, and the use of alkali activated fly ash in soil stabilisation. At the end of the chapter, the knowledge gaps in the available scientific literature on soils stabilised with fly ash and alkali activated fly ash are described.

2.1 Fly ash in soil stabilisation

Fine-grained soils such as clay or silt typically show low mechanical strength and significant volume variation under loading (Ramaji, 2012; Rajpura et al, 2017). The low strength of fine-grained soils causes more damage to civil engineering structures than natural hazards, such as floods and earthquakes (Rajpura et al, 2017). In many countries, damages to structures constructed on soft soils amount to billions of dollars (Kumar and Sharma, 2004; Ramaji, 2012). Thus, it is important to apply appropriate soil stabilisation methods to prevent damage and achieve the desired engineering properties of the soil, such as compressibility, durability, plasticity, and permeability (Behnood, 2018). In general, soil stabilisation methods can be classified as physical, mechanical, and chemical (Hejazi et al, 2012; Ramaji, 2012; Zuber et al, 2013). However, depending on the soil type and application, some of the methods could be expensive or ineffective.

Therefore, there is a need to investigate new methods to improve the strength and reduce swelling and/or settlement characteristics of problematic soils (Hejazi et al, 2012). Chemical stabilisation is commonly used to improve the behaviour of clay soils by modifying the physicochemical properties for permanent stabilisation (Petry et al, 2002). The chemical reactions provide a strong bond network in soil structure, leading to more durable, stronger, and higher quality soil compared to unstabilised soil (Zuber et al, 2013; Mahvash et al, 2018). Using chemical binders in soil stabilisation is also preferable owing to the ease of adaptability (Prabakar et al, 2003). Based on soil type and chemistry, a single binder or two binders can be added to stabilise soil (BS EN 16907-4, 2018).

Common chemical stabilisers can be classified into three groups. These are traditional stabilisers (lime and cement), by-product stabilisers (cement kiln dust, lime kiln dust, other forms of lime by-product, fly ash); and non-traditional stabilisers (potassium compounds, polymers, sulfonated oils, etc.) (Petry et al, 2002). Lime and cement are the two most widely used chemical binders in soil stabilisation (Britpave, 2017; Mahvash et al, 2018; Behnood, 2018; Raj S. et al, 2018). Lime can start pozzolanic reactions that require water and some chemical species such as Si and Ca, generally dissolved from soil, while Portland cement produces hydraulic reactions which only require water to develop (Mahvash et al, 2018). However, the production of these binders has a negative impact on the environment in terms of CO_2 emissions as they have high embodied energy (Behnood, 2018). For example, producing 1 tonne of cement releases approximately 0.7 - 1.1 tonne of carbon dioxide (Corrêa-Silva et al, 2018; Ghadir and Ranjbar, 2018; Ridtirud et al, 2018; Firdous and Stephan, 2019; Wong et al, 2019). Therefore, the utilisation of fly ash as an alternative cementitious agent for

soil stabilisation is encouraged due to its pozzolanic characteristics, cost-effectiveness, environmental sustainability, and ease of adaptability. The use of fly ash offers many benefits as summarised below:

- Disposal of fly ash could lead to the pollution of air, surface water, and groundwater. This is because, the heavy metals in fly ash can leach to the surface soil, deep soil, and underground water. Hence, using fly ash can avoid environmental pollution (Asokan et al, 2005; Nawaz, 2013; Turan et al, 2019).
- A large amount of fly ash is disposed to landfills or placed in storage in developing countries (Ahmaruzzaman, 2010; Consoli et al, 2012, 2014), thus the disposal/storage cost of fly ash increases every year. The disposal space and disposal cost of fly ash can be minimised by increasing the use of fly ash in industry (Nawaz, 2013).
- Utilisation of some expensive natural resources can be reduced by replacing them with by-products (Ahmaruzzaman, 2010).
- The use of fly ash by-products instead of the use of Portland cement in geotechnical applications can be a solution to reduce the CO_2 emissions caused by cement production.
- Fly ash stabilised soil can be used as an effective material in geotechnical applications due to its enhanced geotechnical characteristics (Bin-Shafique et al, 2004; Amiralian et al, 2012b).

2.2 Coal fly ash

Coal fly ash is one of the waste materials obtained from burning of coal in thermal power plants (Dahale et al, 2017). The World-Wide Coal Combustion Products Network (WWCCPN) gives the global definition of fly ash as generated from a coal-fired power station, collected by electrostatic precipitators. In some countries, it is called pulverised fuel ash (PFA). In general, fly ash represents 85 % of the total ash. Other ash types are furnace bottom ash (FBA) and hollow ash particles (WWCCPN, 2020).

2.2.1 Classification of fly ash

Fly ash classification systems are different in the US, China, India, Russia, Canada, Europe, Australia, and Japan, thus, fly ash has no universal classification system (Kelly, 2015). Kelly (2015) proposed a global fly ash classification system considering the classification schemes of eight countries and building an intermediate classification system. Based on the literature, it appears that, generally, the preferred standard is that of the American Society for Testing Materials (ASTM C618). According to the ASTM C618, fly ash can be categorised as class C fly ash or class F fly ash. When fly ash includes more than 70 wt% SiO_2+Al_2O_3+Fe_2O_3 and is low in lime (less than 10% CaO), it is categorised as class F fly ash, whereas if it includes between 50 wt% and 70 wt% SiO_2+Al_2O_3+Fe_2O_3 and is high in lime (more than 20% CaO), it is categorised as class C fly ash (ASTM C618-05, 2005).

There are essentially four types/ranks of coal: lignites, sub-bituminous, bituminous, and anthracite (Bhatt et al, 2019). Class C fly ash is produced from burning of low rank (lignites or sub-bituminous) coals. The calcium content of class C fly ash varies between 20% and 40%, therefore it is also called high

calcium fly ash. On the other hand, class F fly ash is produced from high rank bituminous coals or anthracites. The calcium content of class F fly ash varies between 1% and 10% and thus it is also called low calcium fly ash (Ahmaruzzaman, 2010).

The main difference between class C and class F fly ash is the different contents of calcium and silica-alumina-iron in the fly ash. Another difference is that class C fly ash generally has more alkalinity than class F fly ash due to the higher content of combined sodium, potassium, and sulphates (Ahmaruzzaman, 2010). In addition, class C fly ash has both cementitious and pozzolanic properties. Due to the self-cementing properties of class C fly ash, it hardens in the presence of water. Conversely, class F fly ash has only pozzolanic properties. Due to the low CaO content of class F fly ash, activators such as hydrated lime or quick lime mixed with water are needed to enhance its cementitious properties (Bhatt et al, 2019).

2.2.2 Properties of fly ash

The properties of fly ash can vary significantly according to the coal quality or source, combustion process, and degree of weathering (Asokan et al, 2005; Nawaz, 2013; Yao et al, 2015; Moghal, 2017; Bhatt et al, 2019). Some properties of fly ash are summarised below.

2.2.2.1 Physical and geotechnical properties

Fly ash consists of fine particles, generally spherical in shape (Figure 2.1), hollow, grey in colour (Asokan et al, 2005), and amorphous (glassy) structure in nature (Ahmaruzzaman, 2010; Bhatt et al, 2019). The sizes of fly ash particles vary, ranging from sand to clays (Asokan et al, 2005), and are normally between 0.5 and 400 μm, with an average size of between 12 and 80 μm (Gonzalez et al,

2009). The specific gravity of fly ash could vary from 1.6 to 3.1 and is often around 2 (Moghal, 2017). This variety might be due to several factors like gradation and chemical composition of fly ash (Bhatt et al, 2019). Fly ash is usually non-plastic (NP), meaning that there is no swelling potential when used in geotechnical applications. Fly ash has low bulk density and high specific surface area (Bhatt et al, 2019). Some physical properties of fly ash, such as water holding capacity, porosity, texture, and bulk density, are also found useful in engineering applications. (Asokan et al, 2005; Gonzalez et al, 2009).

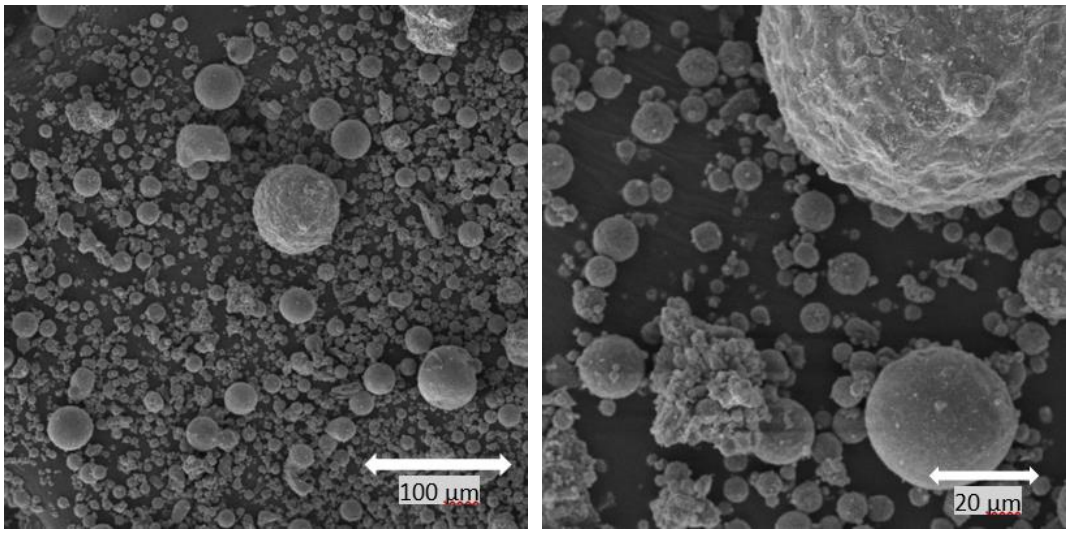

Figure 2.1 Scanning electron microscopy (SEM) images of pure fly ash.

Based on compaction tests, maximum dry density (MDD) of fly ash could vary from 1.01 to 1.78 Mg/m^3 (Bhatt et al, 2019). MDD values of 'silt and clay', and 'sand' are between 1.28 and 1.92 Mg/m^3 and 1.68 and 2.08 Mg/m^3, respectively. Hence, it can be said that MDD values of fly ash are slightly lower than silt and clay and are significantly lower than sand. Optimum moisture content (OMC) of fly ash varies from 11 to 53% (Bhatt et al, 2019). OMC of sand, silt, and clay vary from 6 to 10%, 11 to 15%, and 13 to 21%, respectively (Bhatt et al, 2019).

Therefore, OMC of fly ash may include the ranges of fine-grained soils (silt and clay).

The permeability of fly ash is affected by internal pore structure, pozzolanic activity, particle size distribution, and degree of compaction achieved. The coefficient of permeability of compacted neat fly ash can range from 10^{-6} to 10^{-9} m/s (Bhatt et al, 2019). The values match the range exhibited by silty sand to silty clay soils (Craig, 2004). The angle of shearing resistance of fly ash usually ranges from 26^{o} to 42^{o} (Moghal, 2017). These values are comparable with the angle of shearing resistance of silt (26^{o} to 45^{o}) and sand (27^{o} to 45^{o}) (Bhatt et).

2.2.2.2 Chemical properties

The main chemical elements composing fly ash are Si, Al, Ca, Fe, and Mg (that form about 95% - 99% of total components), while the minor components of fly ash are titanium (Ti), sodium (Na), potassium (K), and sulphur (S) (about 0.5% - 3.5%) (Nawaz, 2013).

Fly ash also includes trace elements, such as arsenic (As), selenium (Se), boron (B), nickel (Ni), molybdenum (Mo), lead (Pb), zinc (Zn), and cadmium (Cd). Most of the trace elements in fly ash are in low concentration (Asokan et al, 2005; Gonzalez, 2009). Some leaching and mobility research has been carried out to determine the possibility of eliminating the trace elements in fly ash, and hence decreasing the environmental damage (Yao et al, 2015). According to the United States Geological Survey (USGS), several trace elements in fly ash are radioactive, such as uranium (U) and thorium (Th). However, these elements have lower toxicity characteristics in comparison with other trace elements, such as arsenic and selenium in fly ash. Also, the amounts of radioactivity in fly ash are comparable with common soils or rocks based on the NORM (Naturally

Occurring Radioactive Materials) (World Nuclear Association, 2020). For example, when fly ash is used in concrete, the radioactivity of fly ash is similar to conventional concrete or building materials such as red brick and granite (USGS, 1997). Sas et al (2019) indicated that naturally occurring radionuclide (NOR) contents of fly ash are lower than red mud samples.

The pH value of fly ash varies from 1.2 to 12.5, while most ashes show alkalinity (Kolbe et al, 2011). According to the Ca/S molar ratio and pH value in ash, it can be categorised into 3 groups of strongly alkaline ash (pH 11 to 13), mildly alkaline ash (pH 8 to 9), and acidic ash (Yao et al, 2015). Class F fly ash tends to be acidic while class C fly ash tends to be alkaline. The cation exchange capacity of fly ash is low due to its non-plastic properties (Moghal, 2017). Fly ash has pozzolanic properties. Pozzolans are siliceous or siliceous and aluminous materials combined with water and calcium hydroxide and thus build cementitious products (Ahmaruzzaman, 2010).

2.2.2.3 Mineralogical properties

The crystalline phases of class F fly ash include quartz, mullite, hematite, and magnetite while class C fly ash includes quartz, lime, mullite, gehlenite, anhydrite, and cement minerals like C_3A and C_2S (Moghal, 2017). Other mineral phases like albite, esperite, nepoutite, and tenorite can also be found (Asokan et al, 2005). Fly ash mainly shows amorphous (glassy) structure (Nawaz, 2013).

2.2.3 Health concerns of fly ash

The inappropriate disposal of fly ash is an important concern due to the environmental threat it poses (Asokan, 2005; Yao et al, 2015; Consoli et al, 2018). Landfilling of fly ash could lead to surface water, air, and groundwater pollution due to the surface run off, wind transport, and leaching of its heavy metals to

surface soil, underground water, and deep soil (Gonzalez et al, 2009; Nawaz, 2013; Turan et al, 2019). The disposal of fly ash in sea, ponds, or rivers can also damage aquatic life (Nawaz, 2013).

Based on the U.S Environmental Protection Agency (USEPA) risk assessment report, living near coal ash disposal areas may increase the risk of cancer considerably (USEPA, 2007). Specifically, long-term exposure to coal fly ash dust can cause stomach cancer, lung cancer pleural abnormalities, and emphysema (Moghal, 2017). Borm (1997) also stated that lung function impairment and respiratory symptoms can be observed with prolonged exposure to fly ash. However, when fly ash is used in geotechnical applications, the cementitious properties of fly ash with water or/and soil create a cemented matrix which does not allow the leaching of any metals due to the immobilisation of fly ash in the matrix (Bhatt et al, 2019).

2.2.4 Availability of fly ash

Coal remains the most consumed fossil fuel for electric power production, even though local policies or international agreements make a change towards alternative energy sources, such as renewable and nuclear. The coal provides about 40% of electrical power production globally (Harris et al, 2019). The coal demand is expected to grow in India, Southeast Asia, and several other countries in Asia, whereas a decline in coal demand is expected in Europe, the United States, and China in the future. Globally, a small increase is expected in coal demand in the next decade. However, over 38% of coal consumption is still predicted in a global perspective (Harris et al, 2019). On the other hand, according to Sifton and Arato (2019), the coal fired power plants are expected to be closed and therefore coal ash production will be stopped in developed

countries in the next 50 years. However, there will still be huge amounts of impounded and landfilled coal ash. For example, the United Kingdom Quality Ash Association (UKQAA) indicated that about 100 million tonnes of landfilled fly ash in the UK will be a 'pozzolanic' reserve for the future (UKQAA, 2020). In the United States, approximately 2 billion tonnes of coal ash material will be stored in the next decades (Sifton and Arato, 2019). Moreover, the production of coal ash is estimated to increase in developing countries. For example, India has the largest resource of energy with approximately 211 billion tonnes of coal reserves (Asokan et al, 2005) whilst no significant alternative energy source has been identified yet (Nawaz, 2013). Therefore, coal consumption in India is expected to increase from 407 to 833 million tonnes of oil equivalent (mtoe) between 2015 and 2035 (Bhatt et al, 2019).

The production (in million metric tonnes - Mt), utilisation (Mt), and utilisation rate (%) of coal combustion products (CCPs) in different countries are shown in Table 2.1 (WWCCPN, 2016). It is seen that China, India, the USA, and Europe were the largest CCPs producing countries. The worldwide production and utilisation rates were over 1.2 billion tonnes (nearly doubling over the previous 5 years) and 63.9% yearly, respectively. However, the utilisation rates vary from country to country because of the different environmental regulations, market situations, and market demand.

Table 2.1 Annual production and utilisation of CCPs (WWCCPN, 2016).

Country	CCPs Production (Mt)	CCPs Utilization (Mt)	Utilization Rate (%)
US	107.4	60.1	56
China	565	396	70.1
Korea	10.3	8.8	85.4
India	197	132	67.1
Japan	12.3	12.3	99.3
Other Asian countries	18.2	12.3	67.6
Europe (EU15)	40.3	38	94.3
Middle East &Africa	32.2	3.4	10.6
Israel	1.1	1	90.9
Canada	4.8	2.6	54.2
Russia	21.3	5.8	27.2
Australia	12.3	5.4	43.5

2.2.5 Cost of fly ash

According to Ahmaruzzaman (2010), fly ash is sometimes available free of charge at the power plants in India. On the other hand, it is a marketed commodity in many western countries such as the UK and in Europe, because of the growing demand for fly ash from the concrete industry. However, fly ash is significantly less expensive than Portland cement (Boral, 2018). Therefore, the costs of fly ash are mainly based on transportation, laying, and rolling costs. If the transportation distance is short, a significant amount could be saved in construction costs. It is recommended that fly ash should not be transported more than about 100 - 200 km (Yao et al, 2015). Kumar and Patil (2006) investigated the cost of fly ash utilisation in road construction. They indicated that the cost of fly ash is directly related to the transportation distance and the cost of resources replaced by fly ash. When the fly ash was evaluated for the use on flexible or rigid pavements of road construction for 0 km transportation distance and 1.5 m of embankment height, the cost saving was found to be about 31%. It was estimated that the fly ash-based road construction can be cost-effective when the transportation distance is less than 60 and 90 km for flexible and rigid pavements, respectively. Suryawanshi et al (2012) pointed out that utilisation of fly ash could

lead to a considerable cost saving in rigid pavement construction by replacing Portland cement.

2.3 Geotechnical properties of fly ash-stabilised fine-grained soils

2.3.1 Effects of fly ash inclusion on consistency limits of soil

The volume change potential of soil can be evaluated by consistency limit parameters, including plasticity index (PI), plastic limit (PL), and liquid limit (LL) (Bhatt et al, 2019). The PI (=LL-PL) indicates the range of water content in which the soil is in the plastic state (Striprabu et al, 2018). Many researchers evaluated the clay soils stabilised with class C or class F fly ash in terms of consistency limits (Table 2.2). In general, it has been shown that the addition of fly ash to soil leads to a reduction in LL, an increase in PL, and a reduction in PI (Ji-Ru and Xing, 2002; Kumar and Sharma, 2004; Parsons and Kneebone, 2005; Zha et al, 2008; Phanikumar, 2009; Mir and Sridharan, 2013; Pal and Ghosh, 2014; Binal, 2016; Kolay and Ramesh, 2016; Seyrek, 2016; Zhou et al, 2019). Kumar and Sharma (2004) showed that PI decreased by approximately 50% in a high plasticity clay (CH) by adding 20% class F fly ash. There are two reasons for changes in consistency limits due to the addition of fly ash (Seyrek, 2016): (i) fly ash has silt-sized particles hence the clay fraction decreases when the fly ash content increases; (ii) fly ash particles lead to a flocculated structure in the clay and reduce the thickness of the diffuse double layer (DDL) of the clay. Striprabu et al (2018) also carried out consistency limit experiments on a clay soil stabilised with class F fly ash and cement. They attributed the decrease in PI to the flocculation and agglomeration of stabilised soil particles. Zhou et al (2019) conducted consistency limit tests on a clay soil stabilised with class F fly ash and

lime. They explained the decrease in PI using the diffuse double layer (DDL) theory. The thickness of water in DDL has a considerable effect on the engineering properties of clay. The plasticity of clay increases by increasing the thickness of DDL. Fly ash includes many high-valent cations. When the concentration of high-valent cations in the DDL increases, the layer is thinned; in this way, the PI of the clay is decreased (Zhou et al, 2019).

The plasticity index of the soil is also a critical indicator of swelling potential (Cokca, 2001; Ji-Ru and Xing, 2002; Seyrek, 2016; Zhou et al, 2019). The swelling potential of stabilised soil decreases with increasing fly ash content. The classification of clay soil generally changes from CH (high plasticity clay) to CL (low plasticity clay), MH (high plasticity silt), or ML (low plasticity silt) with addition of fly ash (Cokca, 2001; Binal, 2016; Seyrek, 2016). Seyrek (2016) showed that CH turns into CL, MH, and ML with addition of 20% class F fly ash, 10% class C fly ash, and 15% class C fly ash, respectively. According to Seyrek (2016), class C fly ash is more effective than class F fly ash in decreasing the PI.

Table 2.2 Consistency limits of soils stabilised with fly ash from different studies.

Type of fly ash	Fly ash content	LL (%)	PL (%)	PI (%)	Soil classification (USCS)	References
class F	unstabilized (0%)	62.2	25.1	37.1	CH	Ji-ru and Xing (2002)
	40%	54.4	27.5	26.9	CH	
	50%	51.4	24.9	26.5	CH	
class F	unstabilized (0%)	80	28	52	CH	Kumar and Sharma (2004)
	5%	77	31	46	CH	
	10%	75	35	40	CH	
	15%	73	40	33	MH	
	20%	70	44	26	MH	
class C	unstabilized (0%)	-	-	30	CH	Parsons and Kneebone (2005)
	12%	-	-	16	-	
	16%	-	-	12	-	
	unstabilized (0%)	-	-	15	CL	
	12%	-	-	11	-	
	16%	-	-	9	-	
	unstabilized (0%)	-	-	17	CL	
	12%	-	-	12	-	
	16%	-	-	9	-	
class F	unstabilized (0%)	59.8	27.5	32.3	CH	Zha et al (2008)
	3%	58.2	29.2	28.9	CH	
	6%	57.3	31	26.2	MH	
	9%	55.1	32.5	22.6	MH	
	12%	53.7	33.3	20.4	MH	
	15%	52.4	35.1	17.3	MH	
class F	unstabilized (0%)	100	27	73	CH	Phanikumar (2009)
	10%	92	32	60	CH	
	20%	86	36	50	CH	
class F	unstabilized (0%)	84	25.4	58.6	CH	Mir and Sridharan (2013)
	20%	72	33	39	MH	
	40%	63	31.6	31.4	MH	
	60%	53	32.5	20.5	MH	
class C	unstabilized (0%)	84	25.4	58.6	CH	
	10%	81	45	36	MH	
	20%	76	49	27	MH	
	40%	66	54	12	MH	
	60%	56.5	45	11.5	MH	
class F	unstabilized (0%)	159	36.9	122.1	CH	Pal and Ghosh (2014)
	50%	91.4	20.9	70.5	CH	
	60%	75.1	23.4	51.8	CH	
	70%	60.8	24.6	36.1	CH	
	80%	45.7	25.9	19.8	CL	
class C	unstabilized (0%)	88.7	35	53.7	CH	Binal (2016)
	5%	-	-	-	MH	
	10%	-	-	-	MH	
	15%	-	-	-	MH	
	20%	-	-	-	MH	
	25%	-	-	-	MH	
class C	unstabilized (0%)	75.8	28.5	-	-	Kolay and Ramesh (2016)
	10%	75.2	25.5	-	-	
	20%	73.9	24.4	-	-	
	30%	69.3	21.3	-	-	
	40%	64.9	19.6	-	-	
	50%	61.5	17.9	-	-	
	unstabilized (0%)	603.1	94.5	-	-	
	10%	512	81.8	-	-	
	20%	432	73.9	-	-	
	30%	346	65.8	-	-	
	40%	283	59.9	-	-	
	50%	237	54.8	-	-	
class F	unstabilized (0%)	-	-	-	CH	Seyrek (2016)
	20%	-	-	-	CL	
class C	unstabilized (0%)	-	-	-	CH	
	10%	-	-	-	MH	
	15%	-	-	-	ML	
class F	unstabilized (0%)	-	-	-	CL	
	15%	-	-	-	ML	
class C	unstabilized (0%)	-	-	-	CL	
	10%	-	-	-	ML	
class F	unstabilized (0%)	48.3	23.4	24.9	CL	Zhou et al (2019)
	30%	43.1	26.5	16.6	ML	

2.3.2 Effects of fly ash inclusion on compaction characteristics of soil

Compaction characteristics can affect many engineering properties of soil like permeability, compressibility, dispersibility, and strength (Seyrek, 2016). Many construction projects, such as roadway subgrades, highway or railway embankments, and earth dams use compaction and soil stabilisers to improve the strength and reduce settlement potential of soils. Compaction tests are carried out to find maximum dry density (MDD) and optimum moisture content (OMC) of the soil. According to Bhatt et al (2019), when fly ash is mixed with soil, the values of MDD and OMC can be changed based on the types of fly ash and fly ash fraction in the mixture. Table 2.3 shows compaction results of unstabilised and fly ash-stabilised soil samples from the literature. The majority of works in the literature show that MDD decreased, and OMC increased as the content of fly ash (class C or class F) increased in the stabilised soil (Ji-Ru and Xing, 2002; Prabakar et al, 2004; Senol et al, 2006; Santos et al, 2011; Mir and Sridharan, 2013; Shil and Pal, 2015; Kolay and Ramesh, 2016; Seyrek, 2016; Nath et al, 2017; Savas et al, 2018; Rajak et al, 2019). Some researchers argued that the decrease of MDD is usually due to the low specific gravity of fly ash in comparison with any fine-grained soil (Shil and Pal, 2015; Kolay and Ramesh, 2016; Seyrek, 2016; Savas et al, 2018; Siddiqua and Barreto, 2018). The change in MDD of mixture could also be due to change in gradation of the mixture (Kolay and Ramesh, 2016). Nath et al (2017) explained that agglomeration and flocculation occur between clay particles and stabilising agents through cation exchange, which creates a larger space and reduces the weight/volume ratio. Seyrek et al (2016) argued that, due to the quick formation of cemented products, the compressibility can decrease during compaction, resulting in a reduction in the

MDD of the soil stabilised with fly ash. Mackiewicz and Ferguson (2005) pointed out that compaction is usually delayed in everyday construction operations. This results in the hydration products in fly ash bonding with the soil particles in a loose state and these bonds cause disruption of material during compaction process. For example, if the compaction is delayed by 1 hour after mixing the materials, MDD values could decrease from up to 0.6 to 1.6 kN/m^3 (Mackiewicz and Ferguson, 2005). Therefore, delays in compaction should be kept to minimum in order to obtain a higher MDD. Dahale et al (2017) and Mahvash et al (2017) used lime and Portland cement, respectively, with fly ash for soil stabilisation. They also observed a decrease in MDD and an increase in OMC. Mahvash et al (2017) argued that these results were obtained when the fly ash content was significantly higher than the cement content. According to Nath et al (2017), the reason of the increase in OMC with addition of fly ash could be that more water is needed for the formation and dissolution of the materials.

On the other hand, some researchers indicated that the MDD increased, and OMC decreased with increase of fly ash in stabilised soil (Kumar and Sharma, 2004 and Phanikumar, 2009). Striprabu et al (2018) showed that the mixture of class F fly ash and a small amount of cement resulted in increase in MDD and decrease in OMC. The reason for the discrepancy of the results of MDD and OMC could be that fly ash shows a significant variety of specific gravity ranging from 1.6 to 3.1. The specific gravity of fly ash varies based on the specific power plant where the fly ash is sourced from. The values even show a variety over the time periods for the same power plant (Bhatt et al, 2019).

Table 2.3 Compaction characteristics of soils stabilised with fly ash from different studies.

Type of fly ash	Type of soil	Fly ash content	MDD (kN/m^3)	OMC (%)	References
class F	CH	unstabilized (0%)	17.5	17.2	Ji-ru and Xing (2002)
		40%	13.9	16.0	
		50%	13.3	18.4	
class F	CH	unstabilized (0%)	13.8	40	Kumar and Sharma (2004)
		5%	13.9	38	
		10%	14.1	35	
		15%	14.2	33	
		20%	14.3	31	
-	CL	unstabilized (0%)	16.8	14.6	Prabakar et al (2004)
		9%	15.5	15.8	
		20%	15.4	17.9	
		28.5%	14.1	20.4	
		35.5%	13.6	22.3	
		41.2%	13.3	25.2	
		46%	13.1	27.2	
		100%	9.2	44.2	
-	MH	unstabilized (0%)	14.0	30.1	
		9%	13.5	29.5	
		20%	13.2	29.5	
		28.5%	12.8	30.1	
		35.5%	12.2	31.9	
		41.2%	12.3	33.3	
		46%	11.9	34.3	
class F	CH	unstabilized (0%)	13.6	34	Phanikumar (2009)
		10%	14	27	
		20%	14.4	21	
-	CL	unstabilized (0%)	17.9	14.0	Santos et al (2011)
		20%	15.5	22.5	
		40%	14.6	25.0	
		60%	13.9	28.0	
		100%	10.4	45.5	
class F	CH	unstabilized (0%)	14.4	28.3	Mir and Sridharan (2013)
		20%	13.9	30.0	
		40%	13.6	31.1	
		60%	12.7	33.0	
		80%	11.8	35.4	
		100%	10.6	38.2	
class C	CH	unstabilized (0%)	14.4	28.3	
		10%	14.1	29.5	
		20%	13.9	29.7	
		40%	13.7	29.9	
		60%	13.5	30.5	
		80%	13.1	31.1	
		100%	12.6	32.0	
class C	CH (kaolinite)	unstabilized (0%)	13.4	30.1	Kolay and Ramesh (2016)
		10%	13.2	31.0	
		20%	13.0	32.2	
		30%	12.9	33.0	
		40%	12.8	34.5	
		50%	12.7	35.4	
	CH (bentonite)	unstabilized (0%)	11.7	40.5	
		10%	11.7	40.5	
		20%	11.5	41.3	
		30%	11.4	41.5	
		40%	11.3	41.6	
		50%	11.3	42.5	

(Table 2.3 cont.)

Type of fly ash	Type of soil	Fly ash content	MDD (kN/m^3)	OMC (%)	References
class C	CH	unstabilized (0%)	16.4	17.2	Seyrek (2016)
		5%	16.1	17.9	
		10%	15.8	18.2	
		15%	15.5	18.2	
		20%	15.6	18.0	
		25%	15.4	18.5	
		30%	15.1	18.8	
	CL	unstabilized (0%)	17.3	15.8	
		5%	17.1	16.1	
		10%	16.8	16.1	
		15%	16.4	16.3	
		20%	16.5	16.0	
		25%	16.3	16.4	
		30%	16.1	16.5	
High-Ca fly ash	Silty clay	unstabilized (0%)	15.3	23	Jafer et al (2018)
		3%	14.5	26	
		6%	14.3	27.5	
		9%	14.2	28	
		12%	14.1	29	
		15%	13.7	30.5	
class C	CL (PI=20)	unstabilized (0%)	16.2	18.7	Savas et al (2018)
		5%	15.7	20.5	
		10%	15.2	22.3	
		15%	15.0	23.0	
		20%	14.9	23.6	
		25%	14.7	24.3	
		30%	14.6	24.9	
	CL (PI-19)	unstabilized (0%)	16.9	15.7	
		5%	16.6	15.8	
		10%	16.2	15.9	
		15%	15.9	15.7	
		20%	15.7	15.7	
		25%	15.5	17.1	
		30%	15.3	17.7	
class F	CL (PI=20)	unstabilized (0%)	16.2	18.7	
		5%	16.0	19.0	
		10%	15.8	19.3	
		15%	15.4	19.9	
		20%	15.1	20.5	
		25%	15.0	21.2	
		30%	14.9	21.8	
	CL (PI-19)	unstabilized (0%)	16.9	15.7	
		5%	16.9	15.7	
		10%	16.7	15.4	
		15%	16.4	15.6	
		20%	16.1	15.1	
		25%	15.9	15.2	
		30%	15.8	15.5	
class F	CL	unstabilized (0%)	17.76	16	Shaunik and Gupta (2020)
		20%	16.28	20	
		40%	12.73	22	
		60%	11.4	24	
		80%	10.24	26	
		100%	8.95	28	
class C	CH	unstabilized (0%)	13.8	30.5	Kumar et al (2021)
		5%	13.4	30.5	
		10%	13.2	31	
		15%	13.1	31.5	
		20%	13.0	31.5	
		100%	11.0	39	

2.3.3 Effects of fly ash inclusion on California Bearing Ratio of soil

CBR values are usually used for designing the subgrade, subbase, and base layers for pavements (Prabakar et al, 2004; Than and Zaw, 2019). CBR values are obtained by evaluating the force and penetration relationship when a cylindrical plunger penetrates the soil at a standard rate (Mahvash et al, 2018). An unstabilised fine-grained soil usually has very low CBR value (< 3%) (Trzebiatowski et al, 2004) and thus it can be considered as poor subgrade material (Bowles, 1992). Adding fly ash to improve a fine-grained soil can increase the CBR value significantly (Ji-Ru and Xing, 2002; Bin-Shafique et al, 2004; Prabakar et al, 2004; Trzebiatowski et al, 2004; Edil et al, 2006; Senol et al, 2006; Binal, 2016; Jose et al, 2018; Than and Zaw, 2019). Table 2.4 shows the CBR values of some unstabilised soils and fly ash-stabilised soils with consideration of general rating and uses (Bowles, 1992). Fly ash has a high potential in improving the bearing capacity of soils, and therefore, fly ash-stabilised soil can be used as a subbase or base material for roads and backfilling (Bin-Shafique et al, 2004; Prabakar et al, 2004; Trzebiatowski et al, 2004; Than and Zaw, 2019). Binal (2016) indicated that the curing time is an important factor affecting the CBR value. A significant improvement was observed in CBR values after 7 days of curing for a fly ash-stabilised soil (Binal, 2016). However, CBR value of fly ash-stabilised soil decreased with an increase of compaction water content (Trzebiatowski et al, 2004; Edil et al, 2006). The CBR values are also affected by the type of fine-grained soil. Senol et al (2006) reported that mixtures of fly ash with organic soil or CH soil had lower CBR values compared to CL soil or silt.

Table 2.4 CBR values of soils stabilised with fly ash from different studies.

Type of fly ash	Type of soil	Fly ash content	CBR (%)	General Rating (Bowles, 1992)	Uses (Bowles, 1992)	References
class F	CH	unstabilized (0%)	2	very poor	subgrade	Ji-ru and Xing (2002)
		40%	17	fair	subbase	
		50%	20.2	good	base, subbase	
class C	CL	unstabilized (0%)	1	very poor	subgrade	Bin-Shafique et al (2004)
		12%	37	good	base, subbase	
	CL-ML	unstabilized (0%)	3	very poor	subgrade	
		10%	32	good	base, subbase	
-	CL	unstabilized (0%)	4.7	poor to fair	subgrade	Prabakar et al (2004)
		9%	7	fair	subbase	
		20%	8.84	fair	subbase	
		28.5%	9.24	fair	subbase	
		35.5%	9.93	fair	subbase	
		41.2%	10.67	fair	subbase	
		46%	11.6	fair	subbase	
class C	CL	unstabilized (0%)	2	very poor	subgrade	Trzebiatowski et al (2004)
		10%	57	excellent	base	
	CL	unstabilized (0%)	3	poor to fair	subgrade	
		10%	47	good	base, subbase	
class C	CH	unstabilized (0%)	2	very poor	subgrade	Edil et al (2006)
		10% (7 days cured)	8	fair	subbase	
		18% (7 days cured)	24	good	base, subbase	
	CL	unstabilized (0%)	5	poor to fair	subgrade	
		10% (7 days cured)	11	fair	subbase	
		18% (7 days cured)	30	good	base, subbase	
	CH	unstabilized (0%)	3	poor to fair	subgrade	
		10% (7 days cured)	12	fair	subbase	
		18% (7 days cured)	15	fair	subbase	
class C	CL	unstabilized (0%)	3	poor to fair	subgrade	Senol et al (2006)
		12% (7 days cured)	34	good	base, subbase	
		16% (7 days cured)	51	excellent	base	
		20% (7 days cured)	56	excellent	base	
	ML	unstabilized (0%)	5	poor to fair	subgrade	
		10% (7 days cured)	32	good	base, subbase	
		14% (7 days cured)	36	good	base, subbase	
		18% (7days cured)	38	good	base, subbase	
	OH	unstabilized (0%)	2	very poor	subgrade	
		18% (7 days cured)	5	poor to fair	subgrade	
class C	CH	unstabilized (0%)	6.7	poor to fair	subgrade	Binal (2016)
		28% (28 days cured)	68.7	excellent	base	
class F	expansive soil	unstabilized (0%)	7.5	fair	subbase	Jose et al (2018)
		10%	12.6	fair	subbase	
		15%	13.2	fair	subbase	
-	CH	unstabilized (0%)	2.1	very poor	subgrade	Than and Zaw (2019)
		4%	4.9	poor to fair	subgrade	
		8%	11.5	fair	subbase	
		12%	21.3	good	base, subbase	
		16%	30.7	good	base, subbase	
		20%	25.1	good	base, subbase	

2.3.4 Effects of fly ash inclusion on Unconfined Compressive Strength of soil

Unconfined compressive strength (UCS) of soil is one of the most important geotechnical parameters used for the design and practice of many geoengineering projects (Sharma and Singh, 2017). UCS tests can be used to understand the deformational behaviour of soil and evaluate its strength. The UCS of fly ash-stabilised soils has been determined by many investigators (Table 2.5) and it has been shown that the strength of soil increased when stabilisation with class C or class F fly ash was carried out (Senol et al, 2002, 2006; Sezer et al, 2004; Bin-Shafique et al, 2004, 2009; Trzebiatowski et al, 2004; Kolias et al, 2005; Silitonga et al, 2009; Santos et al, 2011; Tastan et al, 2011; Seyrek, 2016; Nath et al, 2017; Premkumar et al, 2017; Samidurai et al, 2017; Jose et al, 2018; Savas et al, 2018; Efthymiou et al, 2019; Mir and Sridharan, 2019; Turan et al, 2019, 2020). However, several researchers have pointed out that there is an optimum level of fly ash addition to stabilise soil. Seyrek (2016) investigated UCS values of class C and class F fly ash-stabilised soil and reported that 25% (by dry weight of the soil) is an optimum level in terms of increase in UCS. In addition, Sezer et al (2006) stated that an increase of fly ash substitution level beyond 15% mass percent of the soil increased the UCS marginally.

Seyrek (2016) and Savas et al (2018) found that the UCS of soil stabilised with class C fly ash is significantly higher than class F fly ash. Savas et al (2018) attributed this difference to the high lime content, better reaction of cation exchange, flocculation, and agglomeration in class C fly ash compared to class F fly ash. The higher the CaO content and CaO/SiO_2 ratio (or $CaO/SiO_2+Al_2O_3$ ratio), the higher the UCS is (Tastan et al, 2011). Dahale et al (2017) indicated

that class F fly ash does not have cementitious properties due to the low calcium content, hence, the marginal increase in strength of class F fly ash in short-term can be related to the soil gradation effects. Some investigators evaluated soil stabilised with class F fly ash and low amounts of traditional stabilisers (cement or lime) and reported satisfactory strength results (Kolias et al, 2005; Dahale et al, 2017; Premkumar et al, 2017; Siddiqua and Barreto, 2018; Striprabu et al, 2018). The amount of increase in UCS also depends on the soil type (Senol et al, 2006; Tastan et al, 2011; Nath et al, 2017). Tastan et al (2011) reported a significant increase in UCS (from 30 kPa for unstabilised soil to 400 kPa with fly ash addition) in clay soil with an organic content less than 10% and a low increase in UCS (from 15 kPa for unstabilised soil to 100 kPa with fly ash addition) in organic sandy silty peat with 27% organic content. Kolias et al (2005) and Senol et al (2006) pointed out that low plasticity clay had higher UCS in comparison with high plasticity clay when stabilised by fly ash.

The curing time has a positive effect on UCS results (Kate, 2005; Sezer et al, 2006; Seyrek, 2016; Nath et al, 2017; Premkumar et al, 2017; Striprabu et al, 2018; Turan et al, 2020). Strength development has been commonly assessed after 1, 7, and 28 days of curing time. It has been shown that stabilised soil after 28 days of curing would achieve much higher strength than 1 or 7 days of curing due to the development of pozzolanic reactions (Seyrek, 2016; Striprabu et al, 2018). Premkumar et al (2017) reported that the UCS of soil would still increase from 28 days to 90 days of curing. It was concluded that, during pozzolanic reactions, dissolved aluminium and silicon from clay minerals react with the Ca^{2+} in the pore solution to create a firm gel of calcium silicate and calcium aluminate. Thus, the increase in UCS over longer periods of curing time is a result of

hydration process followed by the formation of cementitious materials (Premkumar et al, 2017).

Table 2.5 UCS of soils stabilised with fly ash from different studies.

Type of fly ash	Type of soil	Curing days	Fly ash content	UCS (kPa)	References
class C	CL	7	unstabilized (0%)	200	Trzebiatowski et al (2004)
			10%	448	
	CL	7	unstabilized (0%)	145	
			10%	490	
class C	CL	7	unstabilized (0%)	140	Senol et al (2006)
			12%	772	
			16%	828	
			20%	863	
	ML	7	unstabilized (0%)	133	
			10%	566	
			14%	614	
			18%	649	
class C	CL	7	unstabilized (0%)	212	Bin-Shafique et al (2009)
			5%	520	
			10%	713	
			20%	804	
	CH	7	unstabilized (0%)	180	
			5%	364	
			10%	456	
			20%	567	
class F	CH	1	unstabilized (0%)	285.7	Seyrek (2016)
		28	25%	1088.3	
class C	CH	1	unstabilized (0%)	285.7	
		1	25%	559.9	
		7	25%	948.4	
		28	30%	1442.5	
class F	CL	1	unstabilized (0%)	215.4	
		28	25%	657	
class C	CL	1	unstabilized (0%)	215.4	
		28	30%	915.5	
High-Ca fly ash	CI	1	unstabilized (0%)	-	Premkumar et al (2017)
			3%	514	
			6%	536	
			9%	437	
			12%	388	
	CL	1	unstabilized (0%)	-	
			3%	401	
			6%	415	
			9%	445	
			12%	407	
class C	CL (PI=20)	1	unstabilized (0%)	257.6	Savas et al (2018)
			5%	459.9	
			10%	476.5	
			15%	729.5	
			20%	765.2	
			25%	784.3	
			30%	862.9	
class F	CL (PI=20)	1	unstabilized (0%)	257.6	
			5%	305.7	
			10%	317.5	
			15%	336.1	
			20%	307.9	
			25%	430.7	
			30%	444.9	
class C	CL (PI=19)	1	unstabilized (0%)	234.8	
			5%	308.9	
			10%	426.1	
			15%	559.6	
			20%	761.7	
			25%	790.4	
			30%	845	
class F	CL (PI=19)	1	unstabilized (0%)	234.8	
			5%	315.8	
			10%	366.5	
			15%	358.9	
			20%	365.2	
			25%	435.1	
			30%	448	
class C	CI	1	unstabilized (0%)	226	Turan et al (2020)
			30%	295	
		7	unstabilized (0%)	245	
			25%	517	
		28	unstabilized (0%)	235	
			25%	599	

2.3.5 Effects of fly ash inclusion on shear strength of soil

Shear strength parameters are required in the analysis of soil stability problems (Craig, 2004). These parameters for a specific soil can be determined by direct shear test or triaxial test. Previous studies have shown that the shear strength parameters of fine-grained stabilised soil increase with increasing fly ash content. It has been shown that the angle of shearing resistance (φ) increases with increasing fly ash content in stabilised clay (Sezer et al, 2004; Binal, 2016; Bryson et al, 2017; Rajak et al, 2019; Keramatikerman et al, 2018) and silt (Prabakar et al, 2004). Prabakar et al (2004) found that the angle of shearing resistance improved from 17^{o} for silty unstabilised soil to 27^{o} for stabilised soil with 46% fly ash inclusion. Binal (2016) and Bryson et al (2017) attributed the increase in angle of shearing resistance to the particle substitution. The silt fraction of fly ash roughens up the surface of clay minerals, decreases clay fraction, and increases of the average grain size of the mixture. The cohesion (c) of soil also increases with increasing fly ash content (Kumar and Sharma, 2004; Prabakar et al, 2004; Sezer et al, 2004; Binal, 2016). Prabakar et al (2004) pointed out that the cohesion of unstabilised CL soil increased from 24 kPa to 39 kPa for stabilised soil with 46% fly ash inclusion. The increase in the cohesion and angle of shearing resistance of soil-fly ash mixture could be due to the pozzolanic reactions and formation of new cementitious compounds, calcium silicate hydrate (CSH) or calcium aluminate hydrate (CAH) from hydration (Keramatikerman et al, 2018; Striprabu et al, 2018). The increase of curing time has also shown to increase c and φ values of fly ash-stabilised soils (Sezer et al, 2004; Binal, 2016). This effect could be related to the pozzolanic properties of fly ash that develop over longer curing period. Binal (2016) reported that the angle of shearing

resistance of CH soil increased 3 times and the cohesion value of the soil increased 16 times for 25% fly ash-stabilised soil with 28 days of curing. Also, higher deviatoric stress (q) was observed by increasing the fly ash content of stabilised soil due to the generation of strong bonds from hydration products, CSH and CAH (Keramatikerman et al, 2018). Prabakar et al (2004) indicated that deviatoric stress of fly ash-stabilised soil showed an improvement by increasing the confining pressure. The maximum deviator stresses of CL were found 361, 467, and 585 kPa at confining pressures of 20, 40, and 60 kPa, respectively, while for the soil stabilised with 46% fly ash, the failure stresses increased to 505, 615, and 729 kPa, respectively, at the same confining pressures (Prabakar et al, 2004).

2.3.6 Effects of fly ash inclusion on swelling, consolidation, and permeability of soil

Expansive soils can cause major damage and distortion in structures, especially in pavements and light buildings, due to significant changes in volume as a result of changes in water content (Zha et al, 2008). Fly ash can also be used as an additive to control volume change and swelling behaviour of expansive soils.

Free swell index (FSI) can be described as 'the ratio of the difference in volumes of soil fraction (<425 μm) in water and air, to the volume of soil in air' as:

$$FSI = \left(\frac{Vw - Va}{Va}\right) * 100(\%)$$

where V_w is final volume of soil in water and V_a is the final volume of soil in air (Zha et al, 2008).

Comprehensive research has demonstrated the successful use of fly ash in controlling the swelling behaviour of expansive soils. It has been shown that free

swell index (FSI), swelling potential, swelling pressure, and swelling index (C_s) decrease significantly with increasing fly ash content (Cokca, 2001; Ji-Ru and Xing, 2002; Nalbantoglu, 2004; Kumar and Sharma, 2004; Prabakar et al, 2004; Kate, 2005; Phanikumar and Sharma, 2007; Zha et al, 2008; Phanikumar, 2009; Amiralian et al, 2012a; Mir and Sridharan, 2013, 2014; Pal and Ghosh, 2014; Binal, 2016; Kolay and Ramesh, 2016; Seyrek, 2016; Vindula et al, 2016; Bryson et al, 2017; Zhou et al, 2019). Table 2.6 shows published results on FSI (%), swell potential (%), and swell pressure (kPa) and Table 2.7 presents the studies of swelling index in unstabilised and fly ash-stabilised soils. Mir and Sridharan (2013) and Seyrek (2016) reported that class C fly ash is more effective in reducing the swelling of soils in comparison with class F fly ash, and that 10% class C fly ash is the optimum content needed to control the swelling of a CH soil compared to 40% class F fly ash. The reduction in swelling of fly ash-stabilised soil can be explained by several reasons. The first reason is the replacement/reduction of plastic fines of expansive soil with non-plastic silt-sized fines of fly ash (Cokca, 2001; Prabakar et al, 2004; Phanikumar and Sharma, 2007; Zha et al, 2008; Mir and Sridharan, 2014; Seyrek, 2016). The diameter of fly ash particles can vary between 0.075 and 0.002 mm which is larger than the diameter of clay particles (<0.002 mm) (Phanikumar and Sharma, 2007). Moreover, the flocculation process in samples creates particles with larger diameter. In this way, when the size of particles increases, the initial suction before inundation of the sample is reduced compared to the expansive soil, resulting in decrease of swelling with fly ash content (Phanikumar and Sharma, 2007). Cokca (2001) and Seyrek (2016) pointed out that fly ash is primarily comprised of silicate, aluminium, and iron oxides, hence it has potential to provide

multivalent cations (Ca^{2+}, Al^{3+}, F^{3+}, etc.), which lead to flocculation of clay particles by cation exchange. In this way, the surface area and water affinity of the stabilised soil could be decreased, resulting in a reduction in swelling. In addition, the cementation occurring at the particle contacts restrains swelling of fly ash-stabilised soil (Phanikumar and Sharma, 2007). Nalbantoglu (2004) also explained the decrease of swelling potential of stabilised soil with fly ash in terms of cation exchange capacity (CEC). CEC is the amount of exchangeable cations held by clay and is equal to the negative charge. Expansive soils with larger specific surface areas have higher CEC and surface activity resulting from higher water absorption potential. It has been observed that CEC decreases with the addition of fly ash. The decrease of CEC could be due to the formation of new phases with coarser particles that leads to lower surface activity, and therefore lower water absorption potential (Nalbantoglu, 2004).

An increase in curing time is also very effective in reducing the swelling behaviour of fly ash stabilised soils (Cokca, 2001; Nalbantoglu, 2004; Zha et al, 2008; Mir and Sridharan, 2013, 2014). This decrease in swelling with the curing time could be mainly due to the time-dependent pozzolanic reactions and the formation of calcium silicate hydrate/calcium aluminate hydrate (CSH/CAH) in fly ash-stabilised soil (Zha et al, 2008; Mir and Sridharan, 2014).

Table 2.6 Swelling parameters of soils stabilised with fly ash from different studies.

Type of fly ash	Type of soil	Fly ash content	Free Swell Index (%)	Swell potential (%)	Swell pressure (kPa)	References
class C	CH	unstabilized (0%)	-	19.6	-	Nalbantoglu (2004)
		15%	-	5	-	
		25%	-	3.7	-	
		25% (30 days cured)	-	0	-	
class F	CH	unstabilized (0%)	250	10.8	90	Kumar and Sharma (2004)
		5%	200	8.8	72	
		10%	165	7.2	60	
		15%	140	6.0	50	
		20%	125	5.5	45	
class F	CH (PI=352)	unstabilized (0%)	377	22	425	Kate (2005)
		20%	260	11	305	
	CH (PI=307)	unstabilized (0%)	326	17.5	345	
		20%	214	8.7	207	
	CH (PI=215)	unstabilized (0%)	230	13.7	259	
		20%	105	6.8	185	
	CH (PI=116)	unstabilized (0%)	168	9	167	
		20%	116	4.7	110	
class F	CH	unstabilized (0%)	165	26.7	330	Phanikumar (2009)
		10%	130	13.9	90	
		20%	110	8.9	74	
class C	CH (kaolinite)	unstabilized (0%)	84	-	1116.19	Kolay and Ramesh (2016)
		10%	75.7	-	755.31	
		20%	70.8	-	514.72	
		30%	64.5	-	240.71	
		40%	59.1	-	150.40	
		50%	54.8	-	75.13	
	CH (bentonite)	unstabilized (0%)	477.1	-	3522.1	
		10%	340.8	-	3281.5	
		20%	307.4	-	2680.0	
		30%	273.3	-	2078.5	
		40%	263.8	-	1356.8	
		50%	246.9	-	1248.5	
class F	CH	unstabilized (0%)	-	7.03	57.6	Seyrek (2016)
		30%	-	2.58	25.5	
class C	CH	unstabilized (0%)	-	7.03	57.6	
		30%	-	1.04	14.8	
class F	CL	unstabilized (0%)	-	4.09	16.4	
		30%	-	1.39	7.9	
class C	CL	unstabilized (0%)	-	4.09	16.4	
		30%	-	0.60	4.6	
Low-Ca fly ash	CH	unstabilized (0%)	125	-	120	Phanikumar and Nagaraju (2018)
		5%	118	-	-	
		10%	100	-	105	
		15%	85	-	-	
		20%	70	-	60	
		25%	50	-	-	
		30%	35	-	20	
class F	CL	unstabilized (0%)	59.4	-	-	Zhou et al (2019)
		20%	35.3	-	-	
class C	CH	unstabilized (0%)	155	15.3	350	Phanikumar et al (2021)
		5%	124	13.5	270	
		10%	110	12.7	330	
		15%	83	12	380	
		20%	77	11.4	290	
		25%	77	10.3	420	

Many consolidation parameters such as compression index (C_c), coefficient of volume compressibility (m_v), coefficient of consolidation (c_v), pre-consolidation pressure, and permeability or hydraulic conductivity (k) were studied using one-

dimensional consolidation tests (Phanikumar and Sharma, 2007; Phanikumar, 2009; Amiralian et al, 2012a; Mir and Sridharan, 2014; Pal and Ghosh, 2014; Shil and Pal, 2015; Kolay and Ramesh, 2016; Bryson et al, 2017; Efthymiou et al, 2019). Compression indices of the unstabilised soil and stabilised soil with different percentages of fly ash are shown in Table 2.7. The results show that the value of C_c decreased with increasing the class C or class F fly ash content in fine-grained soils. However, Phanikumar (2009) reported that the value of C_c initially increased up to certain content of class F fly ash, and thereafter it decreased. The decrease of C_c with fly ash content indicates an improvement in compressibility of the stabilised soil owing to the formation of cementitious bonds (Mir and Sridharan, 2014) and pozzolanic reactions (Amiralian et al, 2012a). The value of C_c also decreased with increase in curing time. This is because the cation exchange reaction leads to flocculation and aggregation which creates an increase in the vertical effective yield stress and decrease in compressibility (Mir and Sridharan, 2014). Shil and Pal (2015) showed that coefficient of volume compressibility (m_v) decreased with addition of fly ash in fine-grained soils. They highlighted that the higher percentage of silt content in fly ash and lower plasticity of fly ash lead to lesser volume change in stabilised soil. Pal and Ghosh (2014) observed that m_v of a CH soil was 2.62×10^{-4} m^2/kN, and it decreased to, 1.41×10^{-4} m^2/kN, 1.01×10^{-4} m^2/kN, 0.72×10^{-4} m^2/kN, and 0.37×10^{-4} m^2/kN when 50%, 60%, 70%, and 80% of class F fly ash were added, respectively. Efthymiou et al (2019) reported that pre-consolidation pressure showed a significant increase with increase of fly ash and curing time. Mir and Sridharan (2014) also showed that the value of c_v increased with addition of fly ash. This is consistent with the increase in rate of permeability (Shil and Pal, 2015).

Table 2.7 Compression and swelling indices of soils stabilised with fly ash based on oedometer tests from different studies.

Type of fly ash	Type of soil	Fly ash content	Compression index (Cc)	Swelling index (Cs)	References
class F	CH	unstabilized (0%)	0.5	-	Phanikumar (2009)
		10%	0.65	-	
		20%	0.5	-	
class F	CH	unstabilized (0%)	0.645	-	Pal and Ghosh (2014)
		50%	0.271	-	
		60%	0.200	-	
		70%	0.125	-	
		80%	0.071	-	
		100%	0.112	-	
-	ML	unstabilized (0%)	0.118	-	Shil and Pal (2015)
		20%	0.063	-	
		30%	0.056	-	
class C	CH (kaolinite)	unstabilized (0%)	1.00	0.23	Kolay and Ramesh (2016)
		10%	0.37	0.21	
		30%	0.15	0.12	
		50%	1.53	0.09	
	CH (bentonite)	unstabilized (0%)	1.07	0.21	
		10%	1.23	0.14	
		30%	1.54	0.11	
		50%	1.42	0.07	
class F (1)	CL	unstabilized (0%)	0.503	0.079	Bryson et al (2017)
		10%	0.508	0.080	
		20%	0.377	0.043	
		40%	0.432	0.069	
		100%	0.041	0.017	
class F (2)		unstabilized (0%)	0.503	0.079	
		10%	0.472	0.073	
		20%	0.425	0.064	
		40%	0.354	0.044	
		100%	0.096	0.013	
class F (3)		unstabilized (0%)	0.503	0.079	
		10%	0.508	0.090	
		20%	0.431	0.063	
		40%	0.356	0.044	
		100%	0.065	0.013	
class C		unstabilized (0%)	0.503	0.079	
		10%	0.469	0.061	
		20%	0.469	0.050	
		40%	0.376	0.025	
		100%	0.036	0.012	

Permeability/hydraulic conductivity of soil stabilised with fly ash is usually assessed through one-dimensional consolidation or permeability tests. It has been reported that permeability increases with increasing the fly ash content in fine-grained soils (Phanikumar, 2009; Mir and Sridharan, 2014; Pal and Ghosh, 2014; Shil and Pal, 2015) (Table 2.8). This is because flocculation and aggregation occur due to the cation exchange reaction, with an increase in porosity and thus permeability (Phanikumar, 2009). In addition, when the silt size particles increase in soil owing to the addition of fly ash, the stabilised soil

becomes comparatively coarser (Mir and Sridharan, 2014). Increase in permeability also indicates an increase in the rate of consolidation of soil (Pal and Ghosh, 2014). Mir and Sridharan (2014) reported that permeability of stabilised soil decreased with an increase of curing time. A possible explanation for this could be that cementitious gel is formed in the soil due to the reaction of CASH or CSH structure which fills the pores during the curing (Kassim and Chow, 2000; Chew et al, 2004).

Table 2.8 Coefficient of consolidation and permeability of soils stabilised with fly ash from different studies.

Type of fly ash	Type of soil	Fly ash content	Coefficient of consolidation (cv)	Permeability (k)	References
class F	CH	unstabilized (0%)	$0.32x10^{-3}$ cm^2/s	$0.10x10^{-9}$ cm/s	Phanikumar (2009)
		10%	$0.8x10^{-3}$ cm^2/s	$1x10^{-9}$ cm/s	
		20%	$2.71x10^{-3}$ cm^2/s	$2.5x10^{-9}$ cm/s	
class F	CH	unstabilized (0%)	$6.343x10^{-9}$ m^2/s	$8.211x10^{-11}$ m/s	Pal and Ghosh (2014)
		50%	$1.418x10^{-8}$ m^2/s	$1.72x10^{-10}$ m/s	
		60%	$2.005x10^{-8}$ m^2/s	$3.63x10^{-10}$ m/s	
		70%	$2.197x10^{-8}$ m^2/s	$5.70x10^{-10}$ m/s	
		80%	$0.026x10^{-4}$ m^2/s	$9.44x10^{-10}$ m/s	
		100%	$2.874x10^{-4}$ m^2/s	$2x10^{-7}$m/s	
-	ML	unstabilized (0%)	$9.07x10^{-3}$ cm^2/s	$3.38x10^{-6}$ cm/s	Shil and Pal (2015)
		20%	$11.4x10^{-3}$ cm^2/s	$3.43\text{-}2.21x10^{-6}$ cm/s	
		30%	$13.4x10^{-3}$ cm^2/s	$2.93\text{-}1.58x10^{-6}$ cm/s	
Low-Ca fly ash	CH	unstabilized (0%)	-	$4.6x10^{-7}$ cm/s	Phanikumar and Nagaraju (2018)
		10%	-	$6.0x10^{-7}$ cm/s	
		20%	-	$8.5x10^{-7}$ cm/s	
		30%	-	$1.8x10^{-6}$ cm/s	

2.4 Field applications of fly ash stabilised soil

There have been limited field studies of fly ash stabilised soil in comparison with the laboratory studies. However, several standards encourage the use of fly ash in field applications. According to the US Federal Highway Administration (FHWA) report (2003), soil + class C fly ash or soil + class F fly ash + lime mixtures can be used in many geotechnical applications, commonly in highway construction. Fly ash can be used to stabilise base or subgrade, backfill for

reducing lateral earth pressure, and embankments for improving slope stability. The main reason for adding fly ash in soil is to improve compressive strength and shear strength of the soil. For field applications, the strength of the soil can be changed with delay in compaction, in situ soil properties, moisture content at time of compaction, and fly ash content. FHWA (2003) indicated that density and strength can be decreased with increasing the delay of compaction. Thus, it is recommended to apply compaction without any delay, or with a one-hour compaction delay in construction. The maximum strength is obtained with moisture content of about 4 to 8% below OMC (for silt and clay). For field applications, the addition of fly ash to the soil is recommended to be typically between 8 to 16% based on by dry weight of the soil. Organic soils are generally not suitable for stabilisation with fly ash. According to ASTM D7762 (2018), self-cementing (class C) fly ash can be applied in road construction, including stabilised subgrade, subbase, and base layers. Fly ash stabilisation method can also be applied to decrease the compressibility of fills below buildings. The fly ash has been shown to be an effective stabilisation material for fine-grained soils used in subgrade for pavements, in decreasing swelling potential of clay soils, in increasing shear strength of fine-grained soils, and in reducing the settlement of fills under foundations (ASTM D7762, 2018).

Senol et al (2002) investigated the performance of class C fly ash-stabilised subbase of a pavement system in a field site in Wisconsin. The subgrade soil was classified as low plasticity clay. Laboratory experiments, including UCS, CBR, and resilient modulus (M_r) tests, were initially carried out with addition of 12%, 16%, and 20% fly ash by dry weight of the soil. Based on the laboratory test results, the subgrade was stabilised with addition of 12% fly ash in the field site.

Post construction tests, including UCS, CBR, and Mr tests, were applied by collecting Shelby tube samples from the field. The values of UCS, CBR, and Mr increased significantly with the addition of fly ash. The CBR value increased from 1 to 25. The general rating of the subgrade soil improved from ‘very poor’ to ‘good’ and the application terms of subgrade soil changed to base or subbase soil (Bowles, 1992). Geo-gauge stiffness (GGS) survey was carried out to measure stiffness, and it was found that the average stiffness increased from 5 MN/m for the unstabilised soil to 13 MN/m for the stabilised soil. Bin-Shafique et al (2004) investigated a case study involving pavements of two sites by mixing class C fly ash and low plasticity clay soil to stabilise a subgrade. Comparison was made between the fly ash stabilised soil and conventional cut and fill method in the field. CBR, M_r, and UCS tests were conducted in the laboratory. Based on the laboratory test results, the most effective fly ash contents were determined in the range 10% to 12% for application in the field sites. It was observed that the strength and stiffness properties of the subgrades were significantly improved with the addition of fly ash. The results of the cut and fill method and the fly ash stabilisation method were similar from field tests. A similar study was conducted by Trzebiatowski et al (2004) to improve the understanding of effects of fly ash in soil stabilisation in highway subgrade. Laboratory tests, including CBR, UCS, and M_r, were carried out on sandy clay with the addition of 10% class C fly ash. Field tests, including falling weight deflectometer (FWD) and soil stiffness gauge (SSG) tests, were also carried out. Based on the laboratory test results, the average UCS of the stabilised soil increased by 1.5 times compared to the unstabilised soil. The average CBR and M_r values increased from 2 to 85, and from 0 to 21 MPa, respectively. The field test results confirmed that the subgrade improved

considerably by addition of fly ash to the soil. The highest strength results were obtained at 28 days curing time according to M_r test results. By contrast, the CBR and UCS results increased marginally after 7 days of curing. Parsons and Kneebone (2005) evaluated a class C fly ash-stabilised clay and unstabilised clay for subgrades of pavements by using laboratory and field tests. Atterberg limit and one-dimensional swell potential tests were conducted with the addition of 12% and 16% fly ash in laboratory. Field tests, including dual-mass dynamic cone penetrometer (strength test) and SSG tests, were also conducted. Based on the laboratory test results, it was concluded that both plasticity index and swell potential of the soil decreased with addition of fly ash, however, the swelling rate of the stabilised soil was still high for subgrade construction. Therefore, it was recommended that utilisation of only fly ash in high plasticity clay soil may not be adequate to prevent swelling. According to the field tests, after 28 days, the stiffness of the stabilised soil increased by around 45% compared to unstabilised soil. The final strength results obtained from dynamic cone penetrometer tests showed improvement of 40-250% compared to the unstabilised soil for the pavement system. Bhuvaneshwari et al (2005) carried out laboratory and field tests for a trial embankment. Atterberg limits and compaction tests were carried out by adding 10%- 50% fly ash in a clay soil. The fly ash stabilised soil with maximum of 25% fly ash was found to be suitable. Li et al (2009) reported mechanical improvement of fly ash-stabilised soil in field and laboratory tests. CBR, M_r, UCS tests were carried out on subgrade soil, recycled pavement material (RPM), and road surface gravel (RSG) using class C fly ash as the stabilising agent. The subgrade soil, RPM, and RSG were described as fine-grained soils (CL, CL-ML, CH), sandy-gravel size particles, and well graded

gravelly sand, respectively. The values of CBR, M_r, and UCS increased with addition of fly ash in both conditions, however with all types of soil, the field-mix values of CBR, M_r, and UCS were found lower than laboratory-mix values. This suggested that mixing the material in the laboratory leads to more uniform distribution of fly ash in the mixture compared to field conditions.

2.5 Geotechnical behaviour of fly ash stabilised soil

Based on the above sections (2.3 and 2.4), the geotechnical behaviour of fly ash stabilised soil can be summarised as the following:

- LL decreases, PL increases, and PI decreases with increasing the fly ash content in the soil.
- The addition of fly ash to soil results in a decrease in MDD and an increase in OMC. However, a number of studies have reported that the MDD increased and OMC decreased with the addition of fly ash. This discrepancy could be due to the differences in the specific gravity of the fly ash used.
- Fly ash stabilised soil could be used as a subbase or base material for roads, backfilling, or other geotechnical structures.
- The addition of fly ash increases UCS, however, the UCS of class C fly ash is often higher than the class F fly ash. An increase in curing time also improves the UCS of soil due to the time-dependent pozzolanic properties of fly ash.
- The shear strength parameters (angle of shearing resistance and cohesion) improve with increasing the fly ash content in the soil.
- Swelling of expansive soils decreases with the addition of fly ash. The compression index (Cc) and coefficient of volume compressibility (mv) of

the soil generally decrease and the pre-consolidation pressure increases with the addition of fly ash. Also, the coefficient of consolidation and permeability increase with the addition of fly ash in the soil; hence, most of the settlement could be completed during the construction stages when fly ash stabilised soil is used.

In general, the technical benefits of using fly ash in soil stabilisation include: increasing strength parameters and CBR values, decreasing plasticity index, preventing swelling of expansive soils, and improving hydraulic conductivity. The ease of adaptability, availability, cost-effectiveness, and being environmentally friendly are the main benefits of using fly ash in geotechnical applications.

2.6 Alkali activated fly ash in soil stabilisation

In recent years, geopolymers have gained a lot of interest as alternative materials to use in the construction industry due to their potential of reducing environmental impacts when compared to Portland cement (Benhood, 2018). Geopolymers are stiff, strong, and long-lasting (Wong et al, 2019), and can offer high mechanical performance and volume stability in soil stabilisation (Ghadir and Ranjbar, 2018). In sections of 2.5.1 and 2.5.2 the detailed definition of geopolymers and geopolymerisation, and previous literature on soils stabilised with alkali activated fly ash (fly ash based geopolymer) are discussed, respectively.

2.6.1 Geopolymers and geopolymerisation

Geopolymers can be defined as amorphous aluminosilicate cementitious materials (Abdullah et al, 2011; Zhuang et al, 2016). They are obtained by the reaction of a solid aluminosilicate (called ‘precursor’) with an alkali activator and are also known as ‘inorganic polymers’ (Duxson et al, 2007). Due to its worldwide availability and silica and alumina contents in amorphous phase, fly ash is one of

the waste materials that is widely utilised as a precursor for producing geopolymers (Abdullah et al, 2011; Al Bakri et al, 2013; Phummiphan et al, 2016; Rios et al, 2016; Zhuang et al, 2016; Murmu et al, 2018; Firdous and Stephan, 2019; Wong et al, 2019; Azimi et al, 2020; de Azevedo et al, 2021; Damrongwiriyanupap et al, 2022). Geopolymerisation allows to immobilise the trace toxic elements in fly ash, slag, or other industrial wastes that could be used as precursors. The geopolymer matrix can capture and fix the hazardous elements such as barium (Ba), cadmium (Cd), cobalt (Co), chromium (Cr), and copper (Cu). The typical processes of metal immobilisation in the fly ash-based geopolymers are chemical stabilisation and physical encapsulation (Van Deventer et al, 2006; Al Bakri et al, 2013; Zhuang et al, 2016; Wong et al, 2019). The three steps of geopolymerisation (proposed by Glukhovsky in 1950s) are '(1) destruction–coagulation; (2) coagulation–condensation; (3) condensation–crystallisation' (Duxson et al, 2007). Other researchers expanded Glukhovsky's model to describe the geopolymerisation process in detail (Duxson et al, 2007), even though studies are still being undertaken to fully understand the mechanisms involved in alkali activation with aluminosilicate materials (Shi et al, 2019). The typical steps used to describe geopolymerisation mechanism are as follows:

- Dissolution of amorphous aluminosilicate powders from the source material by the action of alkali hydroxide;
- The transfer of precursor ions into monomers and their condensation;
- The formation of geopolymer structures by polycondensation or polymerisation of monomers into polymers (van Jaarsveld et al, 2003; Abdullah et al, 2011; Al Bakri et al, 2013; Gado et al, 2020).

Davidovits (1994) proposed the name ‘polysialate’, as an abbreviation of aluminosilicate oxide. It is possible to formulate the polysialate/three-dimensional network of aluminosilicate structures as follows:

$M_n\ [-(SiO_2)_z - AlO_2]_n.wH_2O$

where M is the alkaline element or cation such as sodium (Na^+), potassium (K^+), or calcium (Ca^{++}), n is the degree of polycondensation or polymerisation, z is the Si/Al molar ratio, and w is the water content (Pacheco-Torgal et al, 2008; Al Bakri et al, 2013; Zhuang et al, 2016). Commonly geopolymeric structures are:

Poly(sialate) Si:Al = 1(-Si-O-Al-O-);

Poly(sialate-siloxo) Si:Al = 2(-Si-O-Al-O-Si-O-);

Poly(sialate-disiloxo) Si:Al = 3(-Si-O-Al-O-Si-O-Si-O-) (Phummiphan et al, 2016).

A combination of sodium hydroxide or potassium hydroxide with sodium silicate or potassium silicate is the most used alkali activator for geopolymerisation (Wong et al, 2019; Wang et al, 2020). The type of alkali solution used has a significant impact on the geopolymerisation process. Studies have found that geopolymerisation may be achieved with a single alkali activator, however, when the alkali activator additionally contains soluble sodium or potassium silicate, the reaction occurs more quickly than when only alkali hydroxides are used. (Abdullah et al, 2011; Wong et al, 2019). A sodium silicate (SS) solution is often combined with a sodium hydroxide (SH) solution to enhance compressive strength (Zhuang et al, 2016). In addition, compared to potassium hydroxide solution, the release of Si^{4+} and Al^{3+} from fly ash in SH solution is greater. (Abdullah et al, 2011). There has been significant investigation focused on the effects of the dosage or concentration of alkali activators with fly ash binders on the mechanical properties of stabilised soil.

2.6.2 The use of alkali activated fly ash/fly ash based geopolymer in soil stabilisation

Ridtirud et al (2018) performed unconfined compressive strength (UCS) tests on mixtures of class C fly ash and silty clayey gravel with sand (GM-SM) with 1.5%, 3%, 5%, 7%, 10%, 15%, and 20% fly ash (by weight of the soil) at 7, 14, and 28 days of curing. SH solution with a concentration of 8 M was prepared from SH flakes. SS solution had 8.9% Na_2O, 28.7% SiO_3, and 62.5% H_2O. The ratios of SH/SS were 1/1, 3/1, 3/2, 2/3, and 1/3. The results indicated that the compressive strength of soil increased with up to 7% fly ash. A possible explanation for this could be that the water and alkali activator solutions were added based on the optimum moisture content; therefore, beyond 7% fly ash, there was not enough solution and water to assist the reaction. The compressive strength of the soil increased over curing time. The best ratio of SH/SS solution was found at 1/1 at room temperature, and at 2/3 at 40 °C.

Trinh and Bui (2018) conducted a series of compressive strength tests on a soil stabilised with activated class F fly ash. An alkali-activated solution (AAS with SS/SH = 2, AAS/fly ash = 0.5) was used. Geopolymer inclusions of 5%, 10%, 15%, and 20% were considered. Sand with different percentages was mixed with clay soil to examine the effects of soil types on compressive strength. It was concluded that the compressive strength of the clay soil increased with the addition of class F fly ash binders and sand contents.

Correa-Silva et al (2018) examined the effects of alkali-activated low-calcium fly ash through UCS and California bearing ratio (CBR) tests on low-plasticity clayey soil (CL). The ratio of SS/SH solution was 2. UCS and CBR tests were also carried out on samples of the same soil stabilised with cement and lime for

comparison with the stabilisation with alkali-activated fly ash. The ratios of fly ash used were 10%, 15%, and 20%, while the ratios of lime and cement were 5%, 7.5%, and 10%, and the curing times were 7, 14, 28, and 90 days. According to the UCS test results, the mechanical behaviour of all stabilised soils with 28 days of curing improved compared to unstabilised soil. Fly ash gave significantly better results compared to lime, but the most effective results were obtained with cement at 28 days of curing. Conversely, between 28 and 90 days of curing, the cement improvement was found to be insignificant, whereas lime and fly ash showed a considerable strength increase due to the long-term chemical reactions. The best mechanical behaviour was recorded for the soil stabilised with 20% fly ash at 90 days of curing. Based on the CBR results performed after 96 h, the strength parameters increased by a factor of 6 with addition of 10% cement, by a factor of 5 with addition of 20% fly ash, and by a factor of 2.5% with addition of 10% lime.

Leong et al (2018) analysed the impacts of class F fly ash, alkali activator, water content, curing time, and curing temperature on the mechanical properties of a silty sand by conducting uniaxial compression strength tests. The aim was to understand the suitability of such soil stabilised with a fly ash-based geopolymer for the production of bricks. SH or potassium hydroxide and SS were used as the alkali activator. The results showed that the highest compressive strength of the stabilised bricks was obtained when the ratio of alkali activator/fly ash was at 0.6 and SS/SH or (potassium hydroxide) was at 0.5, with an additional 10% water content. In addition, the compressive strength of the bricks increased by increasing the curing temperature and the ratio of fly ash/soil. On the other hand, the compressive strength of the bricks decreased by increasing the curing

temperature above 100° and with an increased curing time. It was therefore suggested that the high temperature created cracks on the bricks, resulting in a decrease in compressive strength. The curing time also resulted in a loss of moisture (in the oven) in the bricks.

Similarly, Dungca and Codilla (2018) carried out UCS and CBR tests on class F fly ash-based geopolymer-stabilised silty sand by applying the dry-mix method. In this method, the alkali activators and fly ash were mixed in dry conditions, and then water was added. An SS/SH ratio of 2 and an activators-to-fly ash ratio of 0.4 were selected. The curing time was 7 days for the CBR and 28 days for the UCS tests. Based on the test results, the obtained UCS values were 78 kPa (medium consistency), 248 kPa (very stiff), and 1350 kPa (hard) with the addition of 10%, 20%, and 30% fly ash-based geopolymer, respectively. The obtained CBR indices were found to be 9.9% and 16.2% (classified as a sub-base material for embankments), and 34.3% (classified as a base material for embankments) with the addition of 10%, 20%, and 30% fly ash-based geopolymer, respectively.

Sukmak et al (2013) also carried out compressive strength tests to evaluate the effects of fly ash-based geopolymer on the stabilisation of a clay soil. The effects of the fly ash (FA)/clay ratio, SS/SH ratio, and alkali activators (L)/fly ash ratio were considered in the study. The ratios of FA/clay chosen were 0.3, 0.5, and 0.7; the ratios of SS/SH were 0.4, 0.7, and 1, and the ratios of L/FA were 0.4, 0.5, 0.6, and 0.7. Based on the results, the maximum compressive strengths of stabilised soils were found with an SS/SH ratio of 0.7 for all conditions of L/FA and FA/clay ratios. The optimum L/FA ratio was recommended between 0.5 and 0.6 for the maximum compressive strength.

Murmu et al (2018) conducted Atterberg limit, compaction, UCS, and California bearing ratio (CBR) tests on black cotton soil, CH, with addition of different fly ash contents (5%, 10%, 15%, and 20%). SH solution was added with a concentration of 5M. The results indicated that liquid limit (LL) decreased, and plastic limit (PL) increased with the addition of fly ash. The highest decrease in LL was found at 20% of fly ash (predicted 17%). Optimum moisture content (OMC) showed an increase up to 10% of fly ash addition, thereafter, started to decrease. Maximum dry density (MDD), on the other hand, decreased up to 15% of fly ash addition, after that it slightly increased. According to the UCS and CBR results, fly ash based geopolymer stabilised soil with 5-20% fly ash and cured for minimum 14 days at more than 25^{o}C is acceptable for subgrade or subbase applications based on the Indian standard (IRC: SP37).

Abdullah et al (2019b) assessed the applicability of fly ash based geopolymer on different clay soils in terms of compaction, plasticity, compressive strength, pH level, and durability. Class F fly ash, ground granulated blast furnace slag (GGBFS), and sodium-based activators (SS and SH) were used as geopolymer components. The precursor (fly ash + slag) was dosed at 10%, 15%, and 20% by weight of the clay. The mass ratios of SS to SH, slag to fly ash, and activator to (fly ash + slag) were chosen as 2.33, 20%, and 40%, respectively. The SH powder was dissolved in water with a concentration of 14M, before mixing the SS solution. Results showed increase in MDD, decrease in OMC, decrease in LL, slight increase in PL, decrease in PI, increase in compressive strength, and improvement in durability for all different clay soils. However, it was observed that 20% geopolymer addition was required to obtain 12 wetting-drying cycles for a negligible volumetric change of 0.12% on 100% kaolin soil sample. On the other

hand, to resist the 12 cycles, the engineered soil samples with composition 80% kaolin + 20% sand and 60% kaolin + 40% sand showed satisfactory behaviour with 15% and 10% of geopolymer addition, respectively. The value of pH increased with addition of geopolymer with 1-hour curing time. 10% geopolymer addition increased the pH from 7.8 to 12.2 for kaolin soil. However, the pH decreased with curing time. The decrease in pH value was related to the consumption of OH^- ions during geopolymerisation.

Rios et al (2016a) investigated the effects of alkali activated class F fly ash on silty sand by running UCS tests, triaxial tests, and scanning electron microscopy (SEM) analysis. The experiment results were compared with results of soil-fly ash mixture (without alkali activator) and soil-cement (from previous investigations). The fly ash percentage used was 20% and the alkali activators of SS/SH were used with a mass ratio of 1:2. SH solution was dissolved in water to obtain 7.5M solution. Activator solutions dosed at 11.7% (equal to the optimum water content), 15.6%, and 19.5% were mixed to prepare samples labelled M1, M2, and M3, respectively. The highest UCS was obtained with M1 sample. The comparison of soil-fly ash and soil-fly ash-alkali activator mixtures indicated that alkali activator effects were significant to increase the UCS strength. The soil-cement and soil-fly ash-alkali activated mixtures gave similar UCS strength results, however, the reaction development over curing time for the two mixes showed remarkable differences. Cement stabilised soil showed a considerable strength increase at an early age, whereas alkali activated fly ash stabilised soil showed slower and long-lasting strength improvement, specifically at 90 days curing which the UCS results almost doubled compared to 28 days curing. However, it was observed that there is no need to wait for such a long period as the strength obtained was

satisfactory in shorter curing periods. According to the consolidated-drained triaxial test results, high angle of shearing resistance, 49^{o} for M3 and 65^{o} for M1 were obtained. They argued that the high values in angle of shearing resistance are typical of granular materials in cemented conditions. Cohesion values, 250 kPa for M3 and 290 kPa for M1, were obtained. SEM analysis also showed the formation of the aluminosilicate gel.

Syed et al (2020) analysed mineralogical, microstructural, and geotechnical characterisatics of a high plasticity clay soil stabilised with alkali activated fly ash. The alkali activator solution was prepared using SS, SH, and water. Class F fly ash was used as dry precursor. Water to solid (w/s) ratios of alkali activated binders were used as 0.3, 0.4, and 0.5. Different percentages (5%, 10%, and 15%) of binder were mixed with soil. The samples were cured during 3, 7, 21, and 28 days. According to geotechnical characterisation, the consistency characteristics of the soil generally decreased with addition of alkali activated fly ash. The PI of the soil decreased from 32% to 15% with addition of 10% alkali activated fly ash at 28 days curing and with 0.4 w/s ratio. MDD increased and OMC decreased with addition of alkali activated fly ash. 10% alkali activated fly ash by dry weight of soil was recommended as optimum stabilisation dosage. UCS did not show considerable improvement at initial stage of curing, however the strength increased with the increase of binders and curing time. Swelling percentages of soil showed a decrease with addition of alkali activated fly ash and curing time. The swelling percentages of the soil were reduced by 62% and 70% with the addition of 10% and 15% of alkali activated fly ash, respectively, at 0.4 w/s ratio and 28 days curing. CBR value showed significant improvement with the addition of alkali activated fly ash. X-Ray diffraction analysis showed that

diffraction patterns changed with the addition of alkali activated fly ash binders. The diffractograms showed new peaks, such as Augite (A), Mullite (Mu), and Portlandite (P). SEM analysis showed unreacted fly ash particles in the stabilised soil at 3 days curing, however, the fly ash particles started to give reaction with clay and the formation of sodium aluminosilicate matrix was observed after 28 days curing time.

2.7 Research gaps

Based on the above-mentioned literature, considerable amount of research has been conducted to evaluate the Atterberg limits, compaction characteristics, unconfined compressive strength, and swelling index tests of soil stabilised with fly ash and with different curing times. However, limited investigation has been carried out on triaxial and oedometer tests to understand the effects of inclusion of fly ash on soil stabilisation. Shear strength parameters are important in investigating the bearing capacity of soils and assessment of the stability of geotechnical structures, while consolidation parameters allow the analysis of settlement behaviour of soils. Therefore, more research should be carried out, using triaxial tests to investigate the shearing behaviour and oedometer tests to analyse the consolidation behaviour of fly ash stabilised soil.

The current understanding of soils stabilised with class C and class F fly ash can be significantly improved by further study on triaxial and consolidation behaviour of fly ash-stabilised soil. This research gap is addressed in the first phase of the thesis in Section 4.1.

The review of the literature shows the mechanical effects of soil stabilisation with different contents of alkali activated fly ash. Previous studies have reported promising results to improve soil properties with alkali activated fly ash by

conducting mainly UCS and CBR tests. The literature has focused on the effects of SS/SH and alkali activator solution/fly ash ratios in these tests. However, SS and SH solutions can be produced and used at different concentrations (e.g., different contents of Na_2O, SiO_2, and H_2O in SS solution); thus, data on their ratio alone, without considering the actual chemical composition of the activating solution, do not provide enough information for meaningful comparisons among different investigations.

In order to provide objective discussions on activator dosages, it is important to focus on the actual contents of Na_2O and SiO_2 in the activating solution. Two dosage parameters that have been used in this thesis: the silica modulus (SM), i.e., the mass ratio of SiO_2/Na_2O, and the alkali dosage (M+), i.e., the mass ratio of Na_2O/binder expressed in percentage. Many studies in the geopolymer literature showed the importance of using SM and M+ as the designation of the alkali activators amount (e.g., Firdous and Stephan, 2019; van Deventer et al, 2006; Wang et al, 2020; Chi et al, 2015; Karakoc et al, 2014, Yusuf et al, 2014). Chi (2015) pointed out that the alkali dosages and alkali modulus/silica modulus are two key factors affecting the compressive strength. Karakoc et al (2014) and Gado et al (2020) indicated that the rate of geopolymerisation can be significantly affected by SM ratios, and this geopolymerisation phase has an important effect on the properties and structure of geopolymers. Van Deventer et al (2006) argued that the SM ratio in the activating solutions can significantly change the elemental ratio Si/Al in fly ash-based geopolymers. Yusuf et al (2014) also emphasised that SS solutions produced for the improvement of alkali activated binders are commercially available with different SM ratios; hence, it is more appropriate and

economical to designate optimum SM ratios to obtain the desired strength, rather than only using the SS/SH ratio.

The literature is quite fragmented when describing the optimal dosages of activators in the field of soil stabilisation. Thus, there is a need to investigate systematically the effects of SM and M+ values on the mechanical properties of alkali activated stabilised clay. This research gap is addressed in the second phase of the thesis in Section 4.2. The compaction and compressive strength tests were applied on soils stabilised with alkali activated fly ash with various M+, SM, and fly ash contents to analyse the optimal dosages.

Many studies on soil stabilisation using alkali activated fly ash have been carried out mainly using, UCS and CBR tests. However, there is a lack of study on triaxial, and consolidation behaviour of soils stabilised with alkali activated fly ash and the limited literature is generally focused on stabilising sand instead of clay soil (Rios et al, 2016a; Rios et al, 2017). Also, detailed investigation of soils stabilised with alkali activated fly ash using triaxial tests in the context of the critical state theory has been highly recommended (Abdullah et al, 2020a). Although there is a small amount of research on triaxial testing of stabilised soils, the tests have been applied with basic dosage concentration of SS/SH and alkali activator solution/fly ash. Thus, detailed study of these tests is necessary to eliminate the research gap by using the optimal dosage parameters. After finding the optimal dosages M+ and SM, the consolidation and triaxial (including critical state) parameters, and XRD and SEM analysis are discussed in the second phase of the thesis in Section 4.2.

Chapter 3 Methodology

3.1 Overview

This chapter presents the detailed description of the materials, sample preparation for soils stabilised with class C, class F and alkali activated fly ash, and the tests procedures including compaction, unconfined compressive strength, one-dimensional consolidation, and triaxial tests as well as scanning electron microscopy and X-Ray diffraction. These tests were aimed to assess the physical, mechanical, microstructural, and mineralogical behaviour of the soils stabilised with fly ash and alkali activated fly ash. The overview of the experimental programme is presented in Figure 3.1.

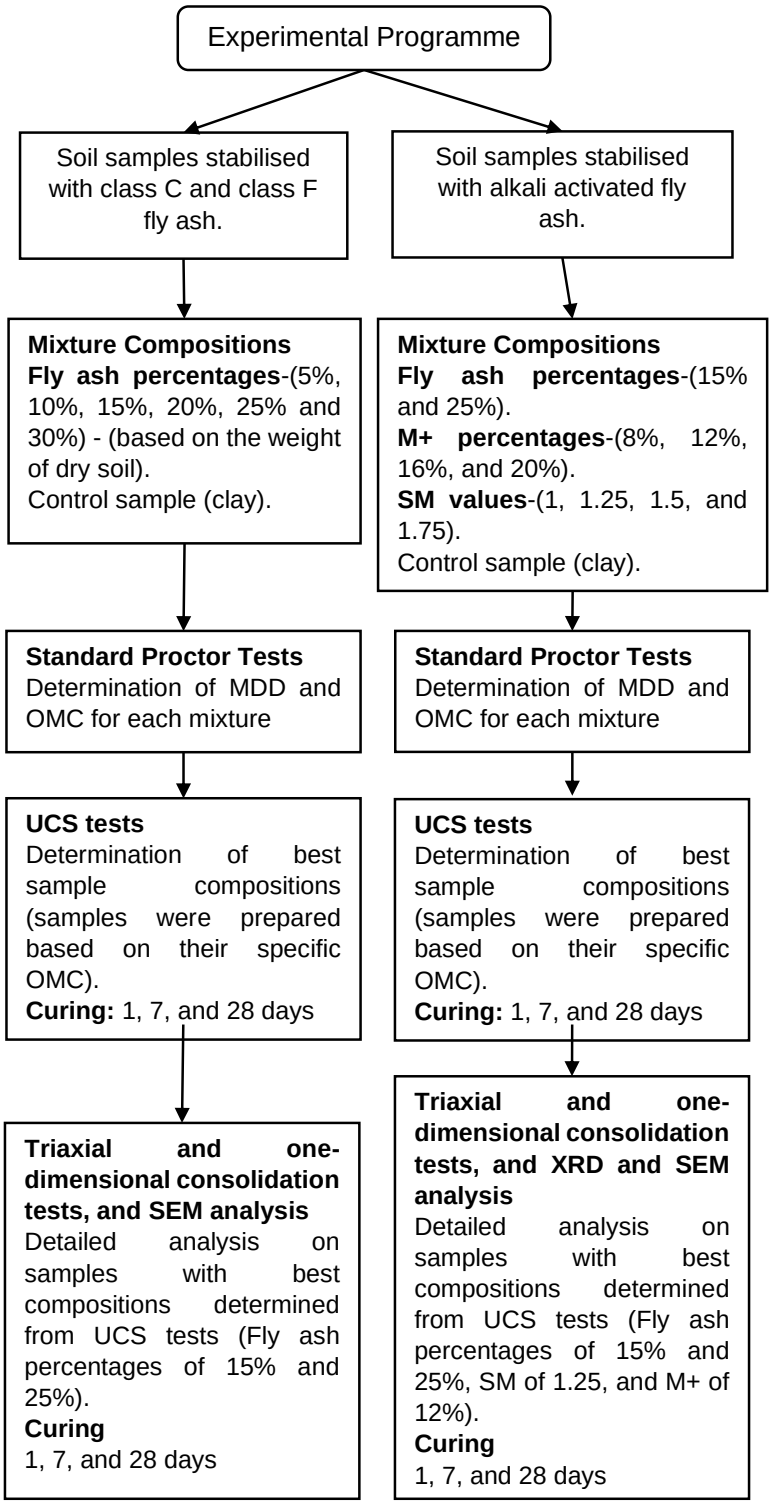

Figure 3.1 The overview of the experimental programme.

3.2 Materials

3.2.1 Soil

A kaolinite powder (China clay), supplied from Mistral Industrial Chemicals, was used in this research. Atterberg limits, standard Proctor (compaction), and small pycnometer tests were carried out to characterise the soil according to British standards (BS 1377-2 and BS 1377-4). According to the results of the Atterberg limit tests, the soil had a liquid limit of 49%, plastic limit of 25%, and plasticity index of 24%. Using the plasticity chart provided in the British standard BS EN ISO 14688-2 (2018), the soil was classified as clay with intermediate plasticity (CI). Based on the compaction tests, the soil was found to have a maximum dry density (MDD) of 15.2 kN/m^3 and optimum moisture content (OMC) of 21%. The specific gravity of the soil was obtained using the small pycnometer test and was equal to 2.6. The average chemical composition of the clay obtained with X-Ray fluorescence (XRF) test is shown in Table 3.1.

Scanning electron microscopy (SEM) analysis was carried out with different magnification factors (Figure 3.2), with the use of TESCAN VEGA 3 SEM detector. Image analysis suggested that the soil had plate-like fragments with different thicknesses.

X-Ray diffraction (XRD) analysis was conducted to assess the mineralogical composition of the soil, with the use of a Bruker D8 advanced XRD equipment. The angular range was recorded as 5 to 65^o (2θ) in a step size of 0.02^o from the X-Ray generator operated at 40 mA and 40 kV. XRD analysis showed that the dominant minerals of the soil were kaolinite, quartz, and illite (Figure 3.3).

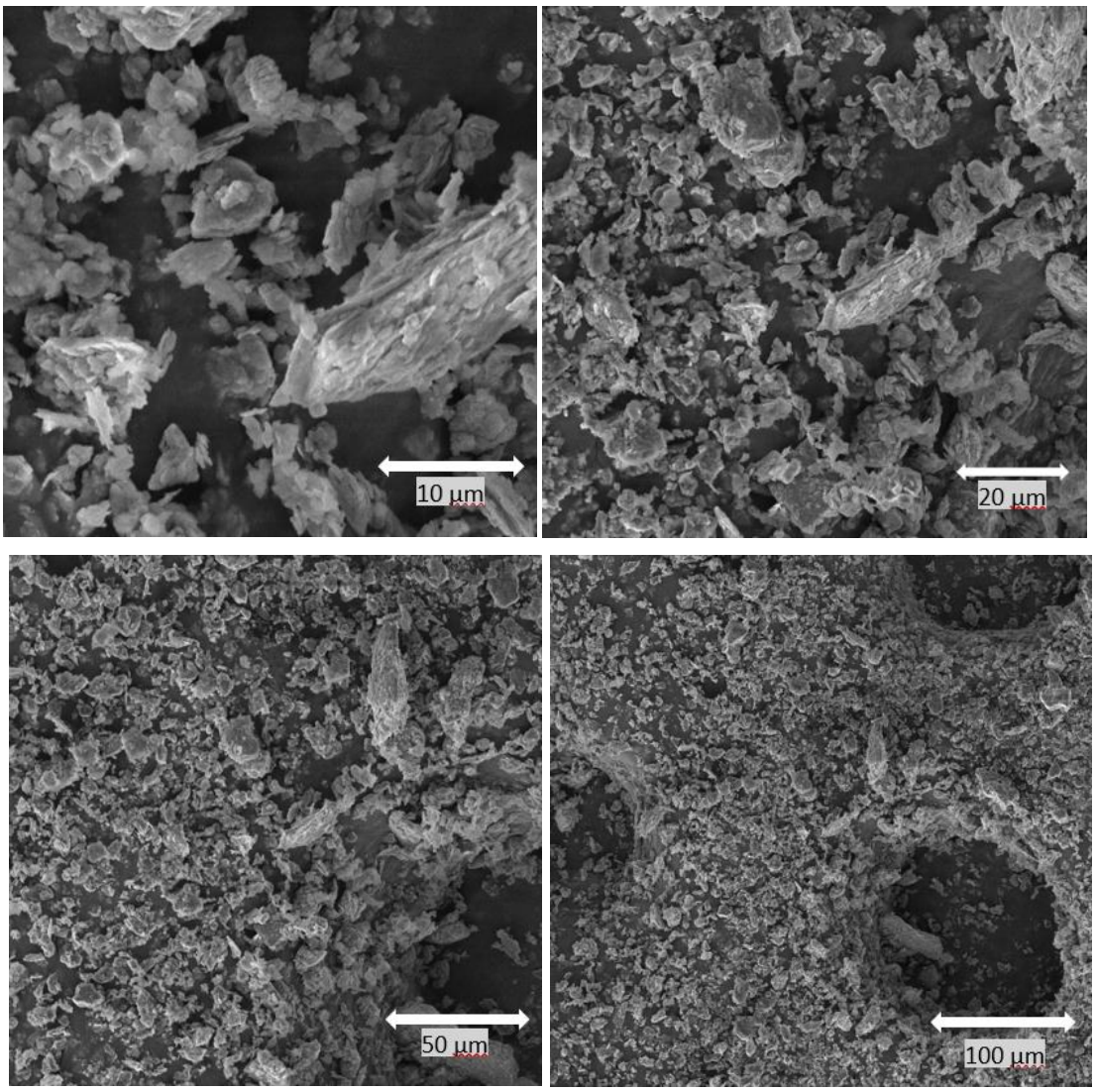

Figure 3.2 SEM images of the soil with different magnification factors.

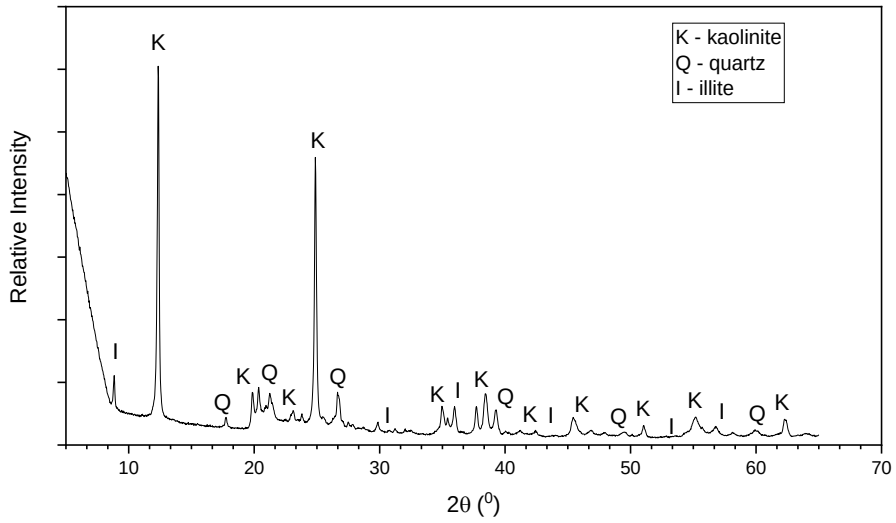

Figure 3.3 X-Ray diffraction pattern of the soil.

3.2.2 Fly ash

Class C fly ash was supplied from the MUEG in Germany and class F fly ash was sourced from Power Minerals Ltd. in the UK. Since the fly ash consists of silt sized particles, the parameters of plasticity index of fly ashes could not be analysed, and they were recorded as non-plastic (NP). The values of specific gravity of class C and class F fly ash were found to be 2.4 and 2.32, respectively (BS 1377-2, 1990). The average chemical compositions from XRF analysis of class C and class F fly ash are shown in Table 3.1. The fly ash was classified according to the ASTM C618 standard.

SEM analysis was carried out on both fly ashes. The SEM images of class C and class F fly ash are shown with different magnification factors in Figures 3.4 and 3.5, respectively. Both class C and class F fly ashes were generally found to be spherical and fine.

XRD analysis was conducted on both fly ashes to obtain their mineralogical compositions. The XRD patterns of class C fly ash and class F fly ash are shown in Figures 3.6 and 3.7, respectively. Based on the XRD analysis, the main crystalline phases of the class C fly ash consist of lime, quartz, anhydrite, and labradorite while the class F fly ash consists of quartz and mullite.

Table 3.1 Oxide composition of clay, class C fly ash, and class F fly ash.

Chemical Composition	Clay	Class C Fly Ash	Class F Fly Ash
CaO (%)	0.1	32.4	2.2
SiO_2 (%)	54.8	28.3	48.6
Al_2O_3 (%)	41.1	15.8	22.5
Fe_2O_3 (%)	1.0	6.6	9.2
K_2O (%)	2.1	0.5	4.1
MgO (%)	0.4	4.2	1.3
Na_2O (%)	0.1	0.3	0.9
P_2O_5 (%)	0.1	0.7	0.2
SO_3 (%)	/	8.6	0.9
TiO_2 (%)	0.1	0.9	1.1

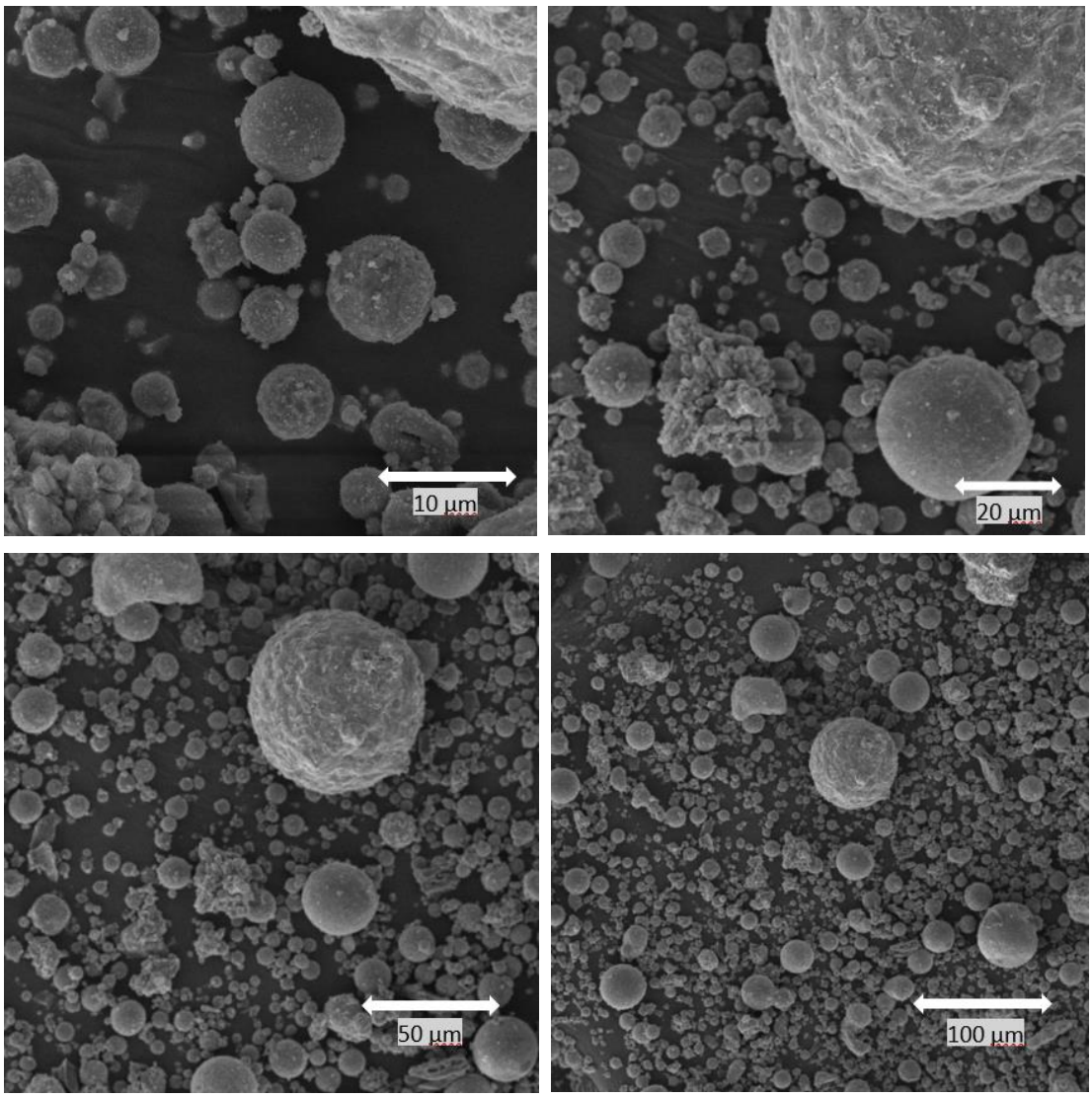

Figure 3.4 SEM images of class C fly ash with different magnification factors.

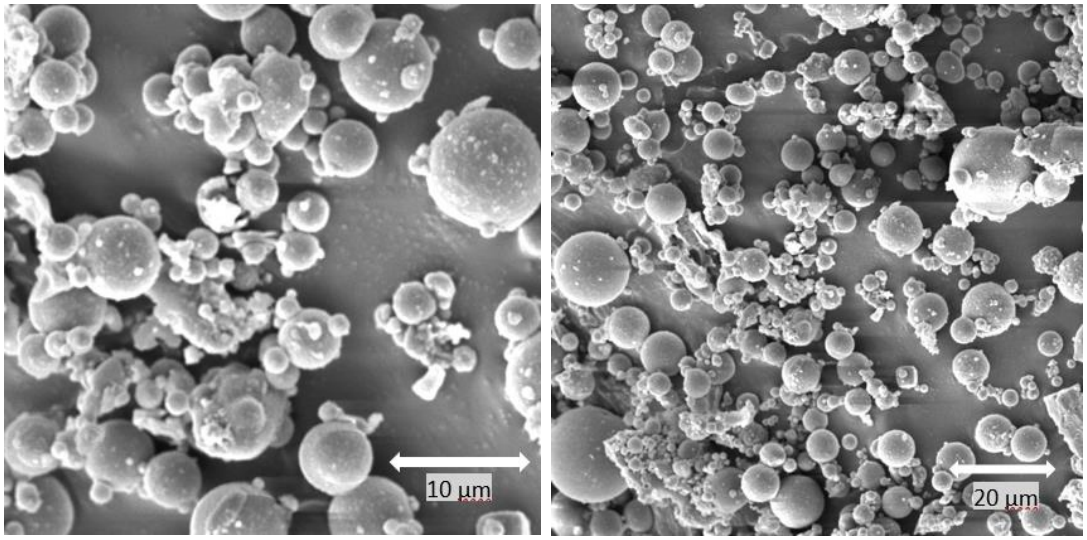

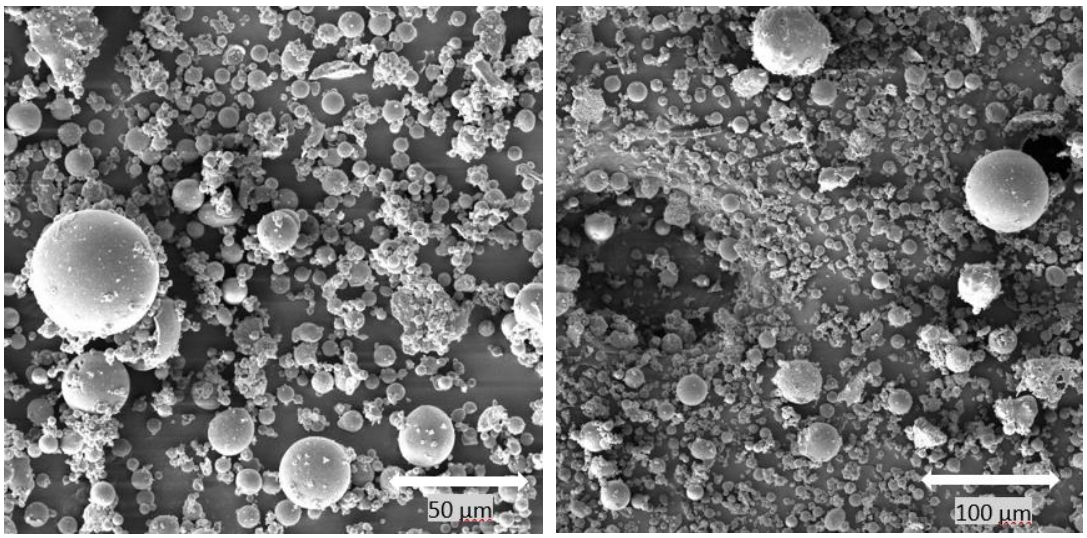

Figure 3.5 SEM images of class F fly ash with different magnification factors.

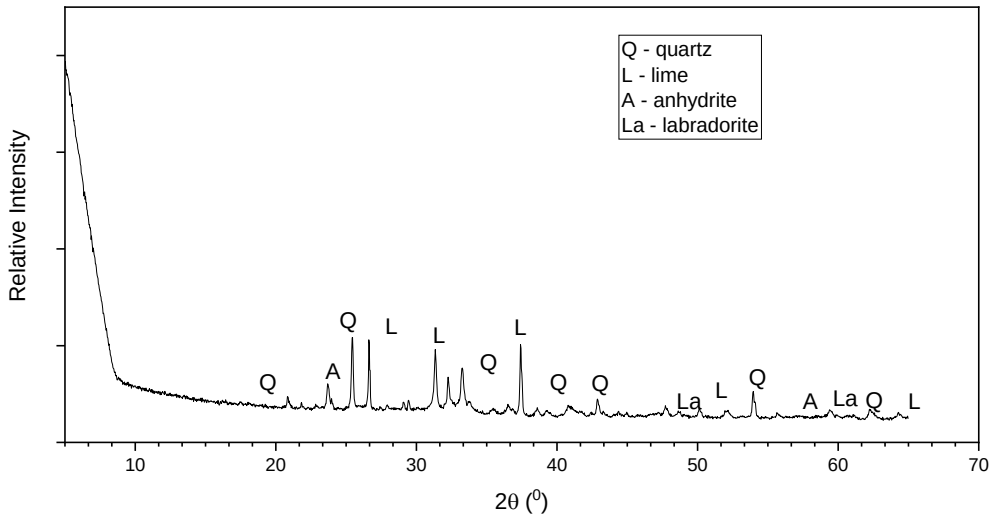

Figure 3.6 X-Ray diffraction pattern of the class C fly ash.

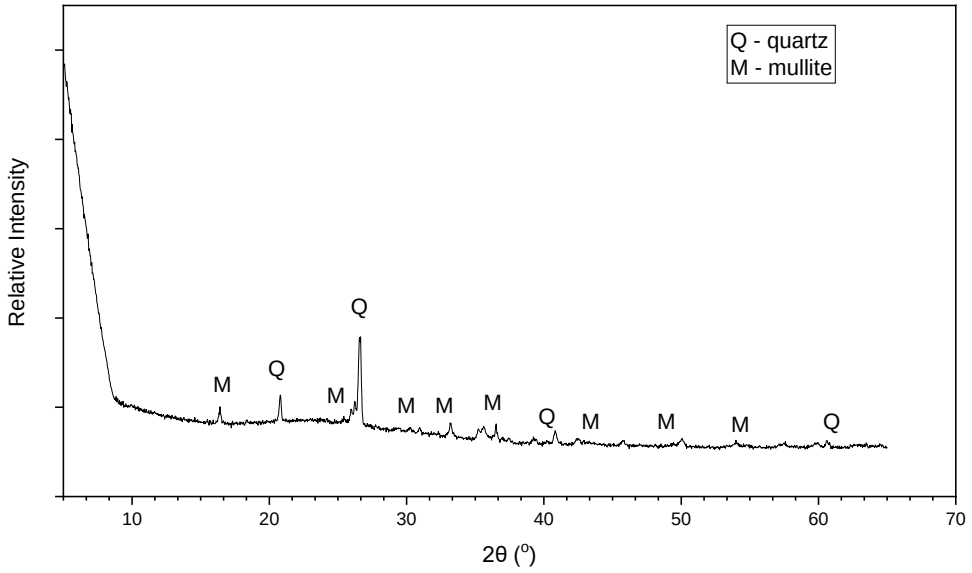

Figure 3.7 X-Ray diffraction pattern of the class F fly ash.

3.2.3 Alkali activators (Sodium silicate and Sodium hydroxide)

Commercially available alkali activators were used in this research. Laboratory grade sodium hydroxide powder with 99% purity was used. Sodium silicate solution was sourced from Fisher Scientific Ltd. in the UK in liquid form. It was composed of 14% Na_2O, 28% SiO_2, and 58% H_2O, by weight. The average molar ratio (SiO_2: Na_2O) of the solution was 2.06.

3.3 Sample Preparation

Control samples and stabilised soil samples were prepared by static compaction using an Instron 3382 Floor Model Universal Loading System for the UCS, triaxial, and one-dimensional consolidation tests. Each layer was compacted by increasing the load at a displacement rate of 2.5 mm/min up to a constant maximum load. The interlocking between layers was achieved by scratching the surface of each compacted layer with a palette. The maximum dry density of the compacted samples was recorded between 13.9–15.2 kN/m^3 based on the different fly ash contents of the stabilised soil samples. The relevant optimum

moisture contents of the control sample and the stabilised soil samples obtained from the standard Proctor tests were used for preparing the samples. After compaction, the samples were sealed and stored in laboratory conditions (23–26 °C) and cured in vacuum desiccators for 1, 7, and 28 days before testing.

Two different mixing methods were applied for the soil samples stabilised with fly ash only, and soil samples stabilised with alkali activated fly ash.

3.3.1 Soils stabilised with class C and class F fly ash

Samples of the soil stabilised with different percentages of class C and class F fly ash (based on the weight of dry soil) were prepared for the tests. The maximum dry density and optimum moisture content of each sample were determined through standard Proctor test. The samples were first mixed to form a homogenous mixture before being compacted based on their relevant optimum moisture contents and were compacted ensuring the desired density was achieved.

3.3.2 Soils stabilised with alkali activated fly ash

For the soils stabilised with alkali activated fly ash, different values of silica modulus used in this study were 1, 1.25, 1.5, and 1.75, while the percentages of alkali dosages were 8%, 12%, 16%, and 20% for the compressive strength investigation. SM is described as the mass ratio of silica to sodium oxide (Na_2O) in the activated solution and M+ is the percentage mass ratio of total Na_2O in the activated solution to the fly ash binder (Soutsos et al, 2016; Rafeet et al, 2017). Fly ash dosage equal to 15% and 25% were investigated. The dosages were selected based on the previous investigations (Turan et al, 2022a).

Two methods have been reported in the literature for mixing the materials. In the first method, the soil and fly ash are premixed, and then alkali solution is added.

In the second method, the fly ash and alkali solution are premixed prior to the addition to the soil. It has been shown that the reaction between fly ash particles, soil particles, and alkali activators, can lead to higher strength following the first method compared to the second method (Leong et al, 2018). Therefore, for the preparation of soil samples stabilised with alkali activated fly ash, the dry soil and fly ash were initially mixed until a homogenous mixture was achieved. Then the mixture of SS and SH solutions, corrected with the required amount of water for achieving the OMC, was added, and further mixing was applied.

The following steps were followed for the preparation of alkali activator solution:

- The required amount of Na_2O was determined based on 8%, 12%, 16%, or 20% of M+ (M+ = Na_2O/fly ash).
- The required amount of SiO_2 was evaluated for SM values of 1, 1.25, 1.5, or 1.75 (SM = SiO_2/Na_2O).
- The required amount of SS solution was determined based on the required SiO_2 (SiO_2 required/SiO_2 % in solution).
- Since the chemical composition of SS includes 14% Na_2O, a corrected amount of Na_2O was determined subtracting the Na_2O already provided with the SS from the total designed amount of Na_2O.
- The shortfall of Na_2O amount was added using SH pellets. Therefore, SH pellets were used to achieve M+ equal to 8%, 12%, 16%, or 20%, considering that the Na_2O content in SH is 77.5%.
- The required amount of SH pellets was dissolved in distilled water to obtain a solution based on the additional water. The additional water content was determined as:

  additional water = water required (OMC) - water in SS solution.

- Finally, the quantities of SH, SS and water determined in the previous steps were mixed, and the resulting activating solution was added to the dry soil-fly ash mixture.

3.4 Experimental Programme

3.4.1 Compaction test

The compaction tests to determine the maximum dry density and optimum moisture content for control samples and the stabilised soil samples were conducted using a standard Proctor machine (BS 1377-4, 1990). For soils stabilised with class C and class F fly ash, 5%, 10%, 15%, 20%, 25%, and 30% fly ash were added to the soil (based on weight of the dry soil). These percentages were selected based on the recommendations from the literature (Cokca et al, 2002; Kumar and Sharma, 2004; Sezer et al, 2006; Phanikumar and Sharma, 2007; Brooks, 2009; Bin Shafique et al, 2009; Seyrek, 2018). For the soils stabilised with alkali activated fly ash, 15% and 25% fly ash were selected as indicated in the sample preparation section 3.3.2.

After the initial mixing of the samples, the compaction was applied without any delay. This is because, MDD can be affected by compaction delays. Mackiewicz and Ferguson (2005) argued that compaction is generally delayed in construction projects. As a result, due to the hydration reaction of fly ash, the reaction products can bond with the soil particles in a loose state and these bonds cause disruption of material during compaction process. For instance, if the compaction is delayed 1 hour after mixing the materials, MDD values could decrease up to 0.6 to 1.6 kN/m^3 (Mackiewicz and Ferguson, 2005). Therefore, the samples were initially mixed and thereafter compacted in 30-45 min to prevent the formation of binders in the soil in the loose state (Figure 3.8).

Figure 3.8 Standard Proctor test equipment.

3.4.2 Unconfined compressive strength test

Control samples and stabilised soil samples were prepared by static compaction with the use of an Instron 3382 Floor Model Universal Loading System for each test (Figure 3.9). The specific optimum moisture contents of the samples, obtained from the Standard Proctor tests (section 3.4.1), were used to prepare the samples. The fly ash percentages were selected from 5% to 30% with an increment of 5% for the soils stabilised with class C and class F fly ash based on the previous investigations as indicated in section 3.4.1. For the soils stabilised with alkali activated fly ash, the fly ash percentages used were 15% and 25%, the SM values used were 1, 1.25, 1.5, and 1.75, the M+ percentages used were 8%, 12%, 16%, and 20% according to the recommendations from the literature (Soutsos et al, 2016; Rafeet et al, 2017).

The samples were 50 mm in diameter and 100 mm in height and were compacted in three layers. Each layer was compacted by ramping the load at a displacement rate of 2.5 mm/min up to a constant maximum load as discussed in section 3.3. In the UCS tests, the samples were loaded between two metal plates at a

displacement rate of 1 mm/min. Each UCS test result was determined from the average of duplicate samples. Figure 3.10 shows the UCS test samples after failure.

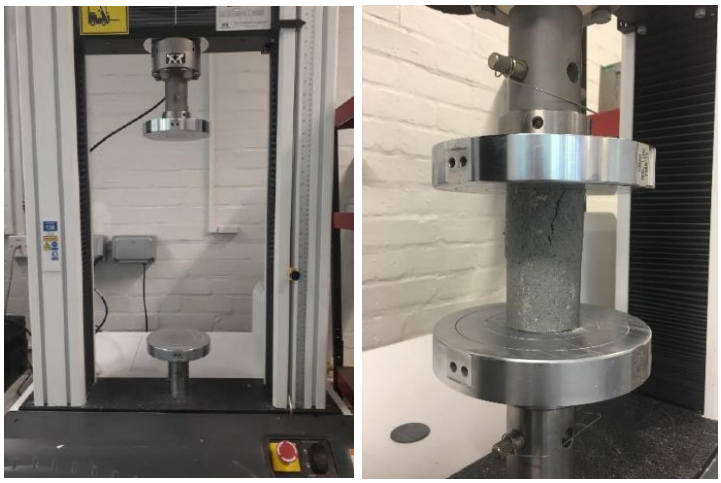

Figure 3.9 Instron testing system.

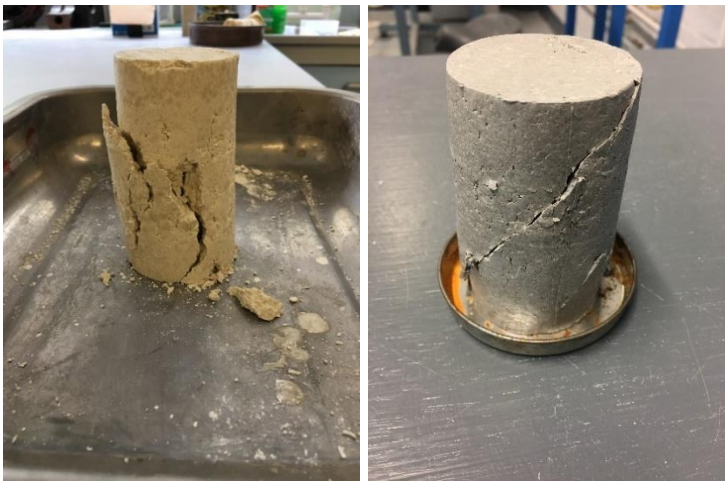

Figure 3.10 Samples after failure – UCS test.

3.4.3 One-dimensional consolidation (oedometer) test

Standard one-dimensional consolidation tests were conducted to evaluate the consolidation properties of the control samples and soils stabilised with class C, class F, and alkali activated fly ash based on BS 1377-5 (1990). According to the UCS test results carried out on soils stabilised with class C and class F fly ash (from 5% to 30% fly ash addition), the fly ash percentages of 15% and 25% were selected for the consolidation tests. Based on the UCS tests, the strength of the

stabilised soils generally decreased after 25% fly ash content. Therefore, 25% fly ash was considered as optimal. Soils stabilised with 15% fly ash were chosen to compare and evaluate the effects of changes in fly ash content from 15% to 25%. The soil samples were prepared by static compaction using Instron 3382 Floor Model Universal Loading System. The samples, 50 mm in diameter and 20 mm in height were prepared in one layer for the 1D consolidation tests. The soil was compacted by ramping the load at a displacement rate of 2.5 mm/min up to a constant maximum load as stated in the UCS tests.

3.4.4 Consolidated-undrained triaxial test

Consolidated undrained triaxial tests were carried out on the control samples and the stabilised soil samples using GDS triaxial apparatus and GDS software (GDSlab v2.8.2.4). The samples were prepared 50 mm in diameter and 100 mm in height by static compaction. For the soils stabilised with fly ash, 15% and 25% fly ash were used (as described in section 3.4.3). The tests were conducted under effective confining pressures (σ'_c) of 200, 400, and 600 kPa. For the soils stabilised with alkali activated fly ash, considering the different combinations of mixtures (different SM, M+, fly ash) that were tested in the UCS section, the mixture that provided the best UCS was selected for triaxial tests. The samples for the triaxial tests were prepared in the same way as the UCS samples.

Two different models of GDS triaxial equipment (Figures 3.11 and 3.12) were used to conduct CU triaxial tests. Figures 3.11 and 3.12 show the models of the triaxial system.

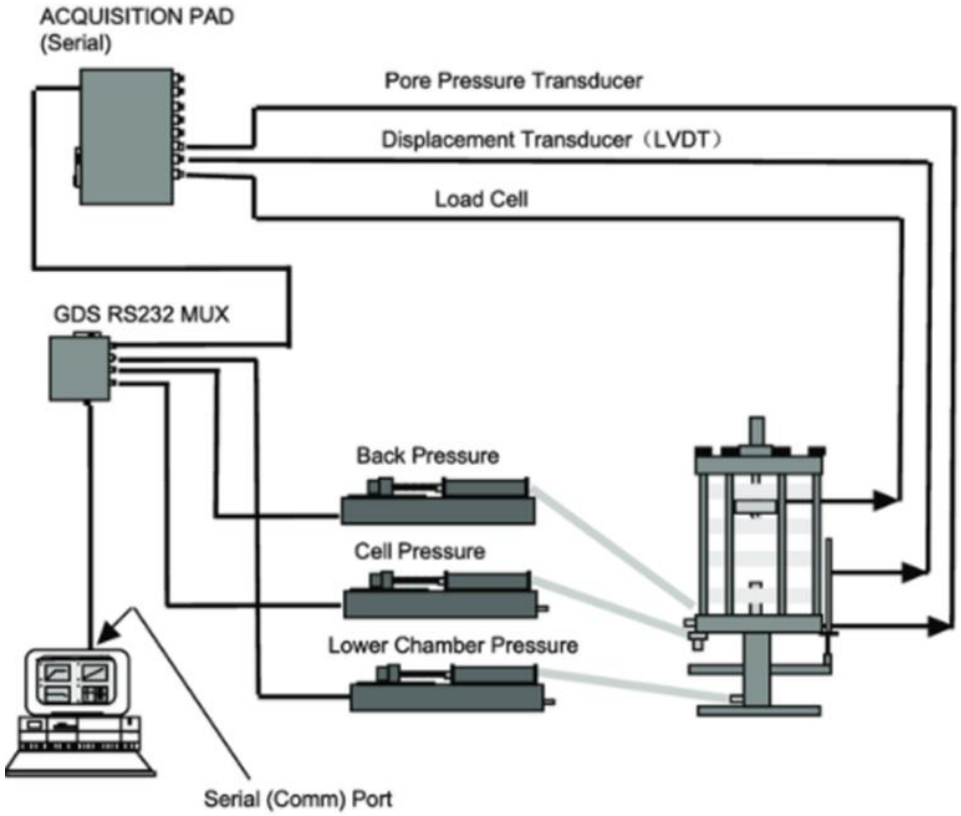

Figure 3.11 GDS triaxial system (Automated stress path type model) (Retrieved from Chen et al, 2018).

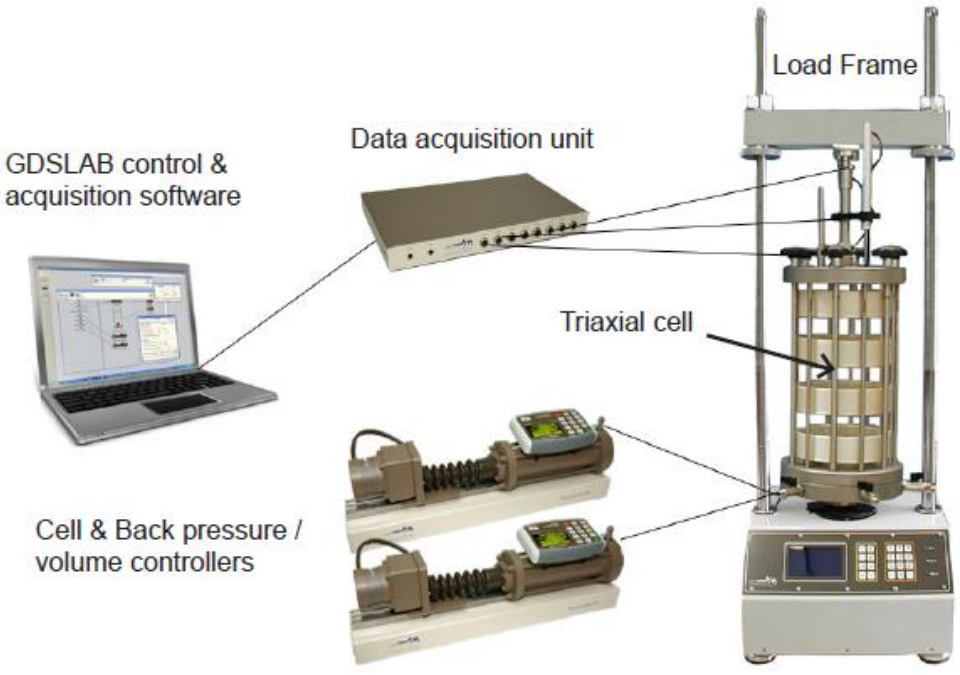

Figure 3.12 GDS triaxial system (Load frame type model) (Retrieved from www.gdsinstruments.com, 2022).

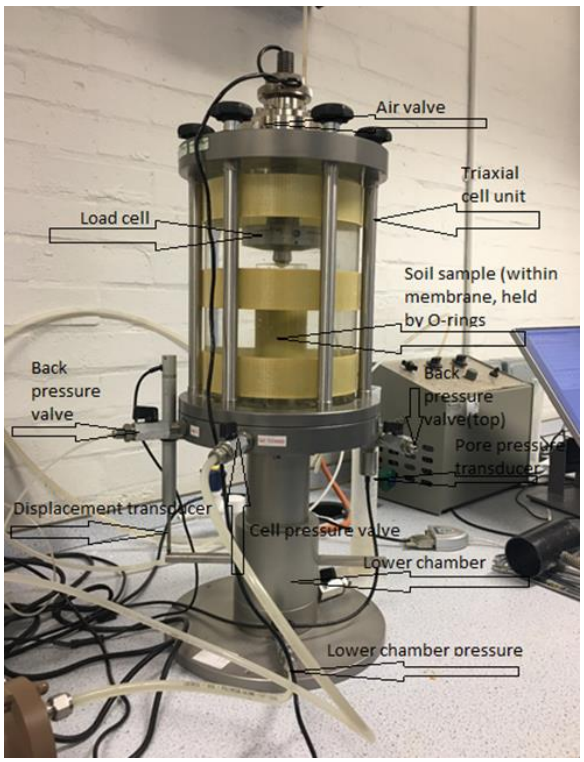

(a)

(b)

Figure 3.13 GDS triaxial system: (a) Automated stress path type model, (b) Load frame type model.

3.4.4.1 Triaxial test stages

- ***Saturation stage***

The aim of the saturation stage is to make sure all voids in the soil sample are filled with water (BS 1377-8, 1990). This can be achieved by raising pore pressure in sample to an appropriate level. Pore pressure can be increased by applying water pressure (back pressure) to sample and increasing the cell pressure at the same time.

The GDS program was set up for the saturation stage, according to the procedures of BS 1377-8 (1990). Cell and back pressures were increased. The cell pressure was set up to 50 kPa, thereafter the increment of cell pressures was applied as 100 kPa. The difference between the cell pressure and back pressure was kept at 20 kPa. For example, the cell pressure was increased to 50 kPa, while the back pressure was increased to 30 kPa for an hour. Then, the cell pressure was increased to 150 kPa, while the back pressure was increased to 130 kPa for 5 hours. The saturation stages were completed after 24 hours. In the final stage of saturation, the cell pressure was 320 kPa and the back pressure was 300 kPa.

After completing the saturation stage, Skempton's B value was determined (B-check) to obtain the degree of saturation. The B-check was performed by increasing the cell pressure ($\Delta\sigma_3$) and recording the corresponding change in the pore pressure (Δu).

$$B = \frac{\Delta u}{\Delta \sigma_3} \tag{3.1}$$

B-value should normally reach 0.95 according to the standards. However, for very stiff soils, it may not be possible to reach this value, therefore a B value of 0.90 would be acceptable (BS 1377-8, 1990). Therefore, the saturation stage was

considered complete when the B value reached between 0.90 and 0.95. Also, the degree of saturation of the samples was examined at the beginning and end of the saturation stage. The initial degree of saturation of samples was determined as (Craig, 2004):

$$S_i = (w_o \times G_s)/e_0 \quad (3.2)$$

The final degree of saturation of samples was estimated based on the relations between pore pressure coefficient B versus degree of saturation graph (Craig, 2004 and Head and Epps, 2014).

Based on the results, the initial degree of saturation was generally found about 82%-85%, whereas the final degree of saturation was between 98%-100%. This indicates the soil samples reached fully saturated soil conditions at the end of the saturation stage.

- ***Consolidation stage***

After obtaining a suitable B-value, the samples were consolidated isotropically. The consolidation stage was applied to bring the sample to the effective stress state required for shearing stage. The effective stress of the sample was increased to the desired value by increasing the cell pressure. The back pressure was maintained constant at the back pressure value in the final step of the saturation stage based on BS 1377-8 (1990). The consolidation stage was maintained for 24 hours until the volume change of the sample was not significant.

- ***Shearing stage***

Before starting the shearing stage, the sample was docked to the top cap, back pressure valve was closed, cell pressure valve was opened, axial displacement and axial strain were set to zero.

During shearing stage, the cell pressure was maintained constant while the soil sample was sheared by applying an axial strain ε_a to the sample at a constant rate of 0.03 mm/min through upward movement of the lower platen. The loading velocity or rate of strain was calculated from the data obtained during the consolidation stage. Based on the ASTM D4767-11 (2020) standard, assuming failure will occur about 15%, a convenient rate of strain can be evaluated as below:

$$\varepsilon = 15\%/(10t_{50}) \tag{3.2}$$

where ε is the rate of strain, t_{50} is a time for 50% primary consolidation.

The t_{50} value was calculated based on the ASTM D2435-11 (2011).

25% axial strain was set to make sure that the samples can reach the critical state. Once the shearing stage was completed, the sample was removed from the membrane and porous discs as quickly as possible to prevent any absorption of water. The sample was weighed and put in the oven for the moisture content determination at the end of the stage.

Figure 3.14 Sheared triaxial samples.

3.4.5 Scanning electron microscopy

Scanning electron microscopy analysis was carried out using of TESCAN VEGA3 SEM detector (Figure 3.15) to observe the microstructural alterations of the soils stabilised with 15% and 25% fly ash, and soils stabilised with 15% and 25% alkali activated fly ash (with the best combinations of M+ and SM). Accelerating voltage of 10 kV and beam intensity of 10 were selected for each sample in this thesis. The SEM images were taken at 20 μm for the analysis.

Prior to the SEM analysis, the dried samples were mounted on the stubs using carbon tape and coated. The soil samples were coated to obtain higher conductivity and therefore higher quality images using the Quorum Q150 TES sputter coater. The sputter coating was done with 20 nm thickness and the samples were coated with a chromium material.

Figure 3.15 Scanning electron microscope (outside and inside views).

3.4.6 X-Ray diffraction

XRD analysis was conducted to obtain the phase composition and mineralogy of the control sample, fly ash, soils stabilised with 15% and 25% fly ash and soils stabilised with 15% and 25% alkali activated fly ash (with the best combination of M+ and SM) using the Bruker D8 advanced diffractometer. The samples were

analysed through CuKα radiation operated at 40 mA and 40 kV with 2θ range of 5^{o} to 65^{o} in a step size of 0.02^{o}. The XRD patterns were analysed using Diffrac.EVA software with the 2017 reference database.

Chapter 4 Results and Discussions

4.1 Soils stabilised with class C and class F fly ash

4.1.1 Overview

The review of the literature section 2.1 suggested that stabilisation of soil with fly ash has great potential for improving the mechanical and physical properties of geomaterials. Common tests used for the study of fly ash stabilised soils are UCS, free swell index, consistency limits, and CBR tests. However, little information is available on shear and consolidation behaviour of fly ash-stabilised clay soils. Furthermore, previous studies did not fully clarify the different effects of using class C fly ash and class F fly ash on shear, consolidation, and microstructural behaviour of stabilised soils. Therefore, there is a need to improve the fundamental understanding of how class C and class F fly ash affect the overall shear, consolidation, and microstructural behaviour on soils.

This section presents a comparison of class C and class F fly ash in stabilisation of a clay soil (kaolinite). Their effects are evaluated through a programme of laboratory tests including compaction, UCS, consolidated-undrained (CU) triaxial, one-dimensional consolidation (oedometer) tests, and scanning electron microscopy (SEM) analysis. The outcome of the study will improve the current understanding of the effects of class C and class F fly ash on the mechanical behaviour and microstructural characteristics of the stabilised soils. It will also help to determine and compare the suitability of class C and class F fly ash as alternative soil stabilising agents and to identify the optimal amounts of two types of fly ash for stabilisation of clay soil.

4.1.2 Compaction tests

Compaction tests were carried out on samples with increasing fly ash content up to a maximum dosage of 30% of fly ash (by weight of the soil). The compaction curves and results of the control sample and the soil samples stabilised with class C and class F fly ash are shown in Figure 4.1(a-b) and Table 4.1. The results show that maximum dry density (MDD) decreased and optimum moisture content (OMC) increased with the increase of the class C or class F fly ash content. This trend is similar to that found by other researchers (Ji-Ru and Xing, 2002; Prabakar et al, 2004; Senol et al, 2006; Mir and Sridharan, 2013; Kolay and Ramesh, 2015; Savas et al, 2018; Seyrek, 2018). The decrease in MDD with the addition of fly ash might be due to the lower specific gravity of fly ash than kaolinite (Shil and Pal, 2015; Savas et al, 2018; Barisic et al, 2019). The specific gravities of class C and class F fly ash were found to be 2.4 and 2.32, respectively. Therefore, the decrease of MDD was smaller for the soil samples stabilised with class C fly ash compared to class F fly ash. Agglomeration and flocculation can be occurred due to the cation exchange reaction which resulted in a change of gradation in the stabilised soil samples (Dahale et al, 2017; Nath et al, 2017). This could be another reason for the decrease in MDD. Seyrek (2018) argued that the immediate formation of cementitious products could decrease the value of MDD in stabilised soil. According to Mir and Sridharan (2013), the increase in OMC with the addition of fly ash is due to the presence of some large and hollow spheres in fly ash situated in stabilised soil.

It is seen from Figures 4.1(a-b) that by increasing the fly ash content, the compaction curves shift to the bottom right of the graph. The OMC and MDD changed from 21% and 15.2 kN/m^3 for kaolinite to 25.8% and 14.2 kN/m^3 with

30% of class C fly ash, and to 28.2% and 13.9 kN/m^3 with 30% class F fly ash addition. Also, the compaction curves for the stabilised soil with 15%, 20%, and 25% class C fly ash showed shallower peak in comparison with kaolinite. The shallow curve indicates that the soil samples stabilised with 15%, 20%, and 25% class C fly ash did not show significant change over a wide range of water content. However, this trend (shallow compaction curves) was not observed for the soil stabilised with class F fly ash. Hence, it can be said that soils stabilised with class C fly ash are more adaptable in field applications than soils stabilised with class F fly ash.

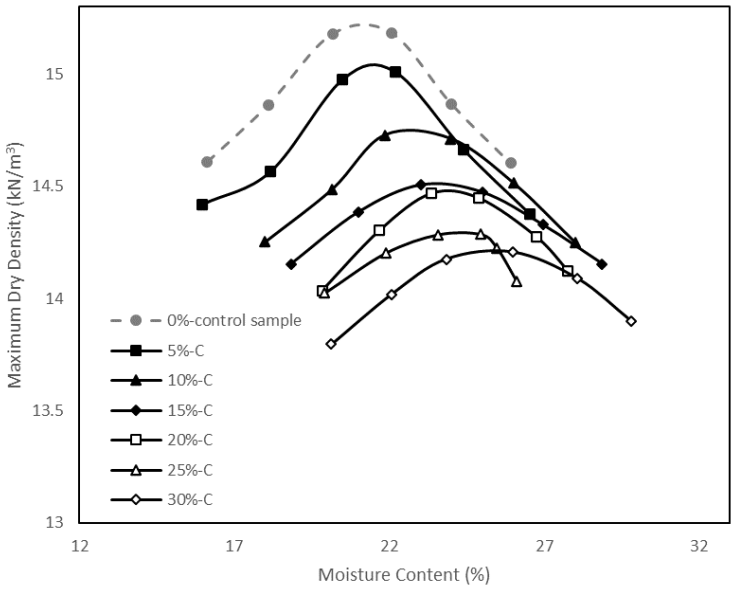

(a)

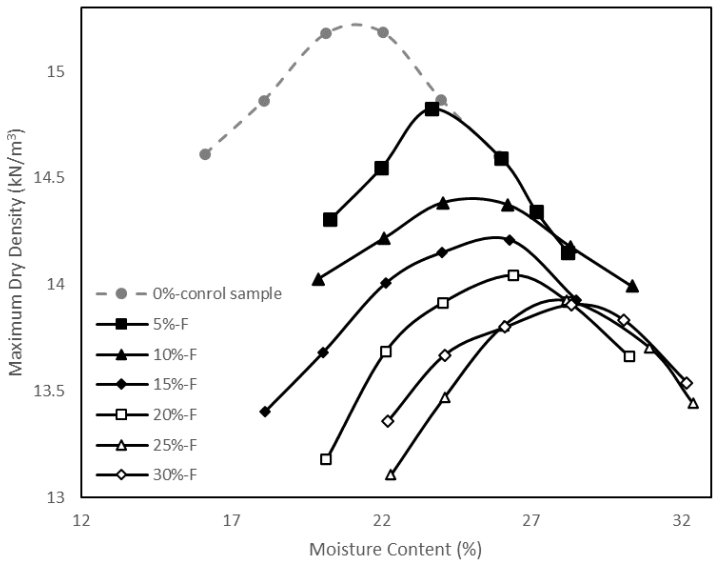

(b)

Figure 4.1 Compaction curves for control sample and soils stabilised with (a) class C fly ash and (b) class F fly ash.

Table 4.1 Maximum dry density and optimum moisture content results for control sample and soils stabilised with class C and class F fly ash.

	class C		class F	
Fly ash content	γ_{dmax} (kN/m^3)	w_{opt} (%)	γ_{dmax} (kN/m^3)	w_{opt} (%)
0%	15.2	21.0	15.2	21.0
5%	15.0	21.4	14.8	23.8
10%	14.7	22.6	14.4	25.0
15%	14.5	23.4	14.2	25.2
20%	14.5	24	14.0	26.0
25%	14.3	24.2	13.9	28.0
30%	14.2	25.8	13.9	28.2

4.1.3 Unconfined compressive strength tests

The relationship between the unconfined compressive strength (q_u) and the fly ash content for different curing periods is presented in Figures 4.2(a-b). The test results clearly demonstrate that the compressive strength increased with increasing the curing time for both types of fly ash (Table 4.2). However, the effect of class C fly ash on the strength of the soil with 7 and 28 days of curing was much higher in comparison with class F fly ash. A similar trend was reported by Seyrek (2018). It is generally accepted that the higher the CaO/SiO_2 ratio in fly ash, the greater the unconfined compressive strength and resilient modulus

(Tastan et al, 2011). The class C fly ash used in the present study had a higher CaO/SiO_2 ratio (32.4%/28.3%) and hence gave a higher compressive strength than the class F fly ash with ratio of 2.2%/46.8%. Furthermore, mineralogical analysis confirmed a non-negligible presence of lime which has self-cementing properties, in the class C fly ash. Also, anhydrite in class C fly ash reacts with water and produces gypsum which has binding effects. On the other hand, class F fly ash does not have enough cementitious properties because of the low calcium content, and thus, it does not give a strong reaction with soil (Dahale et al, 2017).

For both fly ash types and all curing times, the maximum value of unconfined compressive strength was found with 25% fly ash, and it showed a decrease from 25% to 30% fly ash, except for mixtures with class C fly ash at 1 day of curing (Table 4.2). These results are consistent with those reported by Dahale et al (2017) and Seyrek (2018). The unstabilised (control) soil samples had maximum axial stresses of 175 kPa, 180 kPa, and 204 kPa at 1, 7, and 28 days of curing, respectively. The results for control sample cured at different ages are very similar, as expected. For the soils stabilised with class C fly ash, the peak stresses were 294 kPa with 30% fly ash at 1 day of curing, 506 kPa with 25% fly ash at 7 days of curing, and 593 kPa with 25% fly ash at 28 days of curing. For the soils stabilised with 25% class F fly ash, the peak stresses were found to be 246 kPa at 1 day of curing, 259 kPa at 7 days of curing, and 325 kPa at 28 days of curing. When the class C fly ash content was increased from 25% to 30%, the maximum axial stresses decreased from 506 kPa to 490 kPa at 7 days of curing and from 593 kPa to 503 kPa at 28 days of curing. For the same increase in the fly ash content (from 25% to 30%), the maximum axial stresses recorded on

samples of soil stabilised with class F fly ash decreased from 246 kPa to 212 kPa at 1 day of curing, from 259 kPa to 187 kPa at 7 days of curing, and from 325 kPa to 274 kPa at 28 days of curing. The unconfined compressive strength was determined based on the average of two samples. Repeatability of the UCS test results was considered to be acceptable within a margin of coefficient variation (up to 3% differences), providing a good reproducibility on the samples (BS ISO 21748, 2017; Diambra, 2010). Typical results of soils stabilised with class C fly ash at 1 day curing are presented in Table 4.3.

It can be concluded that class C fly ash was more effective in improving the compressive strength of the soil than class F fly ash. In addition, the curing time is an effective parameter in improving the strength and behaviour of stabilised soil with class C and class F fly ash owing to their pozzolanic characteristics.

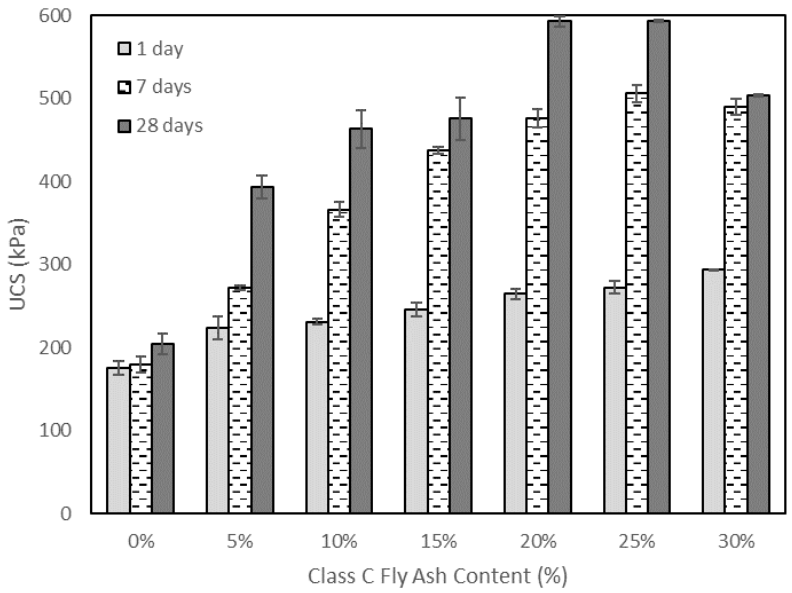

(a)

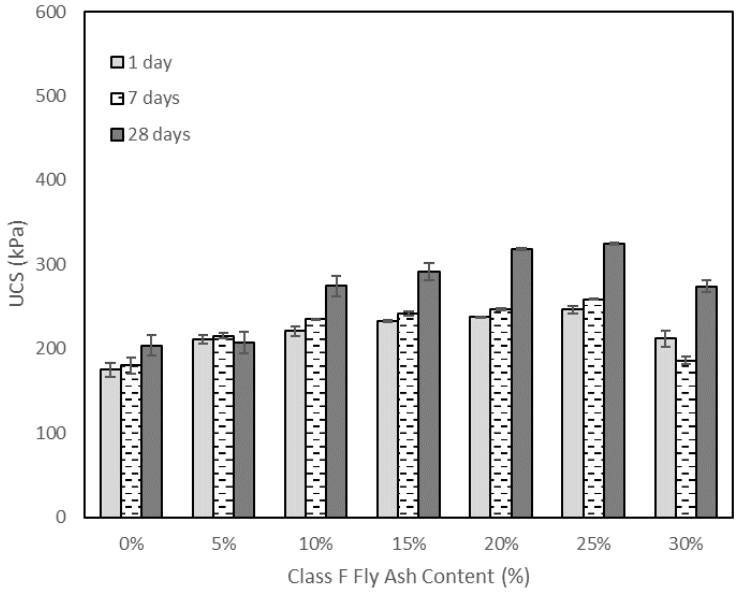

(b)

Figure 4.2 Effects of (a) class C and (b) class F fly ash contents on unconfined compressive strength with 1 day, 7 days, and 28 days of curing.

Table 4.2 Unconfined compressive strength results for soils stabilised with class C and class F fly ash with 1 day, 7 days, and 28 days of curing.

	1 day curing	7 days curing	28 days curing
Fly ash content	Unconfined Compressive Strength (kPa)		
0% (control sample)	175	180	204
5% class C	224	272	393
10% class C	231	366	463
15% class C	246	438	476
20% class C	265	476	592
25% class C	272	506	593
30% class C	294	490	503
5% class F	211	215	207
10% class F	221	235	275
15% class F	233	242	292
20% class F	238	247	318
25% class F	246	259	325
30% class F	212	187	274

Table 4.3 Results from repeatability tests for UCS (1 day curing-class C fly ash)

Fly ash content (%)	0%	5%	10%	15%	20%	25%	30%
1st results (kPa)	178.1	220.7	227.8	240.5	258.3	278.2	294.5
2nd results (kPa)	172.8	226.2	234.7	250.6	270.7	266.3	293.5
Mean results (kPa)	175.5	223.5	231.3	245.6	264.5	272.3	294.0
Standard deviation	3.7	3.9	4.8	7.1	8.8	8.4	0.7
Coefficient of variation (%)	2.1	1.7	2.1	2.9	3.3	3.1	0.2

The values of elastic modulus (E) for the soils stabilised with class C and class F fly ash, obtained from the results of the UCS tests at 1, 7 and 28 days of curing are presented in Table 4.4. The elastic modulus was determined as the slope a tangent line of the linear part of the stress-strain curve (Zhang et al, 2013). The results indicate that, in general, for both types of fly ash, the elastic modulus increased with increasing the fly ash content up to 25%, beyond which, further increases in fly ash content resulted in decrease in elastic modulus. However, the effect of class C fly ash in increasing the elastic modulus of the stabilised soil was greater than class F fly ash. It can be deduced that the improvement of the stiffness of the soil stabilised with class C fly ash is significant.

Table 4.4 Elastic modulus of class C and class F fly ash stabilised soil from UCS tests with different curing times.

	1 day curing	7 days curing	28 days curing
Fly ash content	Elastic Modulus (E) (MPa)		
0% (control sample)	5.9	9.5	9.4
5% class C	16.5	21.3	23.1
10% class C	20.2	25.9	39.1
15% class C	25.2	33.7	42.6
20% class C	25.4	51.0	62.9
25% class C	26.2	53.6	64.9
30% class C	27.5	35.0	37.5
5% class F	8.8	12.5	14.7
10% class F	9.0	13.5	18.2
15% class F	14.0	14.1	21.0
20% class F	14.8	16.8	21.3
25% class F	18.5	21.2	24.8
30% class F	14.8	9.0	14.6

4.1.4 Triaxial tests

4.1.4.1 Effects of fly ash on the stress-strain behaviour

Figures 4.3(a–c) show the deviator stress (q) - axial strain (ε_a) behaviour of the control sample and the soil samples stabilised with 15% and 25% class C and class F fly ash, cured for 1, 7, and 28 days, at 600 kPa effective confining pressure (σ_c'). It is seen that at a given axial strain, the deviator stress of the soil stabilised with both types of fly ash increased with increasing the fly ash content.

This trend is consistent with the findings from Prabakar et al (2004). However, a smaller improvement was observed with the class F fly ash compared to the class C fly ash. For both types of fly ash stabilised soil, the deviator stress increased by increasing the curing time. In addition, there was a significant increase in the deviator stress at 28 days of curing for the soils stabilised with class C fly ash, and the stress-strain curve showed a brittle post-peak strain-softening response (Figure 4.3c) compared to the generally observed post-yield ductile behavior in soils stabilised with class C fly ash at 1 day and 7 days of curing (Figures 4.3(a-b)). The results also show that for the soil stabilised with class C fly ash with 28 days of curing, the axial strain corresponding to the peak deviator stress decreased. For example, in the control sample the peak deviator stress (q_{max}) reached 359 kPa at around 11% axial strain, while in the soil stabilised with 25% class C fly ash, the sample reached the q_{max} of 889 kPa at around 2% axial strain. This could be that the cementitious properties of class C fly ash produced stiff bridges in the soil structure, and lower strains were enough to break such bridges.

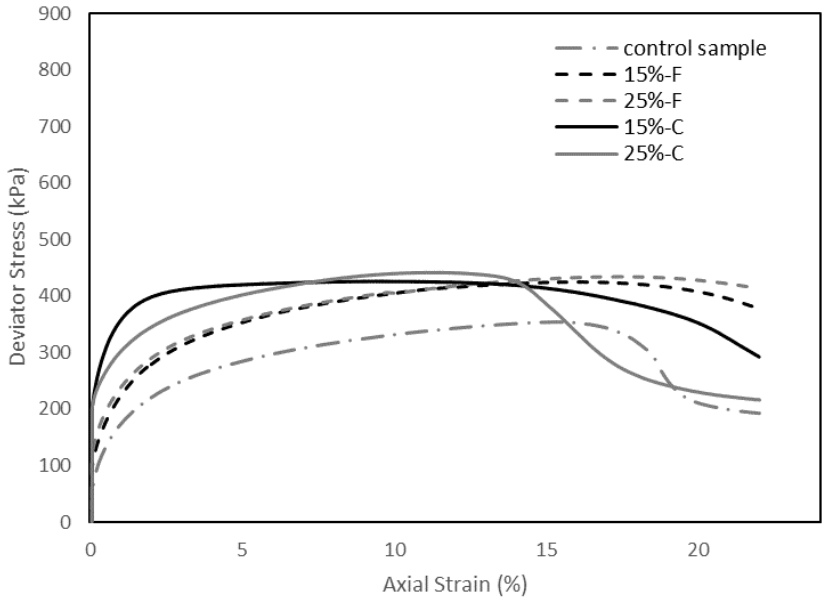

(a)

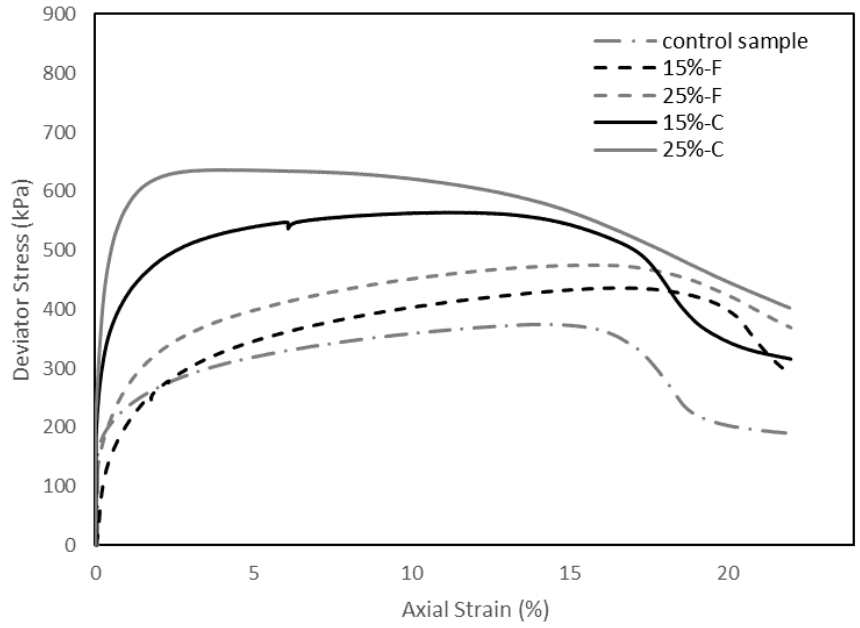

(b)

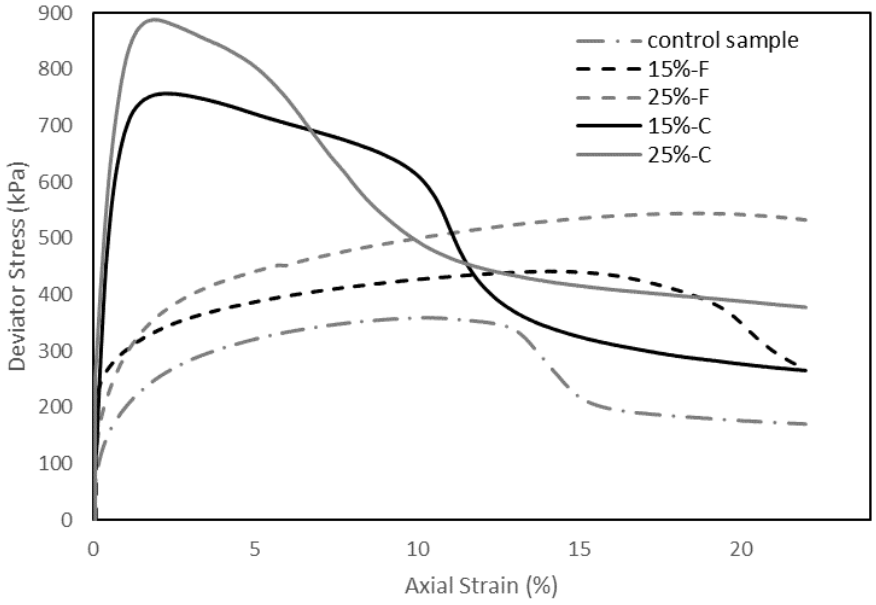

(c)

Figure 4.3 Stress-strain behaviour of control sample and soils stabilised with class C and class F fly ash at a confining pressure of 600 kPa at (a) 1 day of curing, (b) 7 days of curing, (c) 28 days of curing.

Figures 4.4(a–c) show the deviator stress-axial strain behaviour of the control samples, and the soil samples stabilised with 25% class C and class F fly ash at 200, 400, and 600 kPa confining pressures, cured for 1, 7, and 28 days, respectively. In general, the deviator stress of the soils stabilised with both types of fly ash increased with increasing the effective confining pressure at all curing times. This is because higher confining pressure during the consolidation stage decreases the void ratio, hence increasing the strength of the soil. The soil samples stabilised with class F fly ash generally showed a similar ductile stress-strain response with the increase of confining pressure. On the other hand, for the samples stabilised with class C fly ash at 1 and 7 days of curing, the stress-strain response changed from ductile to slightly brittle strain-softening behaviour with increasing the confining pressure (except for the sample tested at 400 kPa confining pressure and 1 day of curing). For the samples stabilised with class C fly ash at 28 days of curing, a brittle strain-softening behaviour was observed for all confining pressures. However, the samples showed higher peaks and became more brittle with increasing the confining pressure. The reason for the brittle strain softening behaviour is a slight destructuration that occurs in the class C fly ash stabilised soil during the consolidation stage, leading to the behaviour governed by cementitious bonds and friction (Abdullah et al, 2019a).

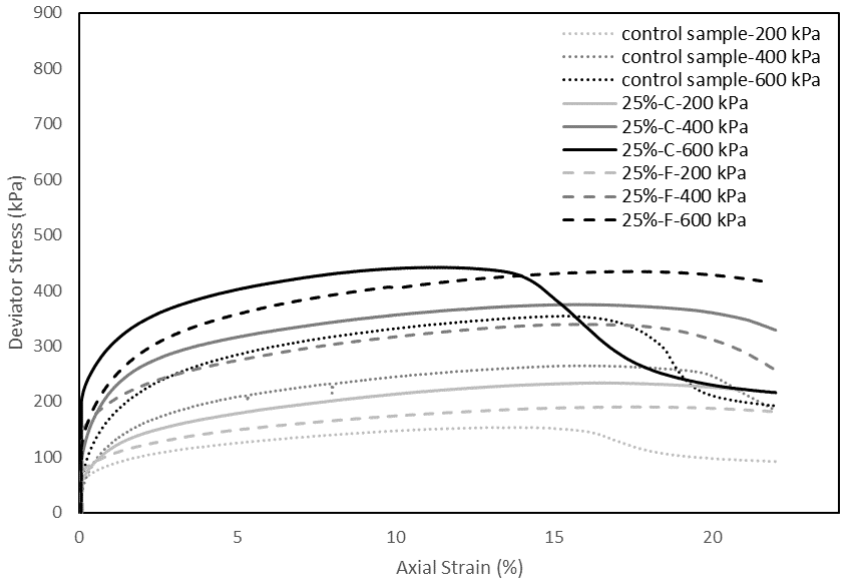
900
800
700
600
500
400
300
200
100
0
Deviator Stress (kPa)
0
5
10
15
20
Axial Strain (%)
control sample-200 kPa
control sample-400 kPa
control sample-600 kPa
25%-C-200 kPa
25%-C-400 kPa
25%-C-600 kPa
25%-F-200 kPa
25%-F-400 kPa
25%-F-600 kPa

(a)

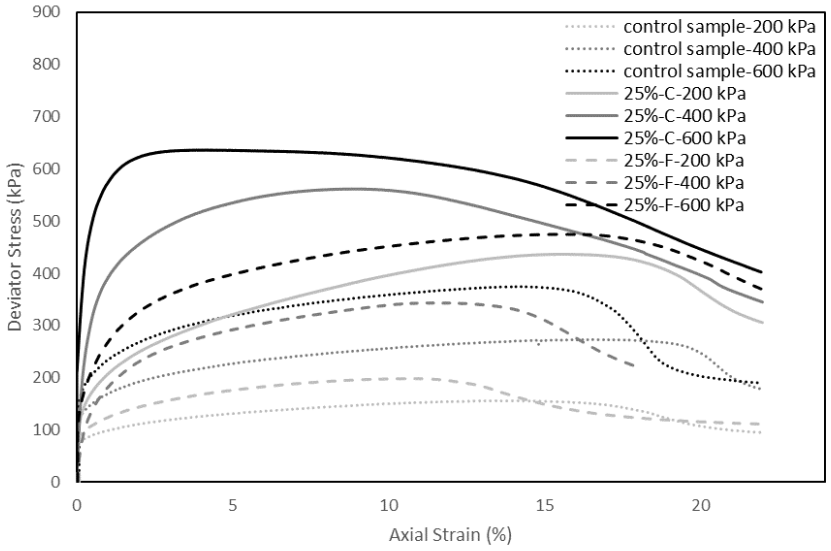
900
800
700
600
500
400
300
200
100
0
Deviator Stress (kPa)
0
5
10
15
20
Axial Strain (%)
control sample-200 kPa
control sample-400 kPa
control sample-600 kPa
25%-C-200 kPa
25%-C-400 kPa
25%-C-600 kPa
25%-F-200 kPa
25%-F-400 kPa
25%-F-600 kPa

(b)

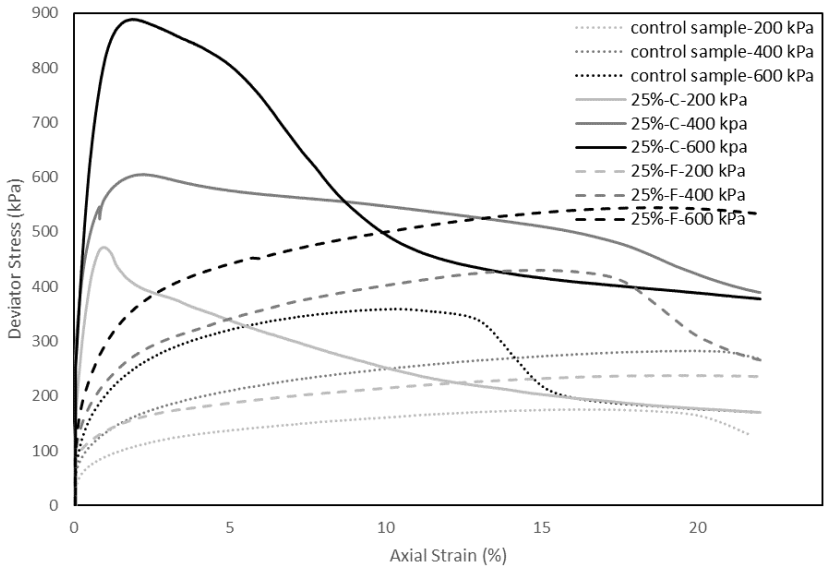

(c)

Figure 4.4 Stress-strain behaviour of control sample and soil samples stabilised with 25% of class C and class F fly ash at confining pressures of 200, 400, and 600 kPa at (a) 1 day of curing, (b) 7 days of curing, (c) 28 days of curing.

4.1.4.2 Effects of fly ash on the shear strength parameters of soil

The shear strength parameters of the soil were obtained from the Mohr–Coulomb failure criterion. Mohr circles were plotted for the control and stabilised soil samples at three different effective confining pressures.

The values of the effective angle of shearing resistance (φ') and effective cohesion (c') are shown in Table 4.5 for the control sample and the samples of soil stabilised with both types of fly ash at 1, 7, and 28 days of curing. The results indicate that the value of c' increased with the addition of class C fly ash. These results agree with the observations made by other researchers (e.g., Sezer et al, 2006; Binal, 2016). For the soil stabilised with class C fly ash, the increase in c' was significant with the increase in curing time. On the other hand, the cohesion of the soil stabilised with class F fly ash was lower than the control sample at 1, 7, and 28 days of curing, although the cohesion of the stabilised soil samples increased with the curing time due to the pozzolanic reactions. This is because

class F fly ash has silty characteristic and includes very low reactive calcium content. Hence, when the cohesionless fly ash mixes with the clay, the structure of the clay changes, leading to the decrease in cohesion. However, for the soil samples stabilised with class C fly ash, the chemical reaction between cementitious class C fly ash and clay has a significant effect in improving the cohesion even though the fly ash is cohesionless. The reason for the higher cohesion value in class C fly ash and lower value in class F fly ash could be the variation of the amounts of cementitious compounds in the soils stabilised with the two types of fly ash.

The values of the effective angle of shearing resistance increased with the addition of both types of fly ash. However, class C fly ash was more effective in comparison with class F fly ash in improving the effective angle of shearing resistance due to its chemical nature. According to Bryson et al (2017), the increase of φ' is related to the particle substitution. The silty characteristic of fly ash decreased the clay fraction and increased the average grain size of the mixture. This contributed to improving the angle of shearing resistance. In addition, the φ' value of the stabilised soils increased with the increase in curing time. This is because the self-hardening and pozzolanic properties of fly ash become more pronounced with curing. Sezer et al (2006) also indicated that the loss of moisture from soil during curing may cause an increase in the value of φ'. However, this statement is not applicable for this study. This is because the samples were stored in vacuum desiccators during curing, hence moisture loss in samples was not observed.

Table 4.5 Shear strength parameters of control and fly ash stabilised soil samples with different curing times.

Fly ash content (%)	Curing days	c'	φ'
0%	1	17.5	18.1
0%	7	18.5	19.6
0%	28	19.0	18.4
15 % class C	1	15.6	21.4
15 % class C	7	43.0	21.8
15 % class C	28	86.6	22.5
25 % class C	1	20.2	21.8
25 % class C	7	77.8	23.0
25 % class C	28	99.1	24.0
15 % class F	1	2.7	20.7
15 % class F	7	4.9	21.1
15 % class F	28	11.1	22.3
25 % class F	1	8.4	21.6
25 % class F	7	10.1	21.6
25 % class F	28	15.1	22.4

Figures 4.5(a–c) show the control sample and the class C fly ash stabilised soil samples with clear shear failure through the samples. The samples reached critical state during the shearing stage of the triaxial tests.

(a) (b) (c)

Figure 4.5 Sheared triaxial samples of: (a) the pure clay (control sample); (b) 15% class C fly ash-stabilised clay; (c) 25% class C fly ash-stabilised clay.

4.1.4.3 Effects of fly ash on the critical state parameters

Figures 4.6(a-c) show the critical state lines (CSL) of the control sample and the samples of the soil stabilised with 15% and 25% class C and class F fly ash cured for 1, 7, and 28 days. Based on the results, the gradient of the CSL (M) increased with increasing the fly ash content for both types of fly ash and with increasing the curing time. There was a greater improvement in the value of M for the soil

stabilised with class C fly ash in comparison with the soil stabilised with class F fly ash for all curing times. The parameter M is directly related to the angle of shearing resistance (Schofield and Wroth, 1968) and indicates the relationship between soil particles and their geometry. It can be said that the increase in angle of shearing resistance with class C fly ash content is because class C fly ash has high cementitious properties and a certain amount of cement is necessary to react with the clay to obtain stiffer cementitious soil matrix, hence, higher improvement in the value of M was observed with the class C fly ash content and lower improvement with the class F fly ash. Subramaniam et al (2015) reported similar observations for M value for a clay soil stabilised with low cement content. The results also indicate that the y-intercept of the critical state lines in the space of deviator stress versus mean effective stress, increased with the addition of class C fly ash for all curing times (except the soil sample stabilised with 15% class C fly ash at 1 day curing). The y-intercept of the CSL is related to cohesion and is a result of cementation (Robin, 2014). It could be concluded that class C fly ash gave higher reaction due to the higher calcium content.

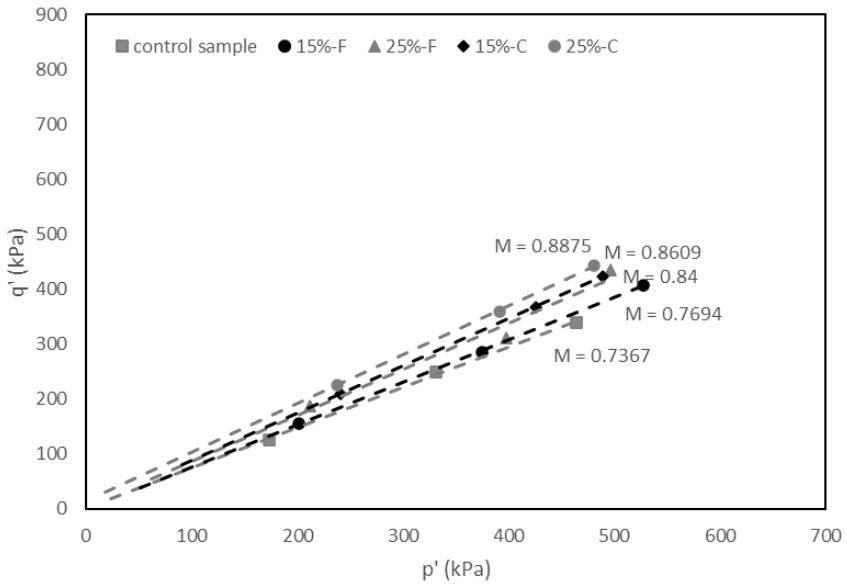

(a)

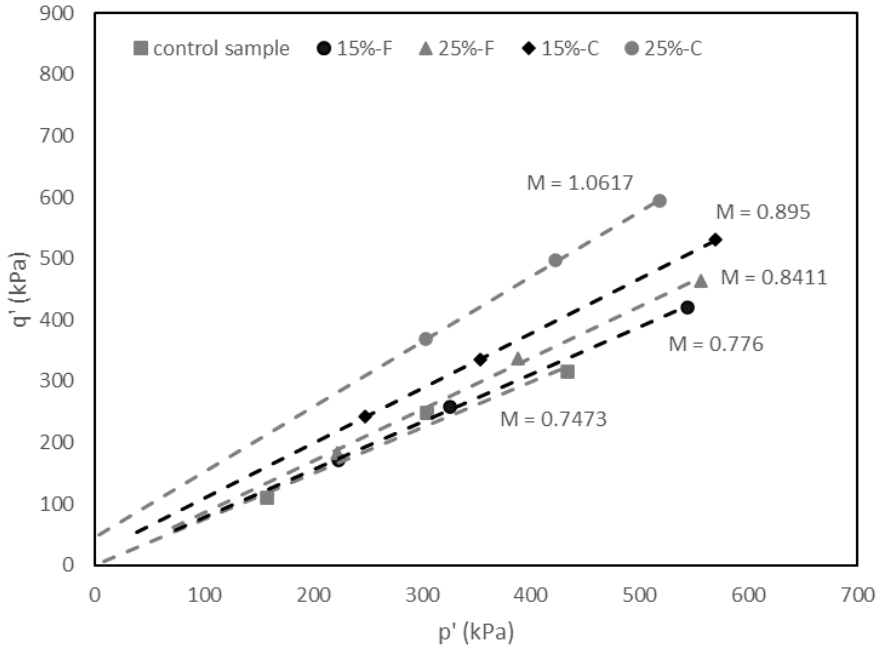

(b)

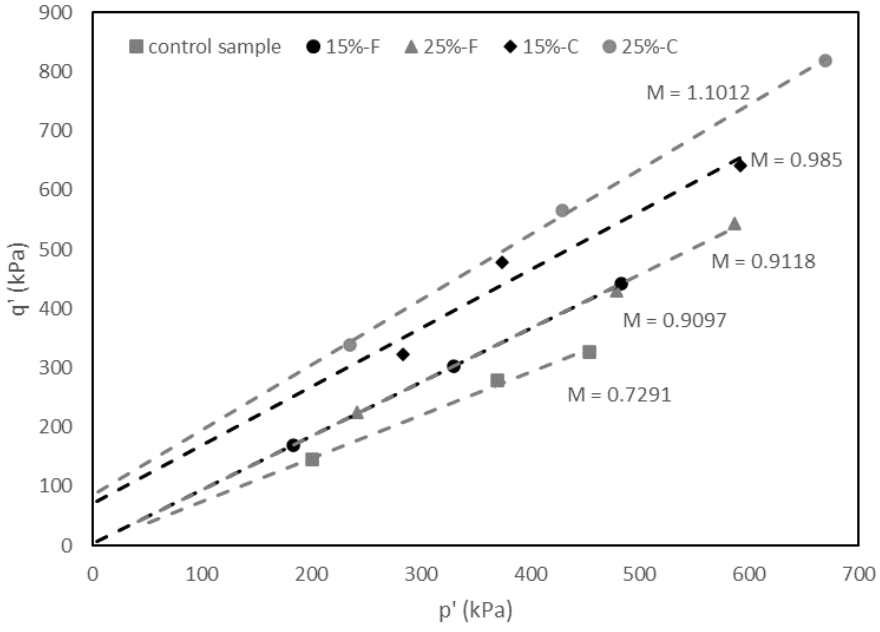

(c)

Figure 4.6 Critical state lines for the control sample and the soil samples stabilised with class C and class F fly ash at: (a) 1 day of curing, (b) 7 days of curing, (c) 28 days of curing.

4.1.5 One-dimensional consolidation tests

One-dimensional consolidation tests were carried out to evaluate the effects of fly ash on the consolidation characteristics of the soil including compression index (C_c), swelling index (C_s), volume compressibility (m_v), coefficient of consolidation (c_v), and permeability (k).

The compression index is an important parameter for determining the consolidation settlement of soft ground. Table 4.6 shows the variation of values of C_c and C_s with different fly ash contents and curing times. The results show that the value of C_c of the soil decreased with increasing the class C fly ash content. This is consistent with the results reported in the literature (Kolay and Ramesh, 2015; Bryson et al, 2018; Amiralian et al, 2012a). After the cation exchange reaction between class C fly ash and clay, the flocculation and aggregation of the soil increase. This improves the vertical effective yield stress and reduces the compressibility of the soil (Ho et al, 2010). In this way, the addition of fly ash decreases the settlement of the soil. However, the compression index of the soil stabilised with 15% class F fly ash (at 1 day of curing) increased (compared with the control sample) and then showed a decrease with increasing the fly ash content to 25%.

The compression index decreased with the increase of curing time for both types of fly ash. This could be attributed to the pozzolanic characteristics of fly ash. When the pozzolanic reaction starts, cementitious particles gradually fill and reinforce the interparticle voids. Thus, the stabilised soil would be less compressible as it cures (Chew et al, 2004).

The results also indicate that the addition of fly ash and the increase of curing time reduced the C_s of the soil (Table 4.6). This trend agrees well with the findings

of Kolay and Ramesh (2015), Bryson et al (2017), and Amiralian et al (2012a). According to Prabakar et al (2004), the non-expansive characteristics of fly ash, and the shape and size of the particles of fly ash lead to the decrease of swelling characteristics.

The results summarised in Table 4.6 also show that that class C fly ash had a better contribution to decreasing the compression and swelling indices of the soil compared to class F fly ash.

Table 4.6 Effects of fly ash and curing time on compression and swelling indices.

Fly Ash Content (%)	Curing days	Compression index (Cc)	Swelling index (Cs)
0 % (unstabilised)	1	0.277	0.054
0 % (unstabilised)	7	0.256	0.046
0 % (unstabilised)	28	0.270	0.046
15 % class C	1	0.164	0.038
15 % class C	7	0.156	0.022
15 % class C	28	0.140	0.015
25 % class C	1	0.154	0.037
25 % class C	7	0.139	0.021
25 % class C	28	0.123	0.015
15 % class F	1	0.288	0.046
15 % class F	7	0.187	0.043
15 % class F	28	0.161	0.037
25 % class F	1	0.227	0.045
25 % class F	7	0.185	0.043
25 % class F	28	0.153	0.029

The coefficient of volume compressibility (m_v) represents the amount of change in unit volume due to a unit change in effective stress:

$$m_v = \frac{\Delta e}{\Delta \sigma'} \frac{1}{1+e_0} \quad (4.1)$$

where $\Delta e/\Delta \sigma'$ is the slope of the e/σ' curve (Whitlow, 1996).

The variations of m_v with different fly ash contents and curing times are illustrated in Figures 4.7(a-b) and 4.8(a-b). Figures 4.7(a-b) show the changes in volume compressibility with the applied effective stress for the control sample and the soil samples stabilised with fly ash at 1, 7, and 28 days of curing. Figure 4.8(a-b) shows the variation of volume compressibility with the fly ash content for an

effective pressure of 80 kPa at different curing time. The results show that for both types of fly ash the value of m_v decreased with increasing fly ash content and curing time. For an effective stress of 80 kPa, the values of m_v for the control sample were 1.14, 1.05, and 1.11 m^2/MN at 1, 7, and 28 days of curing, respectively. The results are expected to be similar in the absence of any reaction for control samples at all curing times. For the soil stabilised with class C fly ash, the results indicated a decrease of 0.61, 0.58 and 0.53 m^2/MN for 15% fly ash, and 0.57, 0.51, and 0.46 m^2/MN for 25% fly ash at 1, 7, and 28 days of curing, respectively (Figure 4.8a). However, for the soil stabilised with class F fly ash, the m_v value slightly increased from 1.14 m^2/MN to 1.15 m^2/MN when fly ash content was increased from 0% to 15% at 1 day of curing. Thereafter, the values of m_v decreased to 0.73 and 0.62 m^2/MN for 15% fly ash at 7 and 28 days, and 0.86, 0.71 and 0.58 m^2/MN for 25% fly ash at 1, 7 and 28 days of curing, respectively (Figure 4.8b).

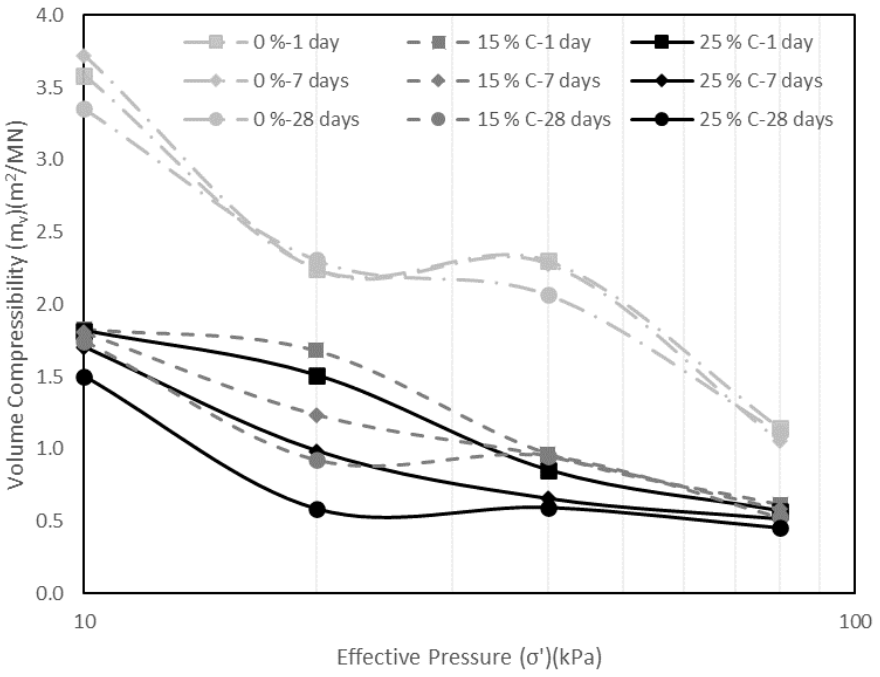

(a)

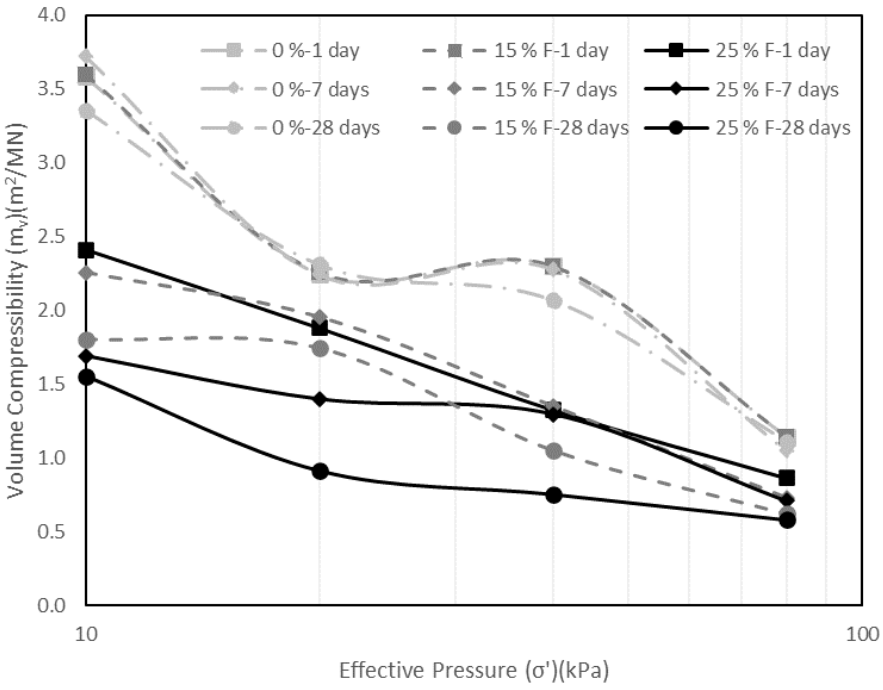

(b)

Figure 4.7 Variation of coefficient of m_v with effective stress (σ') for: (a) different class C fly ash contents, (b) different class F fly ash contents, and curing times.

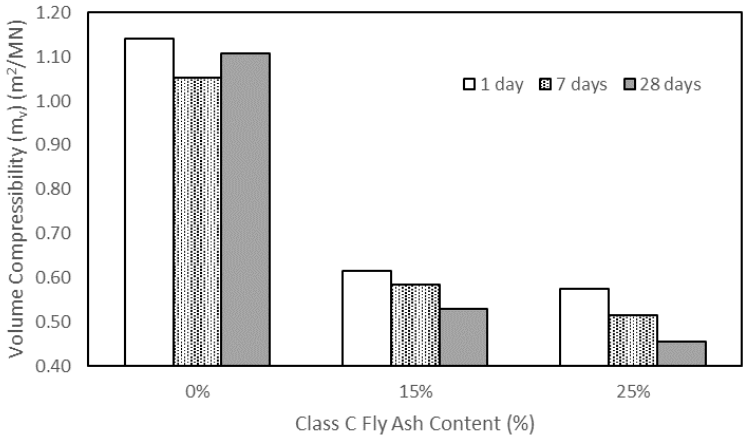

(a)

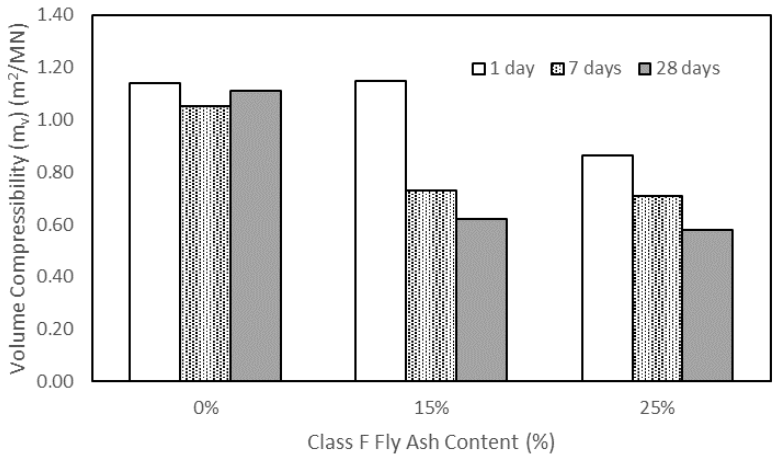

(b)

Figure 4.8 Variation of coefficient of m_v at effective pressure of 80 kPa with different curing times and different fly ash contents: (a) class C and (b) class F.

The coefficients of consolidation of the control samples and fly ash stabilised samples at different curing days were estimated based on Taylor's square root of time method (Amiralian et al, 2012a).

The coefficient of permeability (k) of the samples was also estimated based on the results of the coefficient of consolidation (c_v), the coefficient of volume compressibility (m_v), and the unit weight of water (γ_w) (Whitlow, 1996):

$$k = c_v m_v \gamma_w \quad (4.2)$$

Table 4.7 shows the variations of coefficient of consolidation (c_v) and permeability (k) for different fly ash contents and curing times for an effective stress increment of 40–80 kPa. The results show that the value of c_v of the soil increased with the inclusion of fly ash. A similar trend was observed from the analysis of permeability results. According to Wang and Tanttu (2018), the increase in c_v leads to an increase in permeability. The permeability of the soil increased with the increase of fly ash content. This trend is comparable with the finding of Phanikumar (2009). According to Chew et al (2004), the presence of Ca^{2+} ions from the fly ash leads to the formation of a flocculated structure in the clay. The flocculation leads to

increase of permeability (Phanikumar, 2009). Mir and Sridharan (2014) also indicated that the soil with inclusion of fly ash becomes coarser in comparison with the control sample. In this way, the stabilisation of soil with fly ash increases the permeability of the soil. The soil stabilised with class C fly ash showed a higher permeability than the control samples with 1 day and 7 days of curing. However, the stabilised soil became less permeable in comparison with the control sample at 28 days of curing. On the other hand, the class F fly ash stabilised soils showed a higher k value than the control samples with 1, 7, and 28 days of curing, although the k value of the stabilised samples decreased with the curing time. The long-term decrease of permeability is due to the reaction that produced calcium aluminium silicate hydrate (CASH) and/or calcium silicate hydrate (CSH) gels (Chew et al, 2004). This cementitious gel is deposited in the pores of stabilised soil during curing (Kassim and Chow, 2000). Chew et al (2004) analysed cement treated clays and found that the permeability of soil increased with an increase of cement content, and the permeability of cement stabilised soil decreased with time. Kassim and Chow (2000) reported a similar trend by testing a clay soil stabilised with lime. They argued that high permeability in early stages of curing and a decrease in permeability during curing can bring an advantage in geotechnical applications.

Table 4.7 Effects of fly ash and curing time on coefficient of consolidation and permeability.

Fly Ash Content (%)	Curing days	Coefficient of consolidation (C_v)(mm^2/min)	Permeability (k)(m/min)
0 % (unstabilised)	1	1.9	2.2E-08
0 % (unstabilised)	7	2.3	2.3E-08
0 % (unstabilised)	28	2.1	2.2E-08
15 % class C	1	8.2	5.0E-08
15 % class C	7	5.5	3.2E-08
15 % class C	28	4.2	2.2E-08
25 % class C	1	9.4	5.3E-08
25 % class C	7	5.5	2.8E-08
25 % class C	28	4.0	1.8E-08
15 % class F	1	6.3	7.1E-08
15 % class F	7	5.7	4.1E-08
15 % class F	28	5.3	3.2E-08
25 % class F	1	8.7	7.4E-08
25 % class F	7	6.0	4.2E-08
25 % class F	28	5.8	3.3E-08

4.1.6 Scanning electron microscopy

The SEM analysis was carried out to evaluate the microstructural changes in the soil with the increase of curing time and fly ash content. Figure 4.9 shows the microstructure of the unstabilised soil. The image shows the plate-like clay particles with dense and regular fabric, features that were also reported by Jaditager and Sivakugan (2017).

The microstructures of the soil stabilised with class C and class F fly ash are shown in Figures 4.10(a–f) and 4.11(a–f), respectively. For 1 day of curing, the microstructures of the soil stabilised with both class C and class F fly ash (Figures 4.10(a-b) and 4.11(a-b)) contained scattered and aggregated clay particles, spherical-unreacted fly ash particles, and pores with hollow cavities. The morphology of the soil stabilised with class C fly ash at 1 day of curing also showed the presence of C-S-H cementitious products around the fly ash particles. For 7 days of curing, more cementitious products were formed and bonded around fly ash particles for the soil stabilised with class C fly ash (see Figures 4.10(c-d)). The soil stabilised with 25% class C fly ash (Figure 4.10(d)) showed

more cementitious products compared to the soil stabilised with 15% class C fly ash (Figure 4.10(c)). For 28 days of curing, class C fly ash particles were covered with the cementitious products, and the products also filled the pore spaces and improved the interlocking structures which contributed to the dense fabric in the stabilised soil (Figures 4.10(e-f)). In addition, the structure of the soil presented a denser fabric, and no unreacted fly ash was observed with the increase of fly ash content and curing time (Figure 4.10(f)). The denser fabric could result in higher strength and stiffness in the stabilised soil (Zhang et al, 2013; Yoobanpot et al, 2017; Murmu et al, 2020; Yoobanpot et al, 2020; Abdila et al, 2021). Therefore, the results of the UCS, triaxial, and oedometer tests in this study are consistent with the SEM observations. The results of the SEM analysis for the soil stabilised with class F fly ash are similar to those for the soil stabilised with class C fly ash. However, the morphology of soil stabilised with class F fly ash presented more unreacted fly ash and less reaction products due to the lack of Ca ions (Figures 4.11(a–f)). For 7 and 28 days of curing, the soil stabilised with class F fly ash showed the presence of reaction products due to the pozzolanic reactions, and therefore the structural bonding of the stabilised soil improved. However, unreacted fly ash and partially dissolved fly ash particles were still observed in the stabilised soil. It can be said that the microstructure of the soil stabilised with class F fly ash was modified insignificantly with the increase of curing times. As a result, the soil stabilised with class F fly ash indicated lower strength compared to the soil stabilised with class C fly ash.

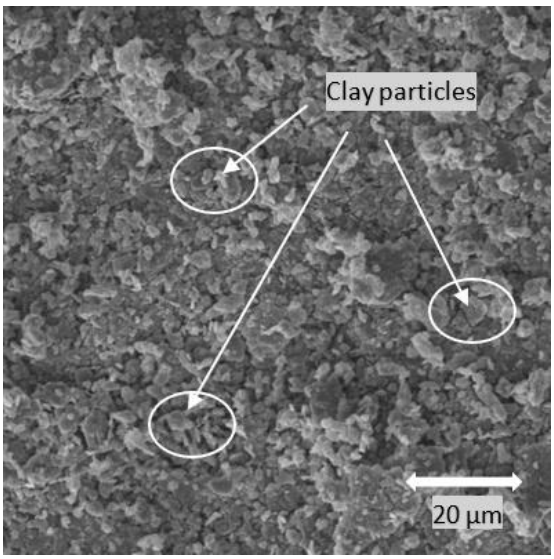

Figure 4.9 SEM images of clay (control sample).

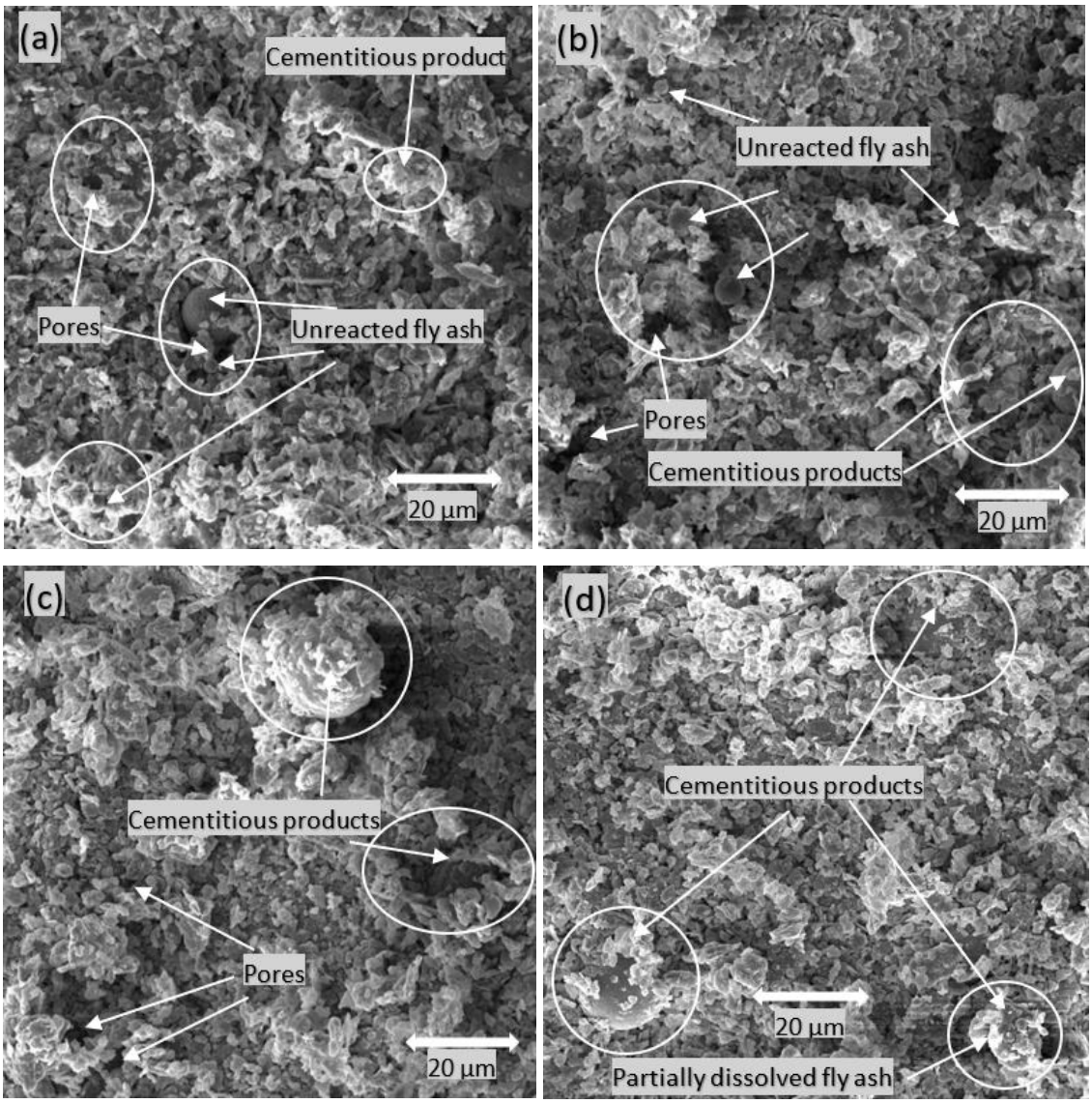

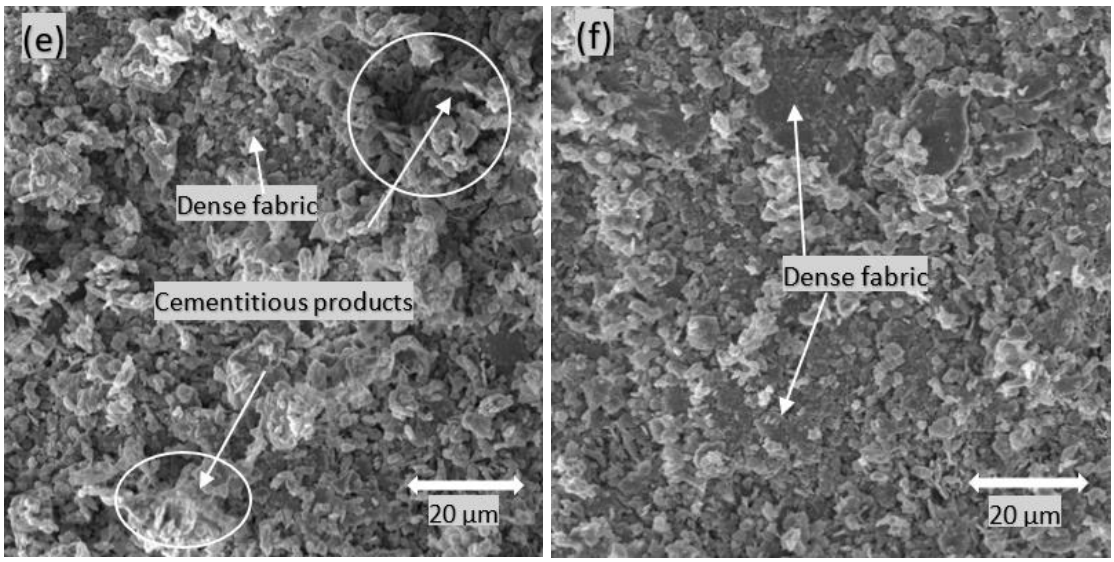

Figure 4.10 SEM images of soil stabilised with class C fly ash: (a) 15% C, 1 day of curing; (b) 25% C, 1 day of curing; (c) 15% C, 7 days of curing; (d) 25% C, 7 days of curing; (e) 15% C, 28 days of curing; (f) 25% C, 28 days of curing.

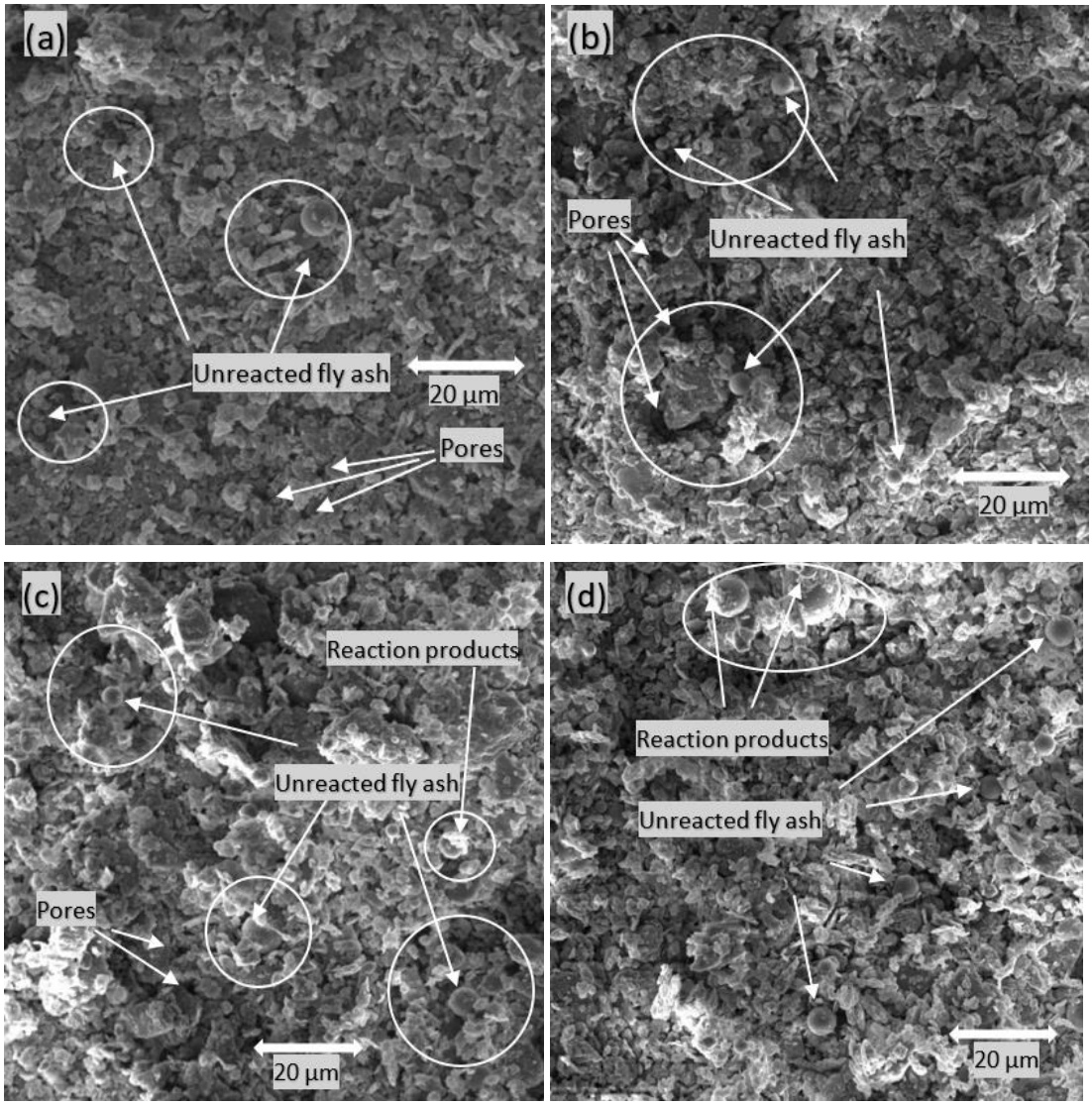

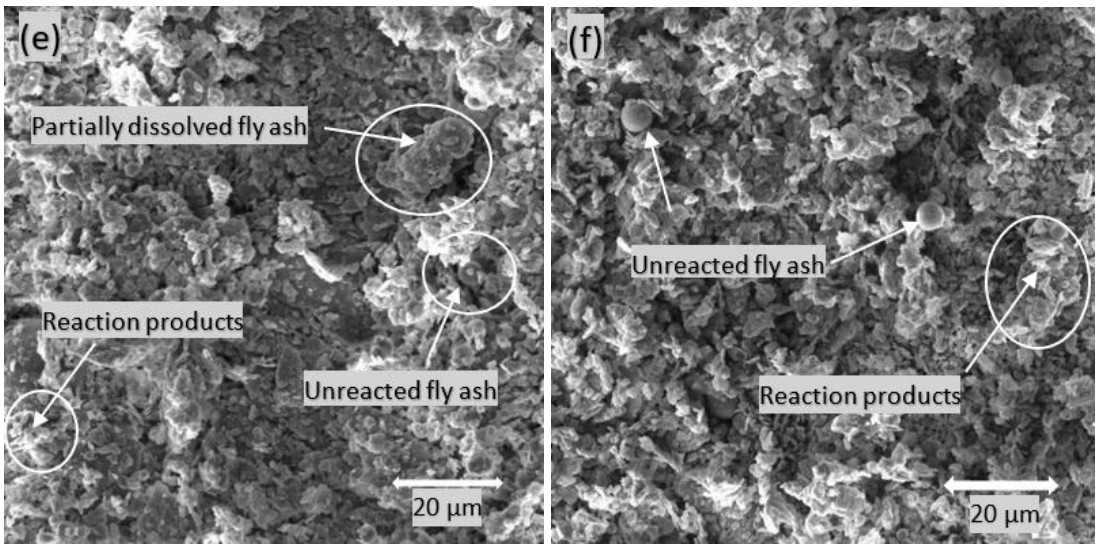

Figure 4.11 SEM images of soil stabilised with class F fly ash: (a) 15% F, 1 day of curing; (b) 25% F, 1 day of curing; (c) 15% F, 7 days of curing; (d) 25% F, 7 days of curing; (e) 15% F, 28 days of curing; (f) 25% F, 28 days of curing.

4.1.7 Summary of the findings

This section investigated the influence of class C and class F fly ash on the strength, consolidation, and microstructural characteristics on a clay soil. The following outcomes can be summarised from the results obtained in this section:

- The maximum dry density of the soil decreased, and the optimum moisture content increased with increasing percentages of both types of fly ash. The soil stabilised with class C fly ash had higher MDD and lower OMC in comparison with the soil stabilised with class F fly ash.
- The compressive strength of the soil increased with the addition of both types of fly ash and with the curing time. However, when the fly ash content increased from 25% to 30%, the compressive strength of the stabilised soil slightly decreased for both types of fly ash and for different curing times. Therefore, the optimal fly ash content appears to be 25% for both types of fly ash. Also, class C fly ash was found to be much more effective in improving the compressive strength of the soil than class F fly ash. The

elastic modulus of the soil increased with the addition of both types of fly ash up to 25% and with increasing the curing time.

- The results of the CU triaxial tests indicated an improvement in the angle of shearing resistance and cohesion intercept with the addition of class C fly ash, whereas the cohesion intercept of the soil stabilised with class F fly ash was lower than the control sample. The curing time was effective in improving the values of c' and φ' for both types of fly ash stabilised soil. The gradient of the critical state line increased with increasing the class C and class F fly ash contents and with increasing the curing time.
- The results from the one-dimensional consolidation tests indicated a decrease in the C_c of the soil stabilised with class C fly ash compared to the control sample. Furthermore, the C_c decreased with curing time for both types of fly ash. However, with class F fly ash, the C_c initially increased up to the particular fly ash content and thereafter decreased at 1 day of curing. The m_v value showed a similar trend to the compression index. C_s decreased by the addition of the class C or class F fly ash. In addition, curing time was found to be an effective parameter in decreasing the swelling index.
- The values of c_v and k increased with the addition of class C or class F fly ash. However, both c_v and k decreased with increasing the curing time for fly ash stabilised soils.
- The SEM analysis conducted on the soil stabilised with both class C and class F fly ash confirmed the gradual improvement in the soil properties and strength due to the formation of reaction products in the soil with the increase of curing time. However, the soil stabilised with class C fly ash

had more reaction products and denser fabric than the soil stabilised with class F fly ash due to the better cementitious properties of class C fly ash. The results from the UCS, triaxial, and consolidation tests were found in agreement with the results from the SEM analysis.

In general, it was observed that class C fly ash is more effective in improving the mechanical properties of the soil compared to class F fly ash. The findings have proven that class C fly ash can be used effectively in the stabilisation of clay soils. Class F fly ash can be used with the other additives such as lime or alkali activators to achieve higher mechanical properties in clay soils.

4.2 Soils stabilised with alkali activated class F fly ash

4.2.1 Overview

The aim of this section is to describe the results obtained investigating the effects of the binder composition on the compaction and UCS of stabilised soils and to assess the other mechanical, mineralogical, and microstructural properties of stabilised soil that showed the highest UCS. The mechanical behaviour of clay soil stabilised with fly ash/alkali activated fly ash was investigated by conducting one-dimensional consolidation and consolidated-undrained (CU) triaxial tests, while XRD and SEM analysis were conducted to observe mineralogical and microstructural composition of clay soil.

The dosage factors silica modulus (SM) and alkali dosages (M+) were used to assess the effects of activator concentration on UCS. Four different silica moduli, four different alkali dosages, and two different fly ash ratios were selected to evaluate the unconfined compressive strength behaviour of alkali-activated fly ash-stabilised soil samples. The effects of SM, M+, curing times, and fly ash dosages on the UCS of the samples were discussed in detail. Before the

mechanical tests, compaction tests were conducted on all samples stabilised with alkali-activated fly ash with different SM and M+ contents to obtain the required optimum moisture content for each sample. The curing times considered were 1, 7, and 28 days for all samples.

The results of the above-mentioned tests and analyses were compared with those of the soil samples stabilised with non-activated class F fly ash to highlight the effect of alkali activators. The outcome of this section will demonstrate the appropriateness of using activating factors M+ and SM in soil stabilisation design to obtain the desired strength. It will foster the use of alkali-activated fly ash as an alternative soil stabilising agent to cement and will show its advantages in terms of geotechnical engineering applications.

4.2.2 Compaction tests

Figures 4.12(a–d) show the compaction curves for control sample, stabilised soil samples with different percentages of fly ash, and alkali-activated stabilised soil samples with different percentages of fly ash, different M+, and different SM. The control sample had higher MDD and lower OMC than the soil stabilised with class F fly ash. A similar trend was reported by Prabakar et al (2004), Mir and Sridharan (2013), Seyrek (2018) and Savas (2018). The lower specific gravity of fly ash (2.32) compared to the specific gravity of clay (2.6) could be one of the reasons for the decrease in MDD. According to Murmu et al (2018), the flocculation and agglomeration of clay particles and fly ash lead to an increase in void ratio, explaining the decrease in MDD with the increase in fly ash. The presence of some broken, hollow fly ash spheres could be the reason for the increase in OMC (Mir and Sridharan, 2013).

Compaction curves of the soil stabilised with alkali-activated fly ash also indicated a decrease in MDD and an increase in OMC in comparison with the control sample. However, the rate of decrease in MDD in soil stabilised with alkali-activated fly ash was less than the soil stabilised with fly ash only. This could be attributed to the alkali activators used in the mixtures being viscous, thereby improving lubrication among fly ash and clay particles and resulting in an increase in MDD (Vitale et al, 2019; Abdullah et al, 2020b). In addition, it is seen that MDD slightly increased with the increase in M+ and SM for the soils stabilised with alkali-activated fly ash. Although the increase in activator amount seemed to provide an increase in the MDD, the variations were modest. The effect of M+ is indicated in Figure 4.12a, where the MDD was 14.5 kN/m^3 at M+ of 8%, and it increased to 14.7 kN/m^3 at M+ of 20% for the soil stabilised with 15% fly ash and an SM of 1. Additionally, MDD was found to be 14.3 kN/m^3 at M+ of 8%, and it increased to 14.6 kN/m^3 for the soil stabilised with 25% fly ash and an SM of 1. Similar modest variations in maximum dry density were reported by Sukmak et al (2013), who compared the compaction tests on clay–fly ash and clay–fly ash–geopolymer mixtures. They indicated that the alkali activators insignificantly affect the soil plasticity, and the liquid limit controls the compaction curve. Therefore, the compaction curves of fly ash stabilised soil and alkali-activated fly ash stabilised soil with different binder ratios have similar maximum dry densities for the same fly ash content (Sukmak et al, 2013).

The OMC of the soil stabilised with alkali-activated fly ash generally decreased with the increase in M+ and SM. Abdullah et al (2019a) argued that the lubrication effects of alkali activators could reduce the required free water to obtain optimum compaction, thereby decreasing the OMC.

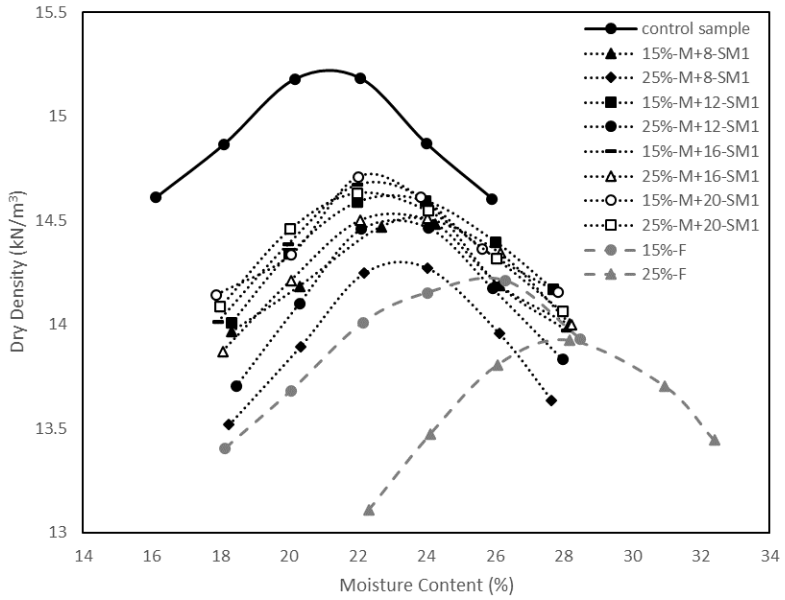
15.5
15
14.5
14
13.5
13
14
16
18
20
22
24
26
28
30
32
34
Dry Density (kN/m³)
Moisture Content (%)
control sample
15%-M+8-SM1
25%-M+8-SM1
15%-M+12-SM1
25%-M+12-SM1
15%-M+16-SM1
25%-M+16-SM1
15%-M+20-SM1
25%-M+20-SM1
15%-F
25%-F

(a)

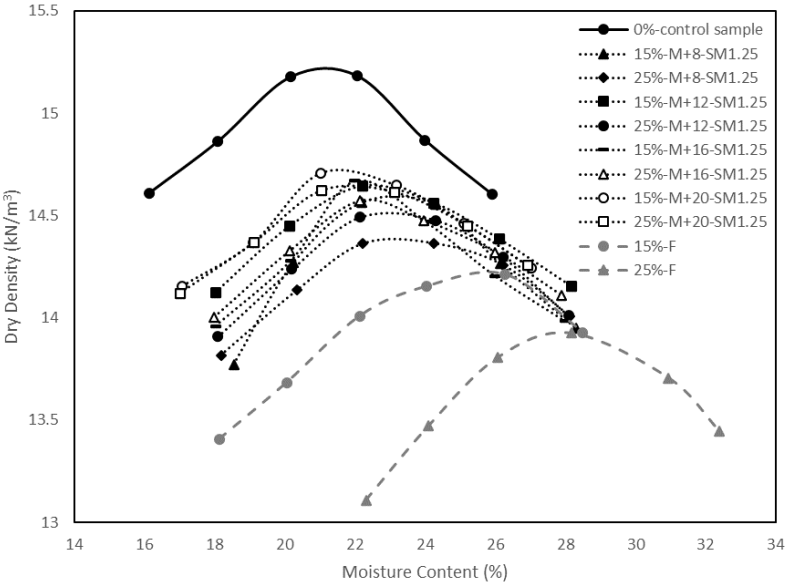
15.5
15
14.5
14
13.5
13
14
16
18
20
22
24
26
28
30
32
34
Dry Density (kN/m³)
Moisture Content (%)
0%-control sample
15%-M+8-SM1.25
25%-M+8-SM1.25
15%-M+12-SM1.25
25%-M+12-SM1.25
15%-M+16-SM1.25
25%-M+16-SM1.25
15%-M+20-SM1.25
25%-M+20-SM1.25
15%-F
25%-F

(b)

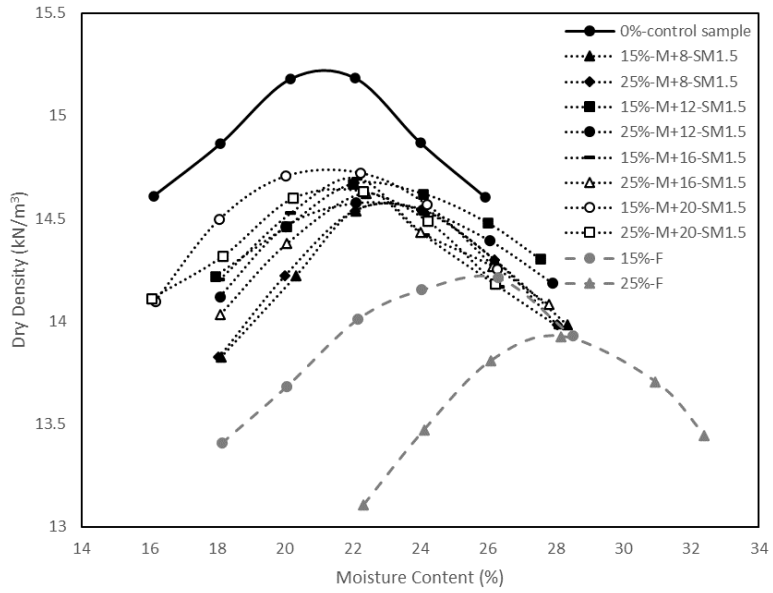

(c)

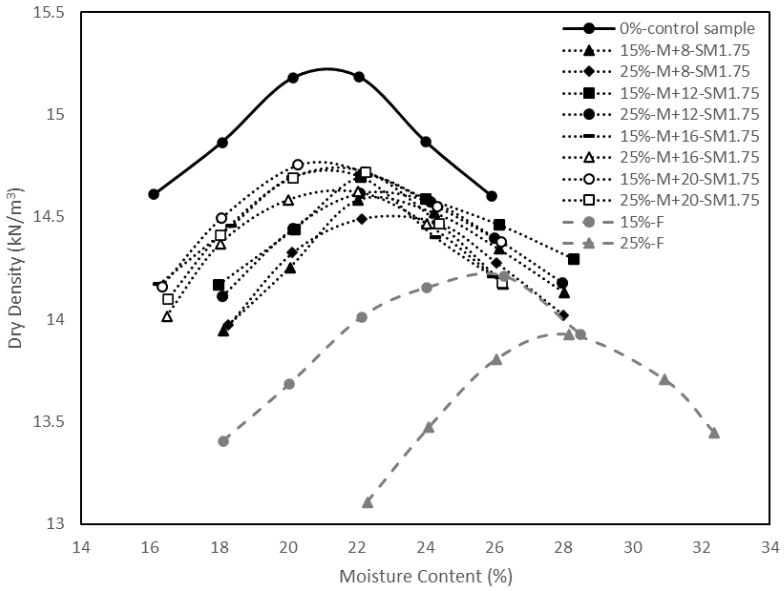

(d)

Figure 4.12 Compaction curves for the control sample, fly ash-stabilised soil samples, and alkali-activated fly ash-stabilised soil samples with different alkali dosages (M+) and silica moduli (SM): (a) SM = 1; (b) SM = 1.25; (c) SM = 1.5; (d) SM = 1.75.

4.2.3 Unconfined compressive strength tests

Unconfined compressive strength tests were carried out to evaluate the effects of M+, SM, curing time, and fly ash content on the strength of soils stabilised with fly ash and alkali-activated fly ash. The results are summarised in Table 4.8. The effects of the different factors on UCS are explained in the following sections.

Table 4.8 UCS in kPa of soils stabilised with fly ash and with alkali-activated fly ash with different alkali dosages and silica moduli.

		1 day curing		7 days curing		28 days curing	
		Fly ash content		Fly ash content		Fly ash content	
M+	SM	15%	25%	15%	25%	15%	25%
0	0	233	246	242	259	292	325
8%	1	210	253	255	373	422	687
	1.25	237	256	309	390	501	748
	1.5	244	276	262	385	413	621
	1.75	230	263	236	311	384	504
12%	1	224	267	280	425	460	998
	1.25	281	345	359	451	629	1144
	1.5	335	373	341	410	470	921
	1.75	271	338	278	378	395	704
16%	1	224	265	306	472	566	1106
	1.25	272	290	387	492	795	1293
	1.5	305	335	342	483	539	1097
	1.75	281	297	313	436	485	838
20%	1	172	201	269	296	441	834
	1.25	201	212	331	347	671	951
	1.5	208	219	277	298	404	782
	1.75	172	197	247	284	352	677

4.2.3.1 Effects of alkali dosages on UCS

M+ mainly represents the alkali concentration in the soil samples. Figure 4.13(a–c) show the effects of M+ on the UCS of the soils stabilised with alkali-activated fly ash with a constant SM of 1.25 at 1, 7, and 28 days of curing. The results for the soils stabilised with alkali-activated fly ash for different SM values generally showed a similar trend; hence, the best UCS results (SM = 1.25) shown in Figures 4.13(a–c) indicate a typical strength improvement of alkali-activated fly ash-stabilised soil with increasing M+ values. It is seen that the compressive strength of the soil samples stabilised with alkali-activated fly ash increased with the increase in M+, up to an optimum value, beyond which a decrease in strength

was observed. Alkali dosages (Na_2O/fly ash) of 8%, 12%, 16%, and 20% were applied on soils stabilised with alkali-activated fly ash in this study, while the previous studies applied generally the ratio of alkali activators (SS+SH) solution/fly ash to find the role of alkalinity in the stabilised soils. According to previous studies, the UCS increased with the increase in the ratio of the SS+SH solution/fly ash up to a maximum, then decreased when the activation exceeded the optimal dosages (Sukmak et al, 2013; Phetchuay et al, 2016). The results obtained in the current study are in agreement with the observations of Sukmak et al (2013) and Phetchuay et al (2016). As explained by Phetchuay et al (2016), a higher alkali hydroxide concentration could dissolve higher amounts of Si and Al ions in fly ash for the geopolymerisation reaction and thus result in a higher compressive strength. Karakoc et al (2014) and Runci and Serdar (2022) also indicated that the alkali concentration is a significant factor affecting the geopolymer strength. They reported that an optimum concentration of alkaline accelerated the geopolymerisation and increased the strength. However, when a concentration higher than the optimum was used, a decrease in strength occurred. This is because the excess alkali concentration can precipitate in early stages before polycondensation and hinder the geopolymerisation reaction, reducing the strength (Phetchuay et al, 2016). Soutsos et al (2016) also reported that the decrease in strength beyond the optimum M+ value is because the geopolymer gel saturated with alkali ions leads to less free water in the mixture; in this way, the speciation of silica and alumina oligomers from the fly ash dissolution cannot be fully completed with very high M+ values.

In this study, the optimum values of M+ were found to be 16% for 7 and 28 days of curing and 12% for 1 day of curing. The difference is because

geopolymerisation is a time-dependent process and the reaction is usually completed in the long term. One day of curing would not be enough for the full reaction of the alkali activators. It is well known that neat fly ash needs a sort of catalyst for the reaction to develop, typically provided in the form of thermal energy, i.e., oven curing, otherwise their reactivity is relatively slow. Therefore, with 7 and 28 days of curing, higher amounts of alkali activators will participate in the reaction, increasing the strength of the soil. On the other hand, although the optimum value of M+ was 16% for 7 and 28 days of curing, after the M+ of 12%, the rate of the strength improvement generally decreased (see Figures 4.13(b-c)). Hence, the M+ was fixed at 12% for further tests as it ensured satisfactory strength results. Moreover, the M+ of 12% was chosen (rather than 16%) to mitigate the environmental impact of activation chemicals and to reduce cost.

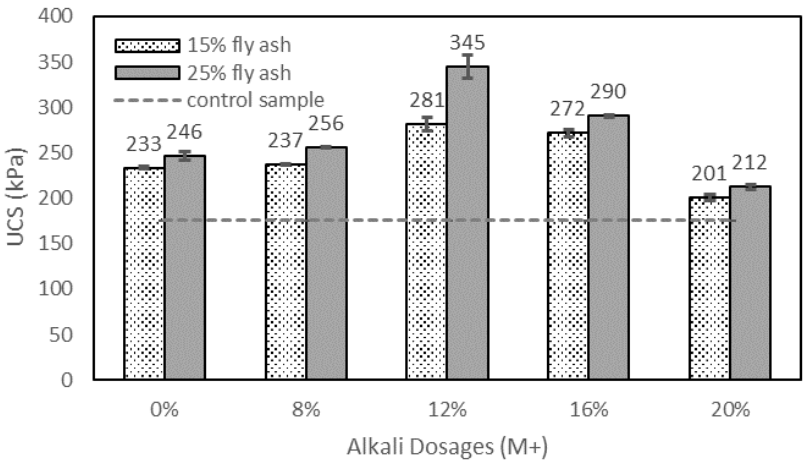

(a)

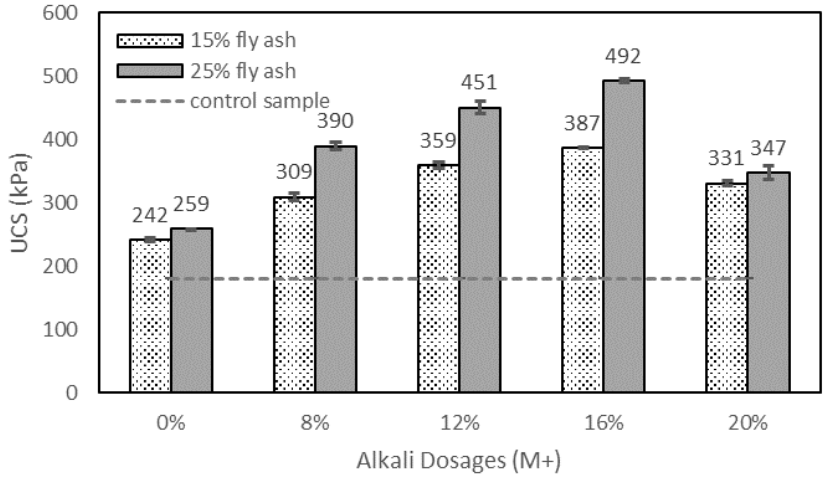

(b)

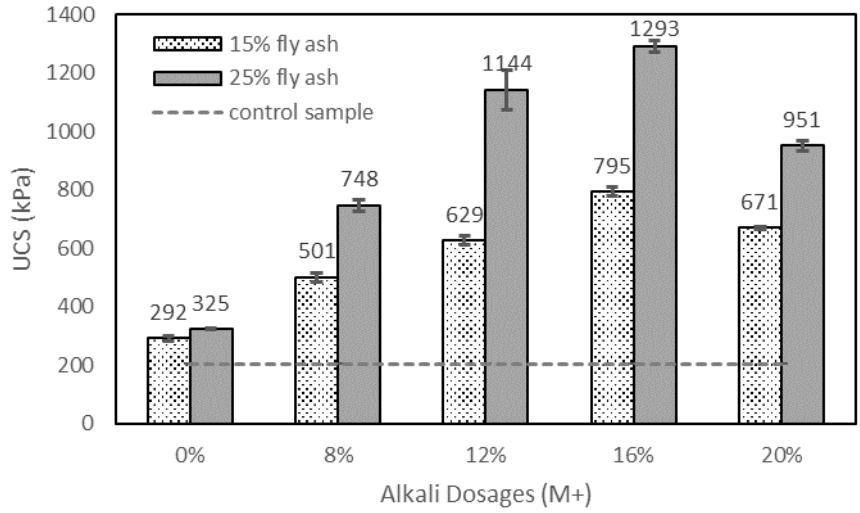

(c)

Figure 4.13 Effects of alkali dosages on the UCS of soils stabilised with alkali-activated fly ash with an SM of 1.25 at (a) 1 day of curing; (b) 7 days of curing; (c) 28 days of curing.

4.2.3.2 Effects of silica modulus on UCS

The SM represents the silica amount in the activating solution, and it is the ratio of SiO_2 to Na_2O in the solution. Figures 4.14(a–c) show the effects of SM on the UCS of the soils stabilised with alkali-activated fly ash with a constant M+ of 12% at 1, 7, and 28 days of curing. For an M+ of 8%, 16%, and 20%, the SM trends found are similar. According to the results, an SM of 1.25 gave the highest compressive strength at 7 and 28 days of curing, while the SM of 1.5 was

generally found to be the highest at 1 day of curing. The reason for the increase in compressive strength after increasing the SM to 1.25–1.5 could be that the available free Si^{+} in the activating solution aids the improvement of the polycondensation of oligomeric precursors during the geopolymerisation process. In this way, the degree of geopolymerisation increases, and subsequently, the compressive strength increases (Karakoc et al, 2014). On the other hand, the decrease in the compressive strength after a certain amount of SM is due to the increase in viscosity and the decrease in the pH of the activating solution (Firdous and Stephan, 2019; Gado et al, 2020). The increase of sodium silicate content in the activating solution increases the viscosity, thus the workability of the geopolymer paste decreases (Gado et al, 2020). When the SM increases, the alkalinity (pH) of the activating solution decreases due to the decrease in available OH groups, which are responsible for the dissolution of materials during the geopolymerisation (Soutsos et al, 2016; Gado et al, 2020).

In general, the silica modulus is inversely proportional to the NaOH and Na_2O amounts in the activating solution. The NaOH participates in the dissolution of aluminosilicates from the reacted fly ash (Leong et al, 2018; Firdous and Stephan, 2019; Gado et al, 2020), while free Si^{+} ions from SS solution are also beneficial for the development of geopolymer reactions (up to an optimum SM amount) (Rafeet et al, 2017). Therefore, the relationship between SM and compressive strength follows a bell-shaped distribution with a distinctive optimum SM/maximum strength apex point, as seen in Figure 4.14(a–c). Although there is a lack of studies using SM in soils stabilised with alkali-activated fly ash, previous studies applied the SS/SH ratio to evaluate the role of SiO_2 in the geopolymerisation process. Sukmak et al (2013), Phetchuay et al (2016), and

Leong et al (2018) used different SS/SH ratios to find the required strength. They indicated that much higher or lower SS/SH ratios in the system are not favourable to balance the SiO_2 amount. These previous studies are in agreement with the trend of SM observed in this thesis.

The SM of 1.25 was found to be adequate to achieve highest strength results with 7 and 28 days of curing. This value was found comparable to the results from Phetchuay et al (2016) who applied UCS tests on soils stabilised with alkali-activated fly ash with 70:30 of SS/SH ratio. On the other hand, the SM of 1.5 gave the highest UCS at 1 day of curing. The reason for the different optimal SM amount (1.5) with 1 day of curing could be that a higher amount of free Si^+ is consumed at a faster rate in the short term (Gado et al, 2020). However, when the SM is lower (1.25), the OH ions increase and high alkalinity provides a better dissolution of aluminosilicates and gelation, resulting in a better compressive strength in the long term. Phummiphan et al (2016) found that the UCS results were higher with curing time for soil samples with lower SS/SH ratios, which means a lower SiO_2 and higher NaOH content. According to their results, the highest UCS was at the SS/SH ratio of 90:10 at 28 days of curing, while the SS/SH ratio of 50:50 gave the highest UCS results at curing times longer than 60 days. This is also attributed to the growth of sodium aluminosilicate hydrate (NASH) gel over time (Phummiphan et al, 2016).

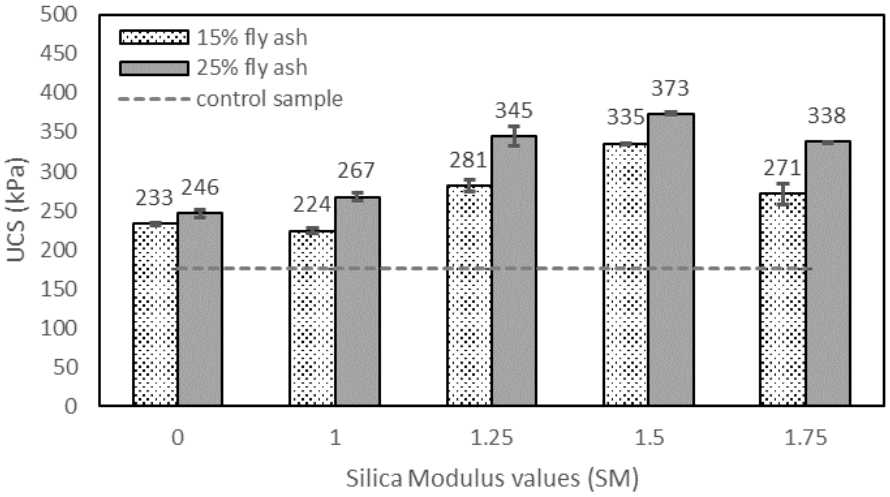
15% fly ash
25% fly ash
control sample
UCS (kPa)
Silica Modulus values (SM)
0
1
1.25
1.5
1.75
233
246
224
267
281
345
335
373
271
338

(a)

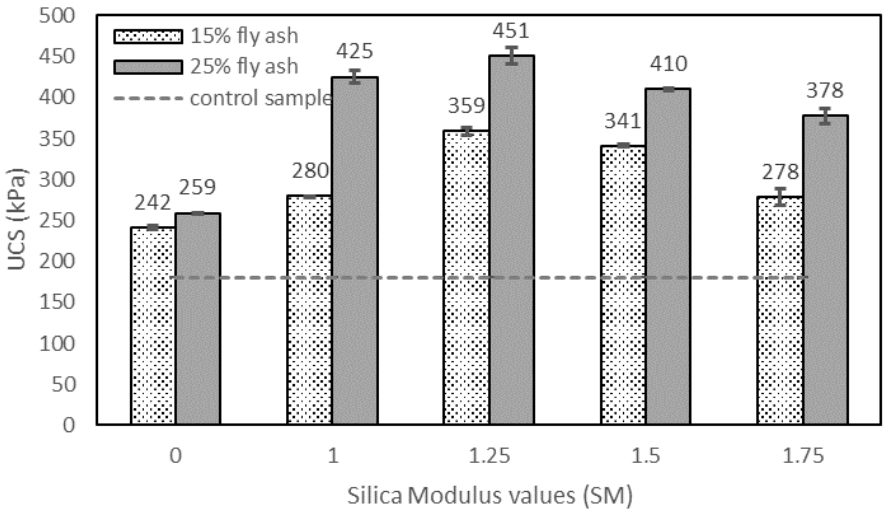
15% fly ash
25% fly ash
control sample
UCS (kPa)
Silica Modulus values (SM)
0
1
1.25
1.5
1.75
242
259
280
425
359
451
341
410
278
378

(b)

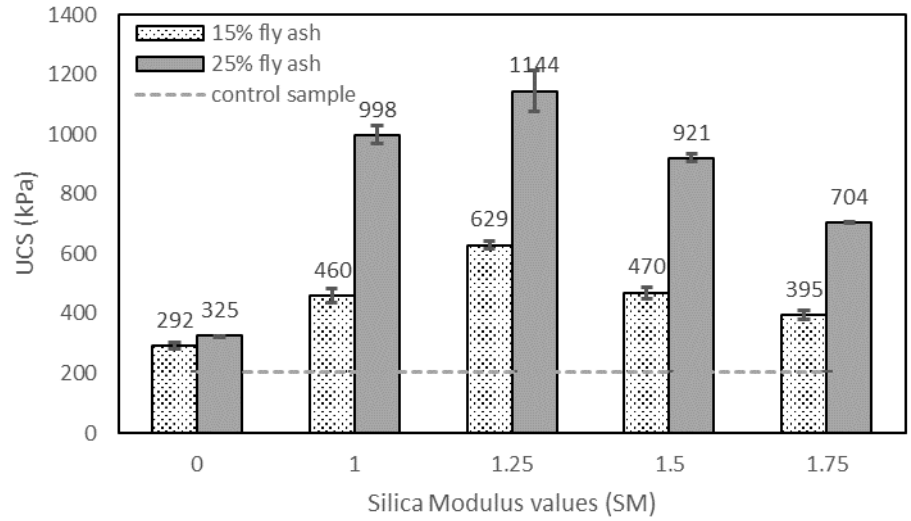

(c)

Figure 4.14 Effects of silica modulus on the UCS of soils stabilised with alkali-activated fly ash with an M+ of 12% at (a) 1 day of curing; (b) 7 days of curing; (c) 28 days of curing.

4.2.3.3 Effects of curing time on UCS

Figures 4.15(a–c) show the variation of UCS with curing time for the control sample, soils stabilised with fly ash, soils stabilised with alkali-activated fly ash with M+ of 12% and SM of 1.25, and soils stabilised with alkali-activated fly ash with M+ of 16% and SM of 1.25, respectively. The increase in UCS with the curing time for the soils stabilised with alkali-activated fly ash with different SM and M+ values generally showed a similar trend (Table 4.7). The UCS results of the soils stabilised with alkali-activated fly ash showed insignificant improvement at 1 day of curing. This can be attributed to the fact that the alkali activators have low reactivity with Si and Al in fly ash in the initial phase (Syed et al, 2020). Parhi et al (2017) argued that the curing time is needed for the reaction to occur and for the products of the reaction derived from the dissolution of Al and Si minerals to accumulate. Sukmak et al (2013) also found that the samples at low temperature or normal room temperature need long curing times to improve the UCS efficiently. The UCS of the soils stabilised with alkali-activated fly ash increased

with curing time for different M+ and SM contents, which is in agreement with the previous literature (Phummiphan et al, 2016; Rios et al, 2016a; Abdullah et al, 2018;2019; Correa-Silva et al, 2018). For example, the UCS of the soils stabilised with 15% alkali-activated fly ash with an M+ of 12% and an SM of 1.25 cured for 1, 7, and 28 days were found to be 1.6, 2, and 3.1 times that of the control sample, respectively. In addition, UCS results of soils stabilised with 25% alkali-activated fly ash for an M+ of 12% and an SM of 1.25 cured for 1, 7, and 28 days were 2, 2.5, and 5.6 times that of the control sample. The highest improvement was observed in soils stabilised with 25% alkali-activated fly ash for an M+ of 16% and an SM of 1.25 cured for 28 days, with the UCS increasing by 6.3 times that of the control sample (Figure 4.15(c)). The improvement in UCS with the curing times is attributed to the continuity of the geopolymerisation reaction (Abdullah et al, 2019). The reactions between fly ash, SS, and SH lead to the NASH products (Phummiphan et al, 2016). Due to the time-dependent availability of NASH products, the UCS of samples increases with the increase in curing time, with the presence of SH. On the other hand, the soils stabilised with fly ash showed a very slight increase with the increase in curing time (Figure 4.15(a)). The increase in UCS in soils stabilised with fly ash with the curing time is due to the development of pozzolanic reaction from fly ash (Turan et al, 2022a).

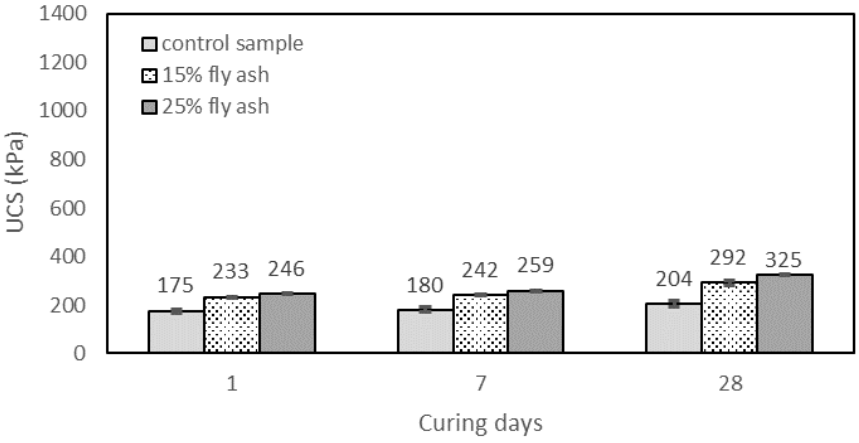

(a)

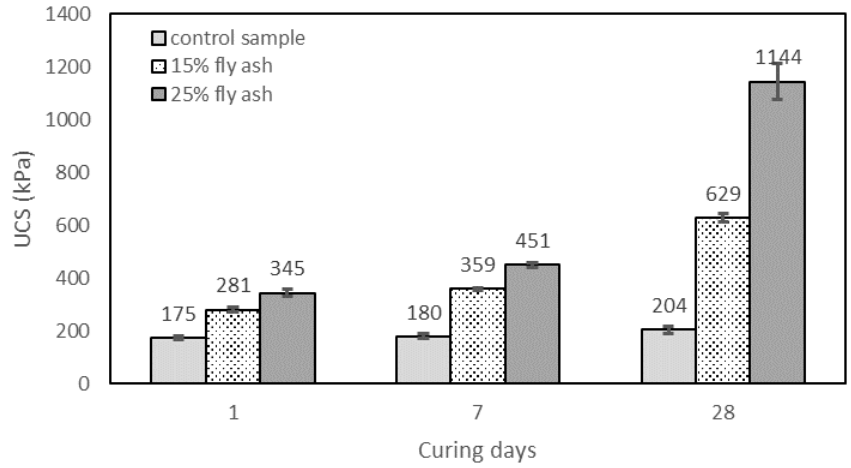

(b)

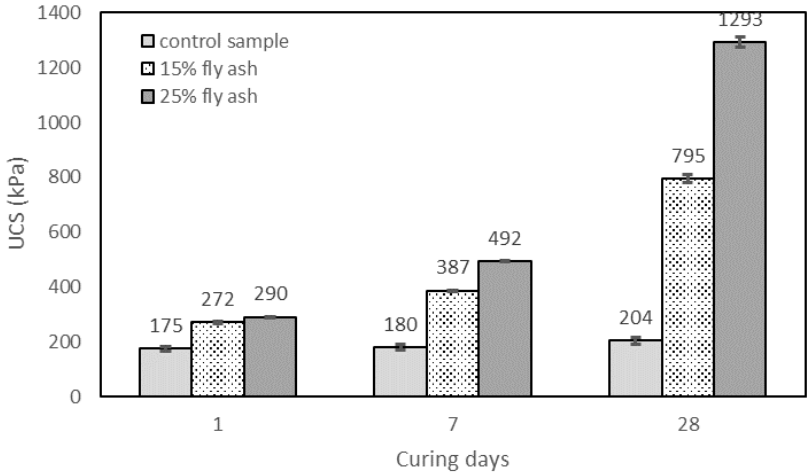

(c)

Figure 4.15 Effects of curing times on the UCS of the control sample: (a) soils stabilised with fly ash; (b) soils stabilised with alkali-activated fly ash with an M+ of 12% and an SM of 1.25; (c) soils stabilised with alkali-activated fly ash with an M+ of 16% and an SM of 1.25.

Figures 4.16(a–c) show the stress–strain behaviour of the control sample, soils stabilised with 15% and 25% fly ash, and soils stabilised with 15% and 25% alkali-activated fly ash with a constant SM of 1.25 and an M+ of 12% and an M+ of 16%, cured for 1, 7, and 28 days. The stress–strain behaviour of the soils stabilised with alkali-activated fly ash for different SM and M+ values generally showed a similar trend. It is seen that the control sample and soils stabilised with fly ash generally showed a ductile behaviour at different curing times. Soils stabilised with alkali-activated fly ash at 1 day of curing showed a similar ductile response. This is because the geopolymerisation at 1 day of curing is in the initial phase due to the relatively low reactivity of the system. With the increase in curing time, the stress–strain behaviour of the soils stabilised with alkali-activated fly ash changed from a ductile to a brittle response at 7 and 28 days of curing. The soils stabilised with alkali-activated fly ash at 7 and 28 days of curing showed higher initial stiffnesses, followed by a sudden strain-softening behaviour. The peak UCS of the control sample was 190.8 kPa at the axial strain of 6%, whereas the peak UCS of the soil stabilised with 25% alkali-activated fly ash with an SM of 1.25 and an M+ of 16% was 1312.3 kPa at the axial strain of 1% and 28 days of curing. A similar trend was reported in previous studies, and the improvement in the stress–strain behaviour of soils stabilised with alkali-activated fly ash was attributed to the formation of cementitious NASH products (Abdullah et al, 2019). Essentially, the cementitious products bound and increased the strength of the soil structure, leading to brittle and stiff bridges in the stabilised soil; hence, the bonds were destructured at very low strain. Kamruzzaman et al (2009) also indicated that the sudden strain-softening behaviour post yield is because the

more the cementitious the bonds, the higher the destructuration in the soil matrix is.

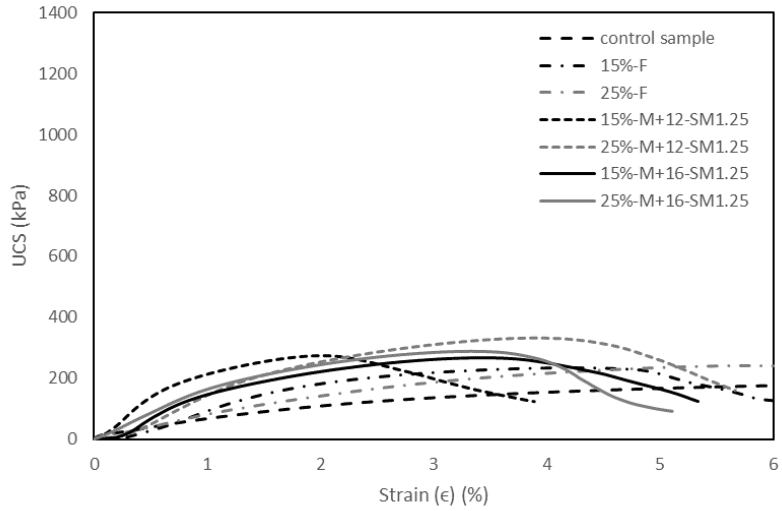

(a)

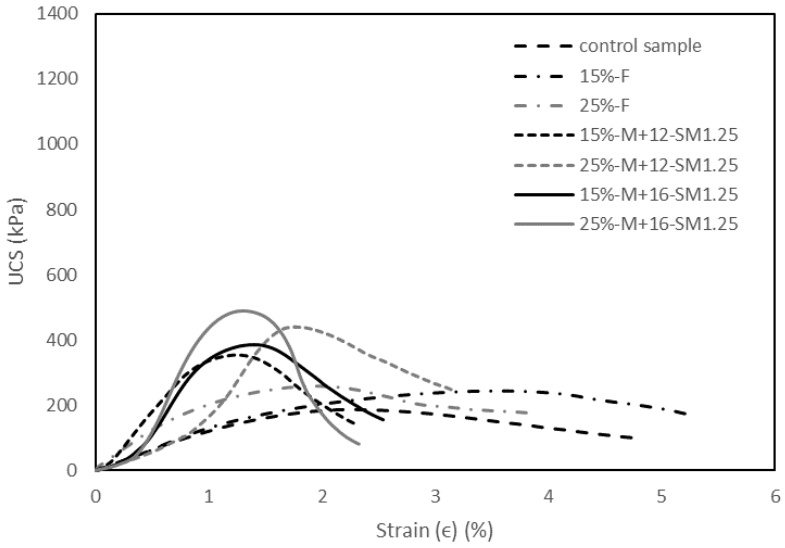

(b)

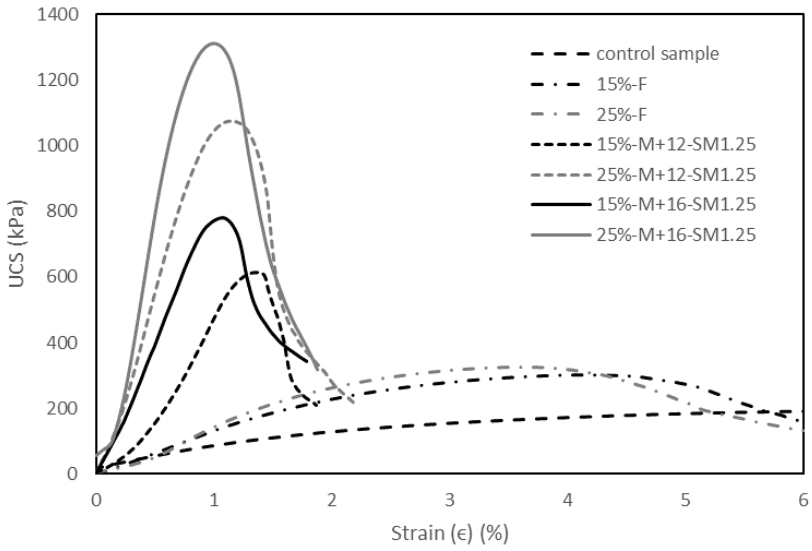

(c)

Figure 4.16 Stress-strain behaviour of the control sample, soils stabilised with 15% and 25% of fly ash, and soils stabilised with 15% and 25% of alkali-activated fly ash with a constant SM of 1.25 and an M+ of 12% or 16% at different curing times: (a) 1 day of curing; (b) 7 days of curing; (c) 28 days of curing.

4.2.3.4 Effects of fly ash content on UCS

Figures 4.17(a-b) show typical results of the effects of fly ash content on the UCS of soils stabilised with fly ash and with alkali-activated fly ash with a constant M+ of 12% and SM of 1.25 at 1, 7, and 28 days of curing. It can be seen that the UCS of the soils stabilised with fly ash or alkali-activated fly ash increased with the increase in fly ash content. This is in agreement with the previous investigations (Sukmak et al, 2013; Phetchuay et al, 2016; Abdullah et al, 2018; Leong et al, 2018). However, the results for the soils stabilised with alkali-activated fly ash at 1 day of curing, and for the soils stabilised with fly ash at 1, 7, and 28 days of curing, were found to be insignificant. This might be due to the fact that class F fly ash has very low reactive calcium content, and this results in the lack of chemical reaction with soil (Turan et al, 2022a). On the other hand, the UCS of the soils stabilised with alkali-activated fly ash increased considerably with the

increase in fly ash content at 7 and 28 days of curing. In general, the UCS of the soils stabilised with alkali-activated fly ash almost doubled, from 15% to 25% fly ash content, at 28 days of curing. When the fly ash content increased from 15% to 25%, the UCS of the soils stabilised with alkali-activated fly ash for the SM of 1.25 and M+ of 12% increased from 281 kPa to 345 kPa, from 359 kPa to 451 kPa, and from 629 kPa to 1144 kPa at 1, 7, and 28 days of curing, respectively. The reason for the increase in the UCS with the increase in the fly ash content in the stabilised soil is that fly ash contains SiO_2 and Al_2O_3 in amorphous (i.e., reactive) phase; hence, it can react effectively with SS and SH. In this way, more geopolymer gel can be formed to bind with soil particles due to the higher consumed SiO_2 and Al_2O_3, leading to higher compressive strengths (Phetchuay et al, 2016; Leong et al, 2018). Sukmak et al (2013) showed, from the results of XRD analysis, that the fly ash is mostly in the amorphous phase; therefore, the leaching capacity of SiO_2 and Al_2O_3 is high. They also indicated that clay includes negative aluminosilicate layer surfaces, resulting in high cation exchange capacity (CEC). As these negative surfaces have high anion capacity, they swarm positive cations (e.g., Na, K). When the fly ash content increases, the negative surfaces in the mixture decrease. In this way, both the increase in amorphous aluminosilicate and the decrease in negative surfaces lead to an increase in the geopolymerisation degree (Sukmak et al, 2013).

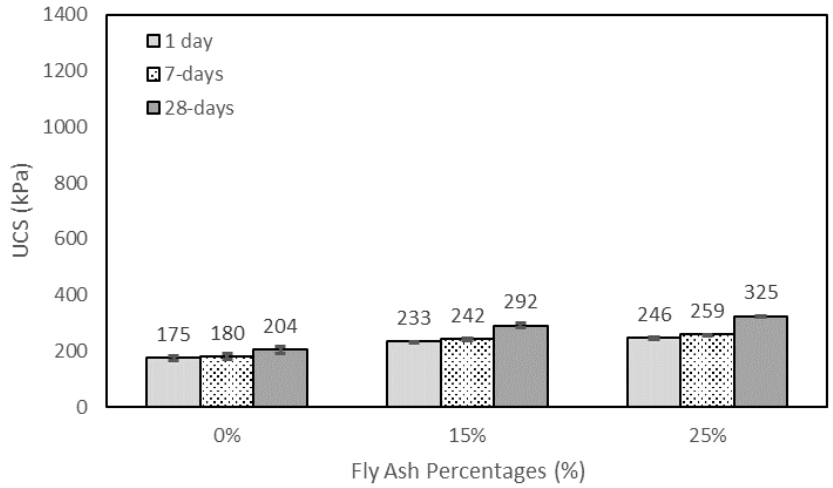

(a)

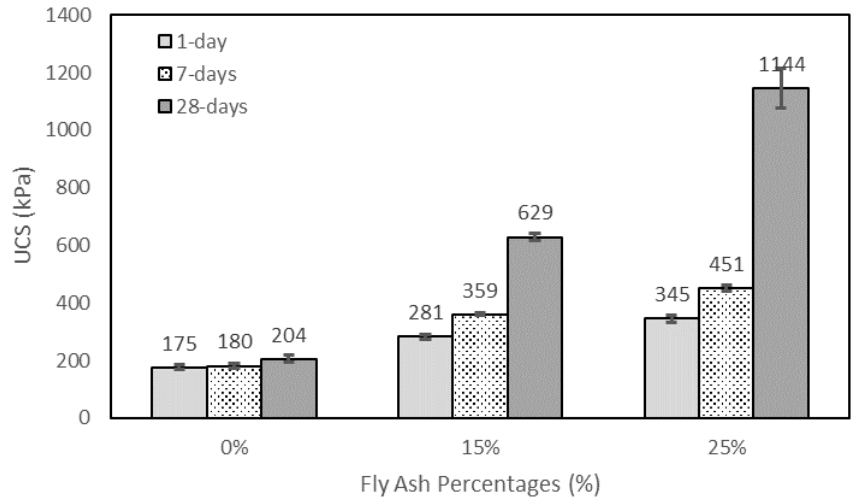

(b)

Figure 4.17 Effects of fly ash content on the UCS of (a) soils stabilised with neat fly ash and (b) soils stabilised with alkali-activated fly ash with an M+ of 12% and an SM of 1.25 and with different curing times.

4.2.4 One-dimensional consolidation tests

One-dimensional consolidation tests were carried out on control sample, fly ash stabilised soil, and alkali activated fly ash stabilised soil, to investigate the following soil parameters: compression index (C_c), swelling index (C_s), pre-consolidation pressure/yield stress (σ_y), and permeability (k).

Table 4.9 shows compression and swelling index results for the control sample, fly ash stabilised soil (F) and alkali activated fly ash stabilised soil (F+AA) samples with different percentages (15% and 25%) at 1, 7, and 28 days curing time. The results indicated that the compression index, C_c, of fly ash stabilised soil increased with 15% fly ash, but decreased with 25% fly ash at 1 day curing. These results agree with the outcomes of Phanikumar (2009), who reported an initial increase of C_c up to a certain dosage, after which a decrease in C_c was observed in clay soil stabilised with class F fly ash. On the other hand, the value of C_c, decreased considerably with increasing alkali activated fly ash content. The significant decrease of compression index was also reported by Mir and Sridharan (2014) with the addition of class C fly ash and they attributed the improvement in compressibility to the formation of calcium silicate hydrate (C-S-H) cementitious bonds (Mir and Sridharan, 2014). For the soil stabilised with alkali activated fly ash, sodium aluminosilicate hydrate (N-A-S-H) cementitious products could be the reason of decrease in compressibility. Another reason could be the effect of change in gradation. Shil and Pal (2015) noted that the proportion of clay size particles decreases and that of silt size particles increases when fly ash is mixed with the soil, resulting in a decrease in compressibility in stabilised soil. It was also observed that the compression index decreased with increasing curing time for both fly ash and alkali activated fly ash stabilised soil

samples. This could be because cementitious bonds are formed in the stabilised soil, which increase the bonding between soil particles during curing, hence reducing the compressibility (Chew et al, 2004; Mir and Sridharan, 2014). For the alkali activated fly ash stabilised soil, geopolymer gel helps with aggregation and flocculation of particles which improves the stiffness and strength of the soil, resulting in reduction in compressibility of the stabilised soil (Jaditager and Sivakugan, 2018).

The swelling index decreased with increasing fly ash or alkali activated fly ash content and with the curing time (Table 4.9). However, alkali activated fly ash was far more effective in decreasing the swelling index of the soil in comparison with fly ash only. The C_s value of the control sample was 0.048 at 28 days curing time, but it decreased to 0.018 with 25% fly ash and to 0.002 (i.e., the soil became non-swelling) with 25% alkali activated fly ash at 28 days curing time. The addition of non-expansive silt-size particles of fly ash to the clayey soil could be one of the reasons for the reduction of the swelling index. As the fly ash is not plastic, it does not absorb water (Cokca, 2001; Phanikumar and Sharma, 2007; Prabakar et al, 2004; Seyrek, 2016; Zha et al, 2008). It might also be due to the fact that NASH is a hydrated reaction product, and it consumes water during its formation. Turan et al (2019) found that the plasticity index of the clay decreased with addition of fly ash, and they indicated that the lower the plasticity index value, the less is the swelling properties. Also, Phanikumar and Sharma (2007) stated that the silicate, aluminium, and iron oxides in fly ash cause flocculation of clay particles due to the cation exchange. The flocculation leads to an increase in the diameter of particles in the stabilised soil, resulting in decrease of swelling characteristics. Kolay and Ramesh (2016) also pointed out that pozzolanic properties of fly ash

significantly decrease the swelling characteristics of expansive soils. The decrease in swelling index with curing time could be due to the time-dependent pozzolanic reaction of fly ashes (Mir and Sridharan, 2013, 2014; Zha et al, 2008).

Table 4.9 Effects of different fly ash and alkali activated fly ash contents and curing time on compression and swelling indices.

Fly ash content (%)	Curing days	Compression index (C_c)	Swelling index (C_s)
0% (control sample)	1	0.314	0.053
0% (control sample)	7	0.312	0.051
0% (control sample)	28	0.314	0.048
15% F	1	0.316	0.048
15% F	7	0.229	0.030
15% F	28	0.139	0.030
25%F	1	0.242	0.031
25%F	7	0.190	0.022
25%F	28	0.124	0.018
15% F+AA	1	0.295	0.040
15% F+AA	7	0.132	0.025
15% F+AA	28	0.097	0.012
25% F+AA	1	0.201	0.024
25% F+AA	7	0.106	0.014
25% F+AA	28	0.024	0.002

The results of permeability of control and stabilised soil samples with different curing times are shown in Figure 4.18. For 1-day curing time, the permeability increased with increasing fly ash or alkali activated fly ash content. Mir and Sridharan (2014) also reported a higher value of k for fly ash stabilised soil compared to control sample at 1 day curing. They argued that the increase in silt-sized particles in clay soil (due to the addition of fly ash) makes the soil more granular, resulting in higher coefficient of permeability. Phanikumar (2009) also highlighted that flocculation (due to the cation exchange) increases permeability. However, the permeability showed a decrease with curing time due to the formation of gel during pozzolanic reaction. This gel forms and fills up the pores

in the soil matrix during curing, leading to a less permeable soil (Kassim and Chow, 2000).

Based on the results, the permeability of the stabilised soil was higher than the unstabilised soil at an early age. Jaditager and Sivakugan (2018) reported that the permeability of dredged mud increased with fly ash based geopolymer. They argued that, due to the increase in the permeability, the pores and hole cavities in the stabilised samples allow easy drainage of water during the primary compression. However, an increase of curing time results in the decrease of c_v and k for the fly ash stabilised soil. In this case, the stabilised soil enabled easy drainage of pore water during primary consolidation (Jaditager and Sivakugan, 2018). As the curing time increased, permeability of stabilised soil decreased considerably. Kassim and Chow (2000) found a similar trend in permeability by testing lime stabilised soil. They pointed out that higher permeability at an early age and stiffer soil during curing can provide an advantage in practical applications.

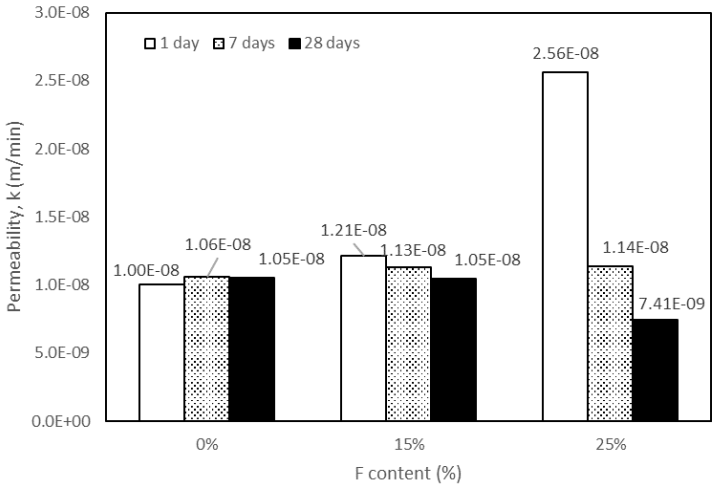

(a)

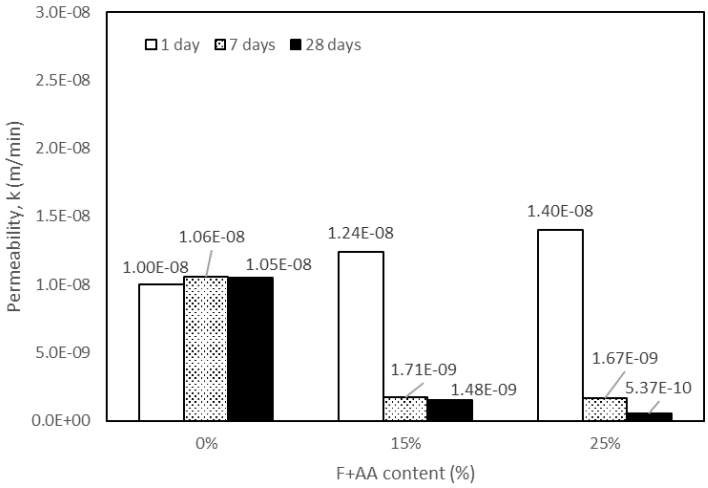

(b)

Figure 4.18 Effects of different (a) fly ash and (b) alkali activated fly ash contents and curing time on permeability.

Figures 4.19 (a-c) show the e - log σ_v relationship of the control sample, samples stabilised with fly ash and samples stabilised with alkali activated fly ash at 1 day, 7 days, and 28 days of curing, respectively. It is seen that the yield stress (preconsolidation pressure) of the stabilised soil increased with the addition of fly ash or alkali activated fly ash and with the increase of curing time. However, the addition of alkali activated fly ash had a significant effect in increasing yield stress in comparison with the addition of fly ash only. The increase might be due to the effect of structuration (formation of NASH cementitious bonds) among fly ash, alkali activators, and clay particles. Similar behaviour was observed by previous researchers who applied one-dimensional consolidation tests on clay stabilised with cement to observe the structuration/cementation effects (Horpibulsuk et al, 2004; Kasama et al, 2006; Kamruzzaman et al, 2009; Subramaniam et al, 2015). They argued that high cementation affects the yield stress considerably.

The effects of curing time were significant with the addition of alkali activated fly ash. Figure 4.20 shows the typical effect of curing time for soils stabilised with 25% alkali activated fly ash. The yield stresses of the stabilised soil were 300, 900, and (higher than) 1100 kPa at 1 day, 7 days, and 28 days curing, respectively. This indicates that the time-dependant pozzolanic reactions lead to strength improvement.

Figure 4.19 shows that the void ratio of the stabilised soil increased with the increase of fly ash or alkali activated fly ash at 1 day of curing. This is consistent with the observations of permeability results as indicated above. Jaditager and Sivakugan (2018) found a similar trend for soils stabilised with fly ash based geopolymer. They indicated that the flocculated structure in soil due to the alkali activation is the reason of the increase in void ratio at 1 day of curing. As the pozzolanic reaction increased and NASH cementitious products formed in the soil structure with curing, the void ratio of the stabilised soil decreased. Although the void ratio of the stabilised soil decreased with curing, it was found to be higher in fly ash-stabilised samples than in control sample. This is due to the modest cementitious properties of class F fly ash (Turan et al, 2022a), and the pozzolanic properties only gave slight decrease in void ratio. On the other hand, the soils stabilised with alkali activated fly ash had higher void ratios than the control sample at 1 day of curing, whereas the stabilised soil had lower void ratio than the control sample at 7 and 28 days of curing. This indicates that the NASH cementitious products have a significant role in forming the soil matrix and filling the voids. Kamruzzaman et al (2009) also argued that the decrease of water content, as a result of the pozzolanic reaction among the particles, can lead to the decrease of void ratio.

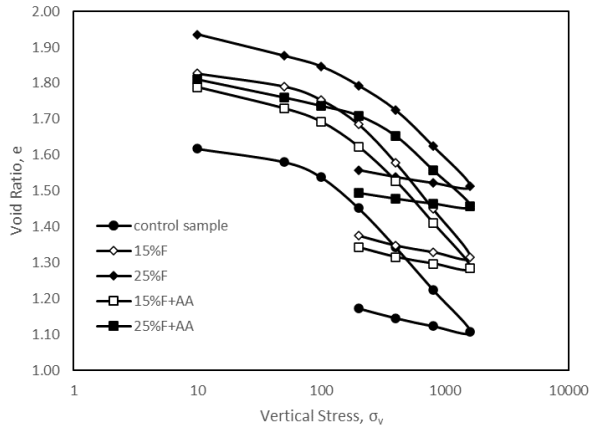

(a)

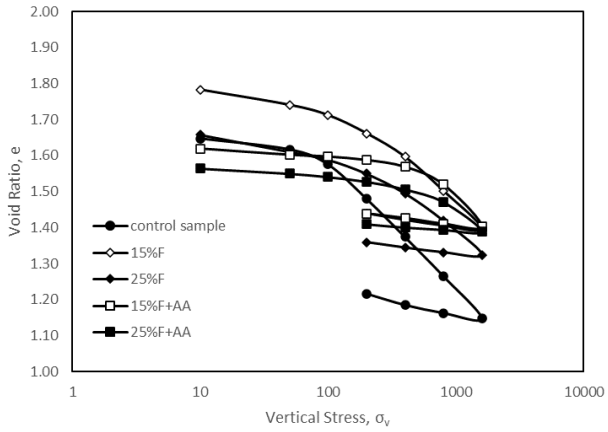

(b)

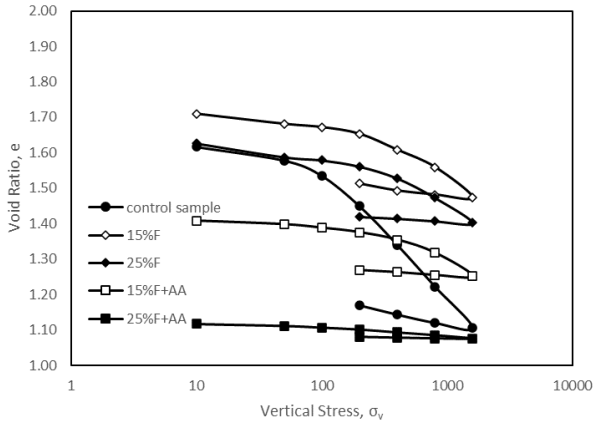

(c)

Figure 4.19 Effects of different fly ash and alkali activated fly ash contents on yield stress (a) at 1 day of curing, (b) 7 days of curing, and (c) 28 days of curing.

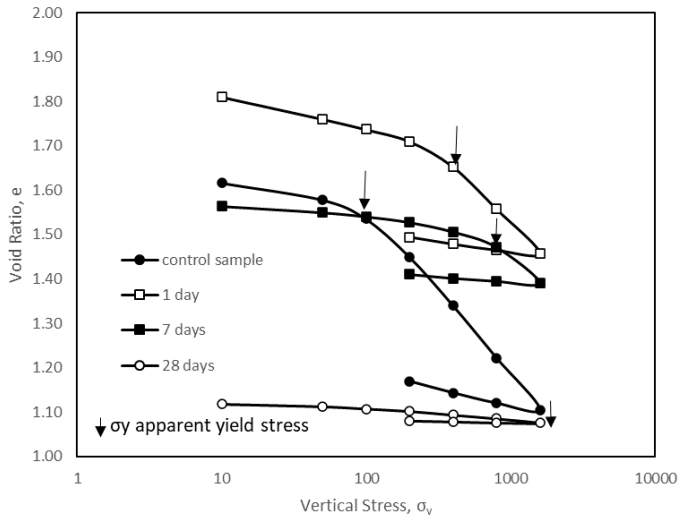

Figure 4.20 Effects of curing time on yield stress for soil stabilised with 25% alkali activated fly ash.

4.2.5 Consolidated-undrained triaxial tests

4.2.5.1 Effects of curing time on maximum deviator stress

Figures 4.21(a-c) shows the effects of curing time (1, 7, and 28 days) for the soils stabilised with class F fly ash and alkali activated class F fly ash with dosages of 15% and 25%, on the maximum deviator stress (q_{max}) under the effective confining pressures (σ'c) of 200, 400, and 600 kPa, respectively. The q_{max} increased with increasing the curing time for the soils stabilised with alkali activated fly ash. The observed trend is in agreement with the observations made by Abdullah et al (2019a). However, considerable changes were observed from 7 to 28 days curing time in comparison with the 1 day or 7 days curing time under all confining pressures. According to Sukmak et al (2013), to achieve a high strength, long curing time is required at low temperatures. Parhi et al (2018) argued that the curing time is needed for the reaction to occur, and for the products of reaction derived from the dissolution of Al and Si minerals to accumulate. For example, the q_{max} of the control sample was around 154 kPa under σ'c of 200 kPa. The addition of 15% and 25% alkali activated fly ash

resulted in q_{max} values of 194 and 319 kPa at 1 day of curing; and 292 and 510 kPa at 7 days of curing, respectively, while the highest q_{max} values were found to be 690 and 1569 kPa at 28 days of curing under the same effective confining pressures. At 28 days of curing, q_{max} of the stabilised soil increased about 9-fold with 25% alkali activated fly ash, compared to the control sample.

The results also show that q_{max} increased with the curing time and with the increase in fly ash content, under 200, 400, and 600 kPa confining pressures. This trend is in line with the results reported by Prabakar et al (2004) and Bryson et al (2017). However, no significant increase in maximum deviator stress was obtained with addition of fly ash only and the curing time. This could be because class F fly ash has low calcium content (2.2%), hence it has limited cementitious properties. Therefore, its chemical reaction (caused by its cementitious properties) with soil is very slow at room temperature (Turan et al, 2022a). Therefore, the small increase in q_{max} of the fly ash stabilised soil could be mainly due to the effect of the class F fly ash on the soil gradation. In general, the highest increase in q_{max} was observed for the soil sample with 25% fly ash at 28 days of curing for all confining pressures. The q_{max} of the soil stabilised with 25% fly ash increased from 191 to 238 kPa under 200 kPa effective confining pressure, while the q_{max} of the soil stabilised with 15% fly ash increased from 158 to 180 kPa under the same σ'c, from 1 day to 28 days of curing.

It can be concluded that the inclusion of alkali activators in the mix has a considerable effect on soils stabilised with fly ash with the increase of curing time. In other words, the effect of activating the fly ash with alkalis on mechanical properties of stabilised soil was evident, confirming that the binding properties of class F fly ash are not significant for the investigated soil even for 28 days curing.

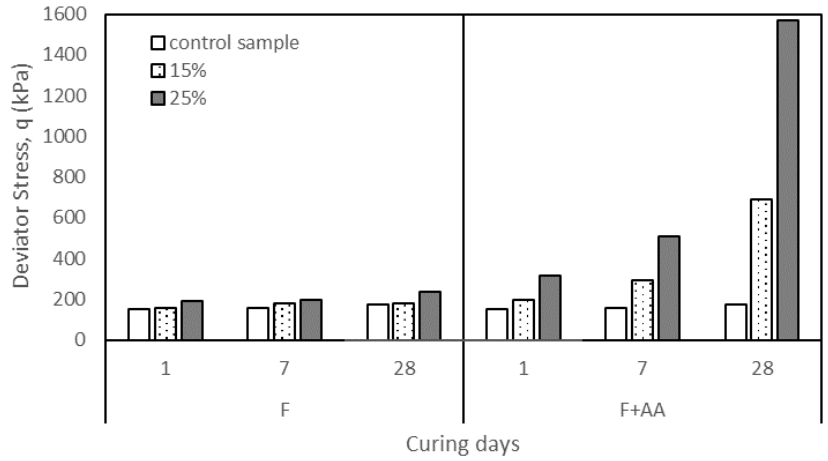

(a)

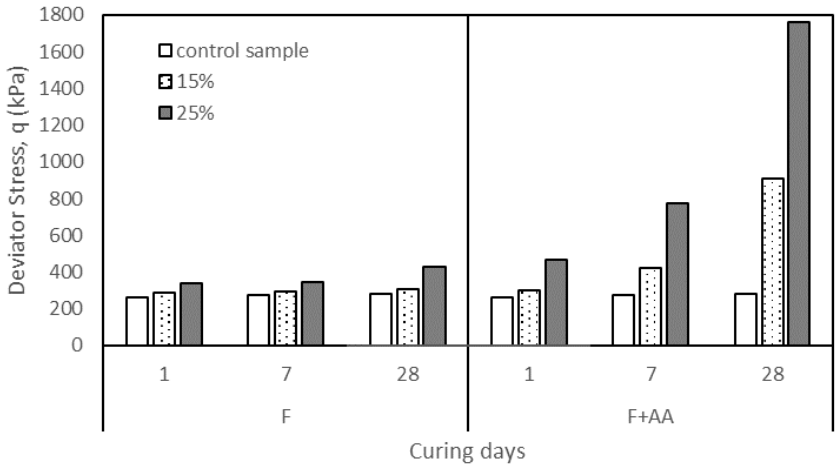

(b)

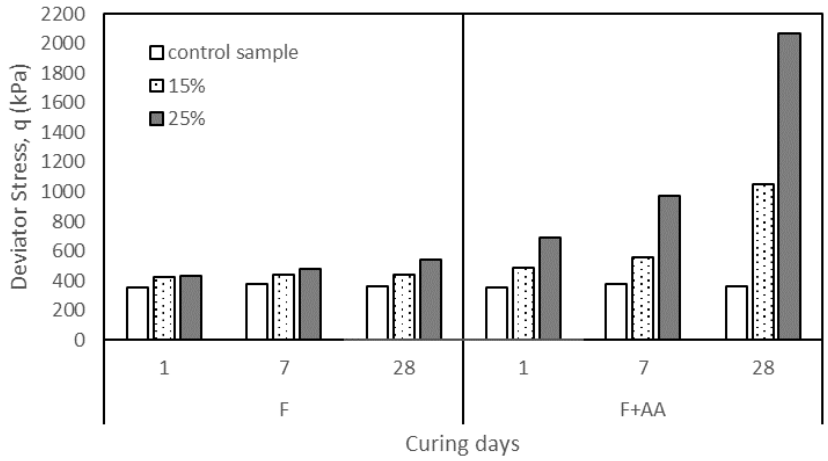

(c)

Figure 4.21 Effects of curing time on maximum deviator stress (q_{max}) of control sample, soils stabilised with 15% and 25% of fly ash and alkali activated fly ash under (a) 200 kPa, (b) 400 kPa, and (c) 600 kPa effective confining pressures (σ'_c).

4.2.5.2 Stress-strain behaviour of soil stabilised with fly ash and alkali activated fly ash

The deviator stress (q) - axial strain (εa) and excess pore water pressure (Δu) - axial strain curves for control sample, soils stabilised with 15% and 25% alkali activated fly ash, soils stabilised with 15% and 25% fly ash, at 28 days curing time under 200, 400, and 600 kPa effective confining pressures are shown in Figures 4.22 to 4.26.

Figure 4.22(a) shows that the control sample has ductile stress-strain response under effective confining pressures (σ'c) of 200 and 400 kPa and a slight strain-softening response under σ'c of 600 kPa. The ductile stress-strain response of the control sample changed to brittle strain-softening response with the addition of 15% alkali activated fly ash under all effective confining pressures (Figure 4.23(a)). The q_{max} of the control sample increased significantly with the addition of alkali activated fly ash for every confining pressure due to the effect of geopolymerisation. With the addition of 25% alkali activated fly ash, the stabilised soil showed more clear and sudden post-peak strain-softening response with higher initial stiffness for all σ'c values (Figure 4.24(a)). The higher initial stiffness is witnessed by the steeper slope of the pre-yield stress-strain line and higher peak value (Bryson et al, 2017). The axial strain corresponding to maximum deviator stress also decreased with the addition of alkali activated fly ash. Under confining pressures of 200, 400, and 600 kPa, the q_{max} values of control sample were 176, 283, and 359 kPa at about 17%, 20%, and 11% axial strain, while under the same confining pressures, the q_{max} values of soils stabilised with 25% alkali activated fly ash were 1569, 1761, 2067 kPa at about 1.1%, 1.0%, 0.9% axial strain at 28 days curing. Similar responses were observed by Abdullah et al

(2019a) who applied tests on fly ash based geopolymer stabilised soils. They explained that alkali activated fly ash improved the geopolymer bonds in soil, leading to high undrained stresses at the pre-yield stage. After shearing, the bonds break and the stress is controlled by frictional response of weak destructured soil matrix during post-yield. Kamruzzaman et al (2009) reported similar behaviours based on tests on cement stabilised soils. They indicated that when stabilised soil incurs strain-softening response, the soil matrix is in destructured stage, and the stabilised soil shows sudden strain-softening response with higher cement content, due to the effect of higher destructuration. In addition, when the strength of cementitious bonds is high, the soil response is comparable with an over-consolidated natural structured soil in which the effective confining pressure is lower than the yield stress (σ_y) (Kamruzzaman et al, 2009). The soils stabilised with 15% and 25% class F fly ash only, showed ductile stress-strain response similar to the control sample (Figures 4.25(a) and 4.26(a)). On the other hand, q_{max} slightly increased with the increase of fly ash for each effective confining pressure.

The deviator stresses of control sample, soils stabilised with alkali activated fly ash and soils stabilised with fly ash, all showed increase with the increase of confining pressure (Figures 4.22(a)-4.26(a)). This is because, the higher the confining pressure, the higher the change in fabric during consolidation stage. Consequently, higher volume change can be observed, therefore the q_{max} of soil sample increases (Horpibulsuk, 2004; Kamruzzaman, 2009). However, this condition is more obvious when the effective confining pressure of the sample is higher than the yield stress (i.e., soil is normally consolidated); this is due to the higher effect of reorientation in clay matrix during consolidation stage. The q_{max}

rate of control sample from 200 to 400 kPa σ'c was 1.7, while the rate of soils stabilised with 25% of alkali activated fly ash showed 1.1 under the same σ'c (Figures 4.22(a) and 4.24(a)). This indicates that the yield stress of soils with alkali activated fly ash is much higher than the control sample.

It is observed that the excess pore pressure – axial strain responses of all samples are similar to that of stress-strain response as shown in Figures 4.22(b)-4.26(b). Positive excess pore pressures were observed under all effective confining pressures for the control sample. The samples generally showed peak state at axial strain of about 6-10%, followed by very slight reduction under 200, 400, and 600 kPa confining pressures (Figure 4.22(b)). For the soils stabilised with 15% and 25% alkali activated fly ash, for all σ'c values (Figures 4.23(b) and 4.24(b)), the excess pore pressures increased initially at low strain up to a peak, and thereafter, showed strain-softening response by a sudden reduction and levelling off at the residual state. Lower strains were observed with the increase of alkali activated fly ash content. At low confining pressure and high alkali activated fly ash content, the volume change response changed from contractive to dilative behaviour. However, as the pore water cannot be drained in undrained shear test, instead of dilation, negative pore pressure was generated, similar to the behaviour of heavily over-consolidated clays. This was observed for the soils stabilised with 15% alkali activated fly ash under 200 kPa confining pressure, and the soils stabilised with 25% alkali activated fly ash under 200 and 400 kPa confining pressures. The excess pore water pressures of the soils stabilised with 15% and 25% fly ash showed a behaviour similar to the control sample (Figures 4.25(b) and 4.26(b)). In general, it can be said that over-consolidated behaviour was not observed with the control sample and the soils stabilised with 15% and

25% fly ash, even under the low σ'c values. This is due to the lack of cementitious properties of class F fly ash.

The increase in confining pressure showed higher excess pore pressure for all samples (Figures 4.22(b)-4.26(b)). Similar observation was reported by other researchers who applied tests on cement stabilised soils (e.g., Porbaha, 2000; Horpibulsuk, 2004; Kamruzzaman et al, 2009; Luis et al, 2019). Luis et al (2019) argued that when σ'c increases, the cementitious bonds become weaker by the σ'c, therefore, the excess pore pressure can be stabilised more rapidly at a higher σ'c.

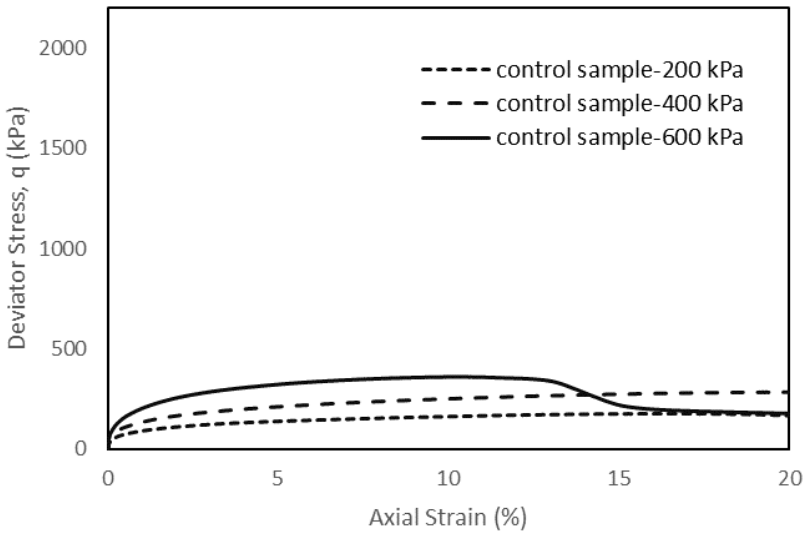

(a)

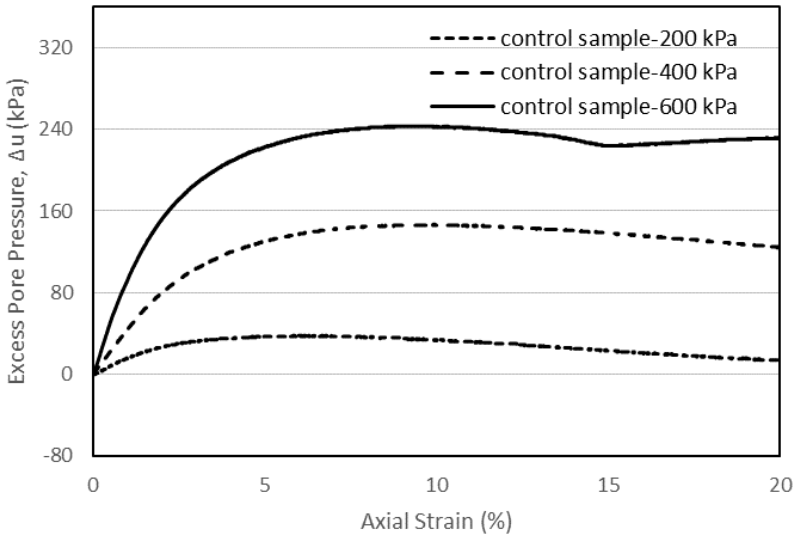

(b)

Figure 4.22 (a) Stress-strain and (b) pore pressure-strain behaviour of control sample under 200, 400, and 600 kPa effective confining pressures at 28 days of curing.

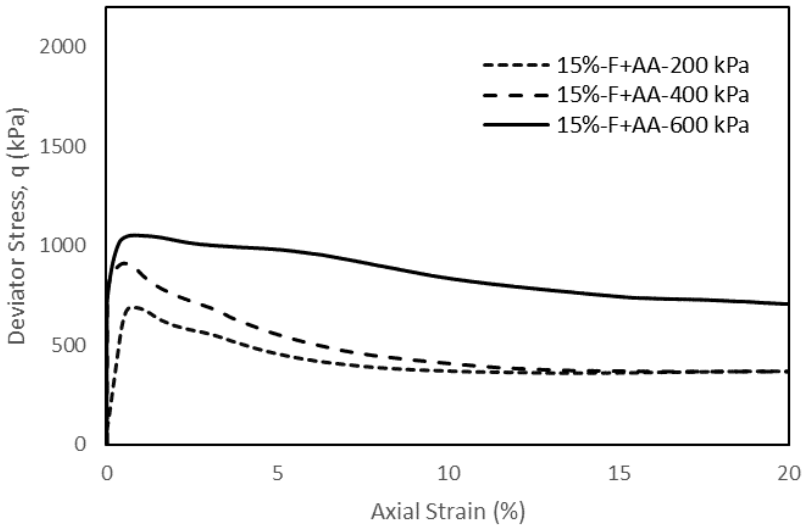

(a)

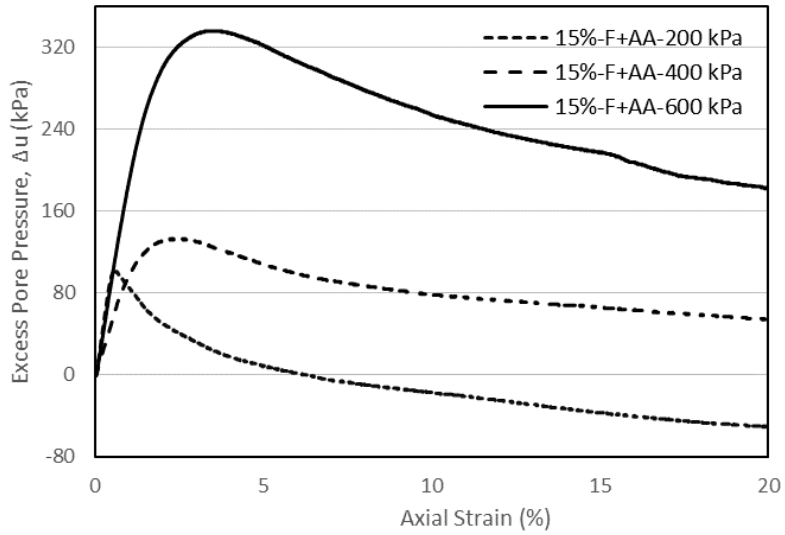

(b)

Figure 4.23 (a) Stress-strain and (b) pore pressure-strain behaviour of soils stabilised with 15% alkali activated fly ash under 200, 400, and 600 kPa effective confining presures at 28 days of curing.

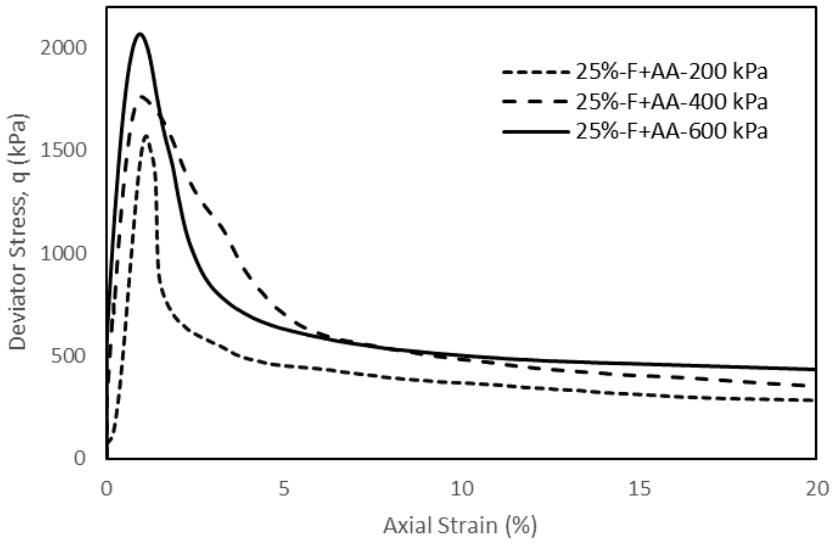

(a)

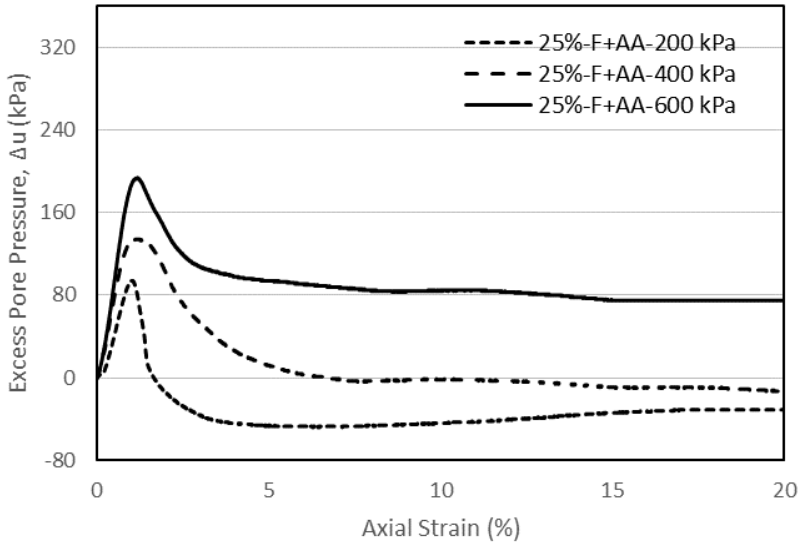

(b)

Figure 4.24 (a) Stress-strain and (b) pore pressure-strain behaviour of soils stabilised with 25% alkali activated fly ash under 200, 400, and 600 kPa effective confining pressures at 28 days of curing.

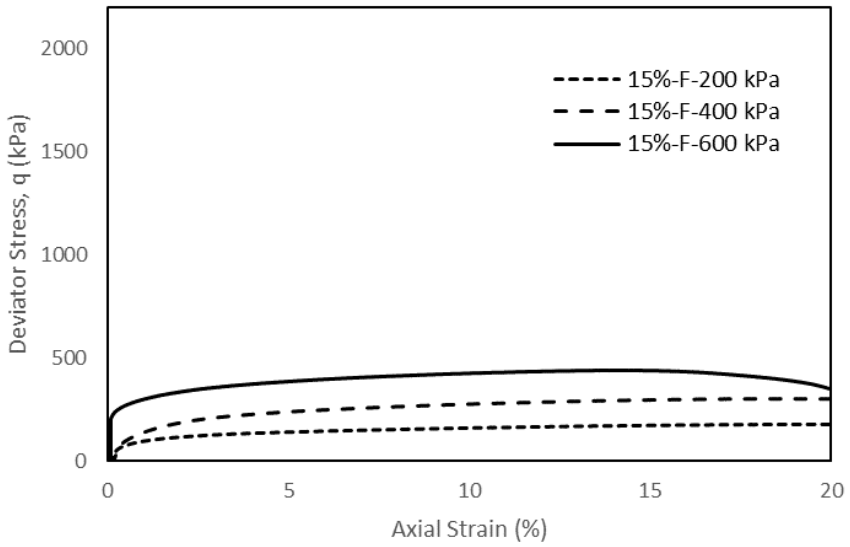

(a)

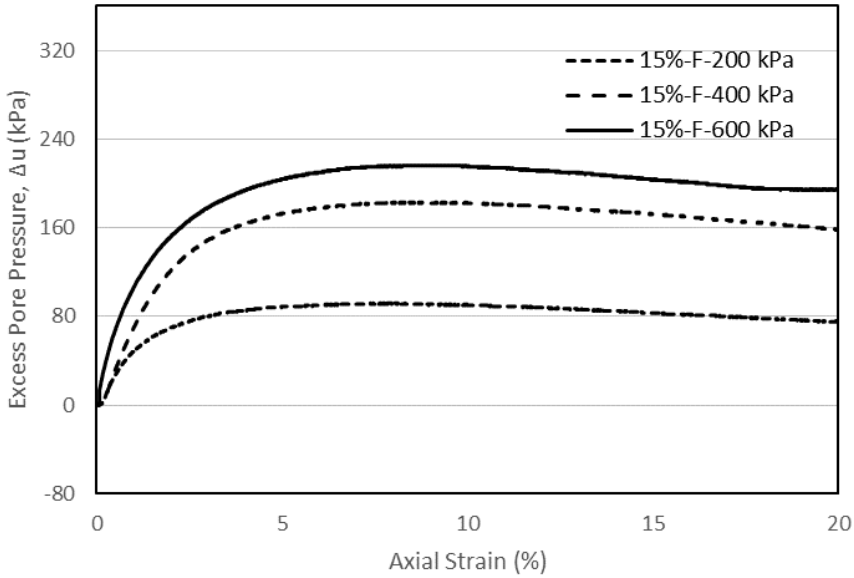

(b)

Figure 4.25 (a) Stress-strain and (b) pore pressure-strain behaviour of soils stabilised with 15% fly ash under 200, 400, and 600 kPa effective confining pressures at 28 days of curing.

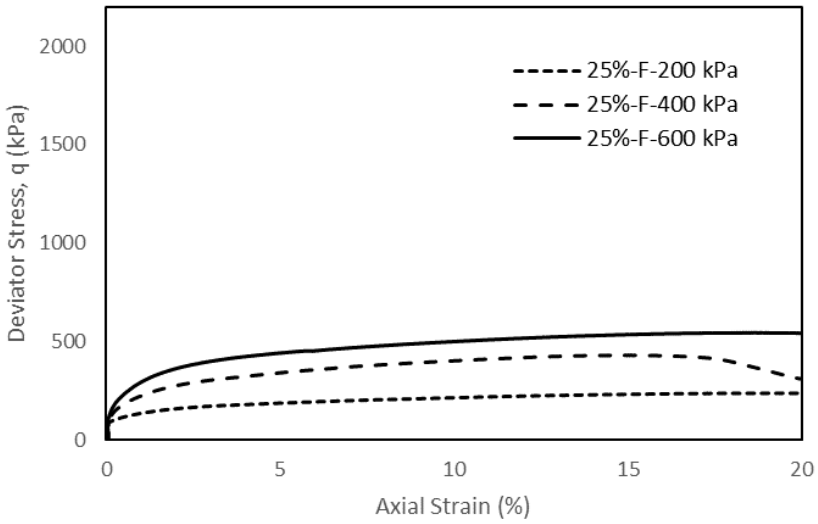

(a)

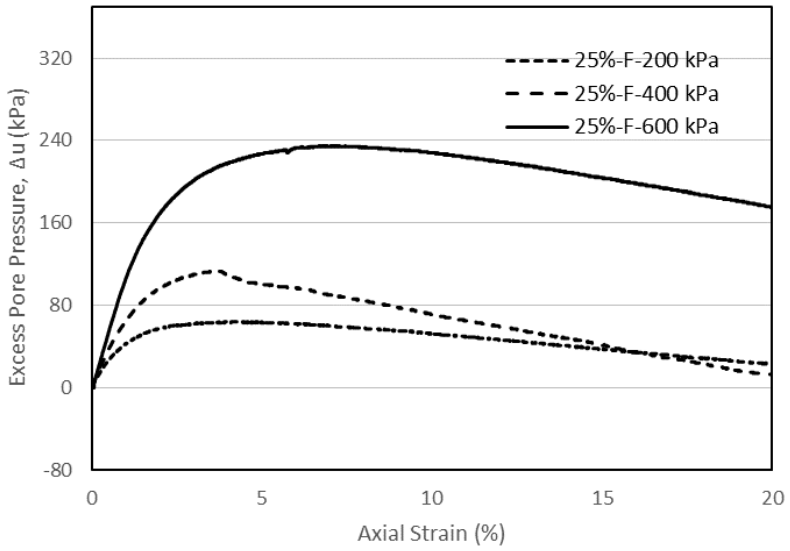

(b)

Figure 4.26 (a) Stress-strain and (b) pore pressure-strain behaviour of soils stabilised with 25% fly ash under 200, 400, and 600 kPa effective confining pressures at 28 days of curing.

4.2.5.3 Shear strength parameters of soil stabilised with fly ash and alkali activated fly ash

Mohr-Coulomb shear strength parameters were obtained from the CU triaxial tests under three different effective confining pressures to determine the effective cohesion (c') and effective angle of shearing resistance (φ') of the control sample, the soils stabilised with alkali activated fly ash and the soils stabilised with fly ash at 1, 7, and 28 days of curing as shown in Table 4.10.

It is seen that the value of effective cohesion in soils stabilised with alkali activated fly ash increased with the increase of fly ash content and curing times. The increase in c' value with the increase in fly ash content can be attributed to more geopolymerisation products and higher bonding with higher fly ash content. Correa-Silva et al (2018; 2020) indicated that alkaline binder affects shear strength considerably as it acts like glue, connecting soil particles and improving the cementitious bonds. The higher the degree of cementitious bonds, the higher the cohesion (Horpibulsuk et al, 2004). Also, increase in c' of the stabilised soil was significant with the increase in curing time. Turan et al (2022b) indicated that the reactions of SS, SH, and fly ash lead to sodium aluminosilicate hydrate (NASH) products which have time-dependent characteristics, hence, the bonding between reaction products and soil particles increases with increase in curing time. In addition, Correa-Silva et al (2020) reported continuous improvement of the reaction products in soils stabilised with alkali activation, leading to increase in c' value between 28 and 90 days of curing. The c' value of soils stabilised with fly ash was lower than the c' value of the control sample at all curing times since class F fly ash has very low calcium reactive content and silty features (Turan et al, 2022a). A similar trend was reported by Rajak et al (2019). However, slight

increase in c’ value of soils stabilised with fly ash was observed with the increase in the curing times due to the pozzolanic properties of class F fly ash.

The values of effective angle of shearing resistance in the soils stabilised with alkali activated fly ash and fly ash were higher than the control sample at all curing times. The addition of 25% alkali activated fly ash to the soil showed an increase in φ’ from 18.4^{o} (control sample) to 29^{o} at 28 days of curing, while the soils stabilised with 25% fly ash at the same curing time had a φ’ value of 22.4^{o}. Studies have indicated that the increase in φ’ with the increase in fly ash content is mainly due to the particle substitution (Bryson et al, 2017; Rajak et al, 2019; Turan et al, 2022a). Due to the silt fraction of fly ash, the clay fraction decreases, leading to an increase in the average grain size of the mixture in the stabilised soils (Bryson et al, 2017). The soils stabilised with alkali activated fly ash had higher φ’ value than the soils stabilised with fly ash. Horpibulsuk et al (2004) argued that the cementitious reaction products weld the soil matrix. Hence, during shearing, higher distortion, resulting in higher angle of shearing resistance was observed in stabilised soils. In other words, the cementitious bonds are not only to improve the cohesion, but they also help the improvement in the angle of shearing resistance (Horpibulsuk et al, 2004). The φ’ values also showed an increase with the increase in curing times. It can be said that, higher cementitious bonds and pozzolanic reactions during curing increase the value of φ’. Also, loss of moisture from a sample with curing time can cause an increase of angle of shearing resistance as indicated by Sezer et al (2006). However, this statement is not applicable for this work as the samples were stored in vacuum desiccators during curing. In this way, moisture loss in samples was not observed.

Table 4.10 Cohesion and angle of shearing resistance values of control sample, soils stabilised with 15% and 25% alkali activated fly ash, and soils stabilised with 15% and 25% fly ash with different curing times.

Fly Ash Content (%)	Curing days	c' (kPa)	ϕ' (º)
0%	1	17.5	18.1
0%	7	18.5	19.6
0%	28	19.0	18.4
15% F+AA	1	17.6	21.3
15% F+AA	7	43.7	22.2
15% F+AA	28	183.3	22.6
25% F+AA	1	26.3	25.7
25% F+AA	7	101.8	27.0
25% F+AA	28	388.6	29.0
15% F	1	2.7	20.7
15% F	7	4.9	21.1
15% F	28	11.1	22.3
25% F	1	8.4	21.6
25% F	7	10.1	21.6
25% F	28	15.1	22.4

4.2.5.4 Critical state behaviour of soil stabilised with fly ash and alkali activated fly ash

CU triaxial tests were conducted at effective confining pressures of 200, 400, and 600 kPa. The critical state lines in the q-p’ plane for the control sample, soils stabilised with alkali activated fly ash and soils stabilised with fly ash, at 1, 7, and 28 days of curing are shown in Figure 4.27. It is seen that the addition of fly ash or alkali activated fly ash increased the gradient of the critical state line (M). M is a function of angle of shearing resistance and indicates the relationship among particles and their geometry (Robin et al, 2014). Thus, it can be said that the silty characteristics of fly ash helped to improve the value of M in the stabilised soils. The soils stabilised with alkali activated fly ash had higher value of M than the soils stabilised with fly ash at 1, 7, and 28 days of curing. These results are consistent with the obtained Mohr-Coulomb shear strength parameters in section 4.2.5.3. Subramaniam et al (2015) and Abdullah et al (2019a) reported similar increasing trend for M for clay stabilised with cement and for clay stabilised with alkali activated fly ash slag, respectively. It is argued that the large particles

formed during geopolymerisation can cause the increase in M value (Abdullah et al, 2019a). The M value was also increased with curing time for all stabilised soils due to the effects of pozzolanic reactions and cementation.

For the stabilised soils, the y-intercept of the critical state line (CSL) in q-p’ plane increased with the increase of alkali activated fly ash and the curing times. The increase of the y-intercept in the stabilised soils can be attributed to the effects of cementation bonding (Robin et al, 2014). In the soils stabilised with alkali activated fly ash, cementation occured during the geopolymerisation process (Abdullah et al, 2019a). A similar modification was observed by Robin et al (2014) who applied triaxial tests on soils stabilised with lime. On the other hand, the y-intercept of the CSL for the soils stabilised with class F fly ash in q-p’ plane was stable due to the low calcium amount and thus low cementation.

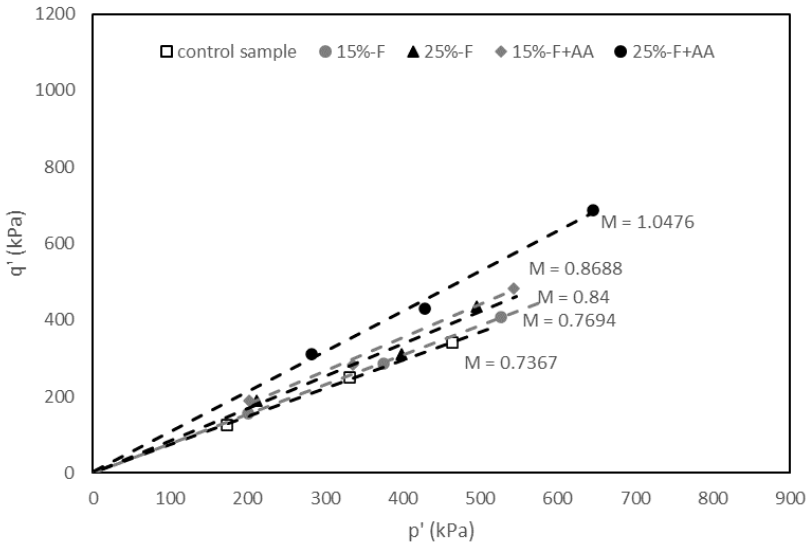

(a)

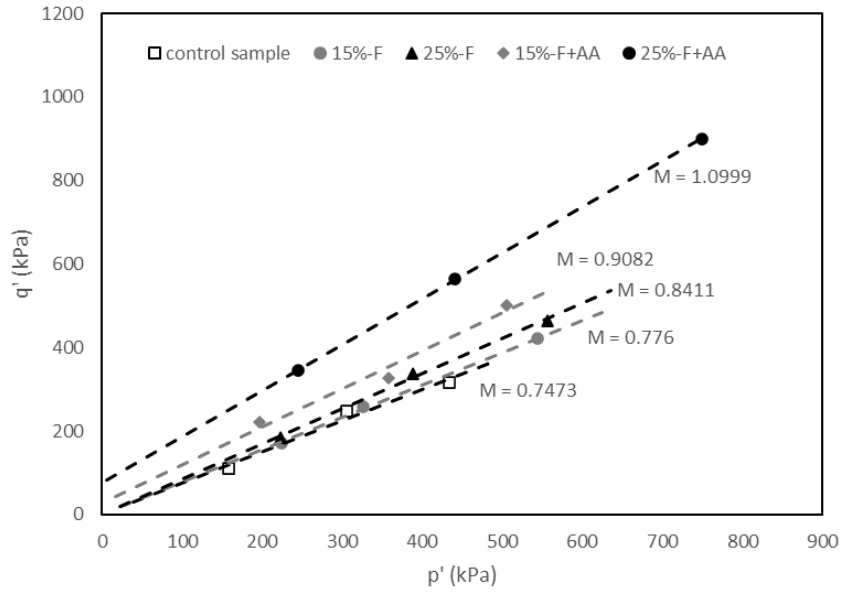

(b)

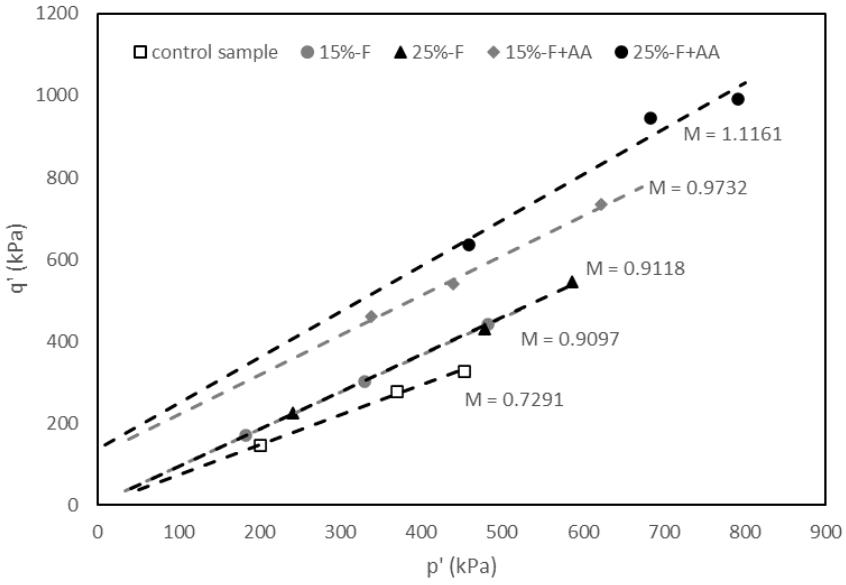

(c)

Figure 4.27 Critical state lines in q'-p' plane for the control sample, soils stabilised with alkali activated fly ash, and soils stabilised with fly ash at (a) 1 day of curing, (b) 7 days of curing, and (c) 28 days of curing.

Figures 4.28 (a-c) show the critical state lines in v-lnp' plane for the control sample and the samples stabilised with alkali activated fly ash and class F fly ash at 1, 7, and 28 days of curing, respectively. The parameters, λ and Γ, were calculated from the equation:

$$v = \Gamma - \lambda \ln (p') \quad (4.3)$$

where Γ is the value of v on the CSL at p' = 1 kPa and λ is the gradient of the CSL (Estabragh and Javadi, 2008).

λ is also related to the compression index (C_c) (Horpibulsuk et al, 2009) which represents the consolidation and settlement behaviour of the soil. According to the results, both λ and Γ decreased with the increase in the alkali activated fly ash at all curing times and with the increase in fly ash at 7 and 28 days of curing. A similar decreasing trend was reported by Kichou (2015) who applied triaxial tests on London clay stabilised with lime. The results indicate that the compressibility of the stabilised soil decreased with the addition of 15% and 25% alkali activated fly ash or fly ash. The results are in agreement with the results reported by Phanikumar and Sharma (2007), Kolay and Ramesh (2015) and Bryson et al (2017). However, for the soil stabilised with 15% and 25% class F fly ash at 1 day of curing, the parameter Γ increased from the control sample and thereafter, it decreased with increasing the curing times to 7 and 28 days. Phanikumar (2009) and Bryson et al (2017) reported that by increasing the class F fly ash, the compression index increased up to a certain point at 1 day of curing. This could be due to the lack of cementitious characteristics in class F fly ash. It can be concluded that, to reduce the compressibility of soils stabilised with class F fly ash, the curing time plays an important role.

The value of Γ was 2.48 for the control sample and it changed to 2.35 and 2.19 for the soil stabilised with 15% and 25% alkali activated fly ash and to 2.38 and 2.36 for the soil stabilised with 15% and 25% class F fly ash at 28 days of curing. The value of λ was 0.095 for the control sample and it changed to 0.075 and

0.053 for the soil stabilised with 15% and 25% alkali activated fly ash and to 0.079 and 0.075 for the soil stabilised with 15% and 25% class F fly ash at 28 days of curing. It can be observed that alkali activators have a significant effect in decreasing the compressibility characteristics of the stabilised soils.

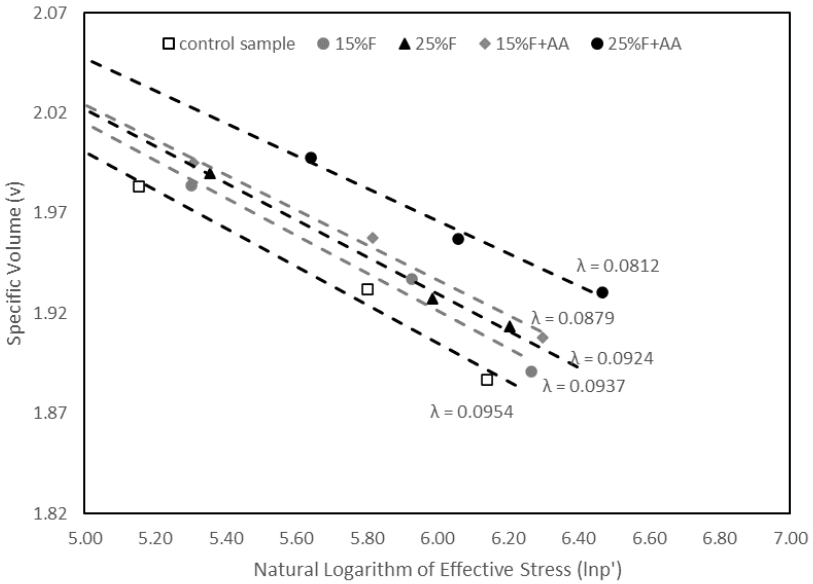

(a)

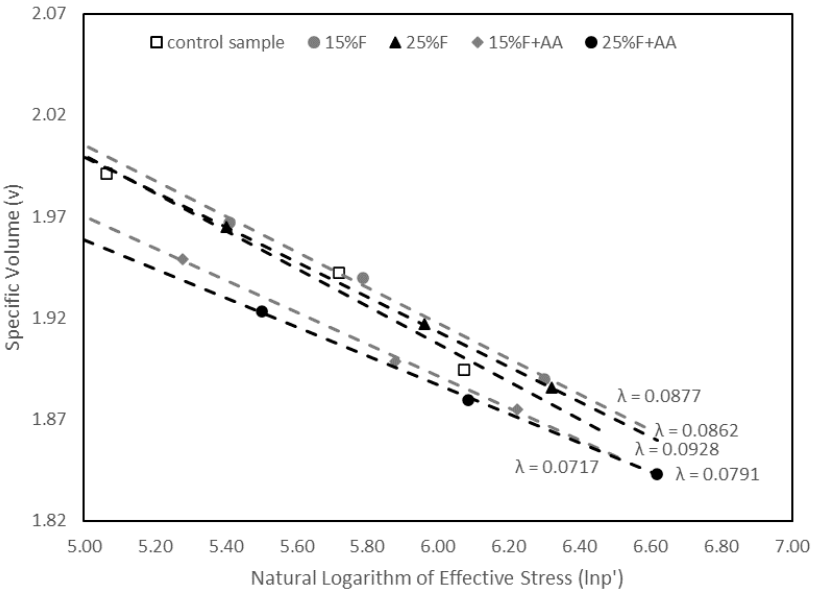

(b)

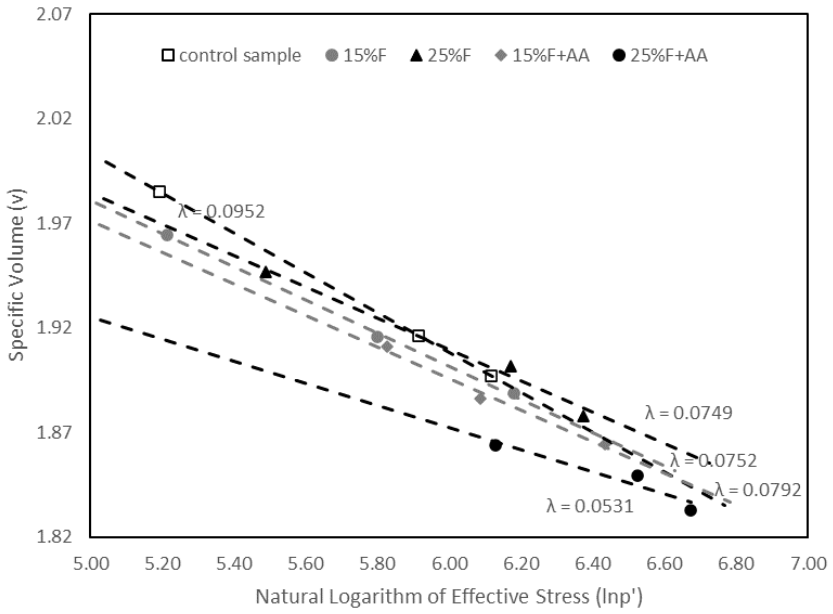

(c)

Figure 4.28 Critical state lines in v:lnp' plane for the control sample, and the samples of the soil stabilised with alkali activated fly ash and class F fly ash at (a) 1 day of curing; (b) 7 days of curing; and (c) 28 days of curing.

4.2.6 X-Ray diffraction analysis

The XRD patterns of the control sample (clay) and class F fly ash are shown in Section 3.2. The clay was mainly composed of crystalline kaolinite, illite, and quartz, while the fly ash showed mostly amorphous phase with some crystalline mullite and quartz.

Figure 4.29 shows the XRD patterns for fly ash, clay, and soils stabilised with 15% and 25% fly ash at different curing times. These patterns are used to analyse the change in mineralogy and crystalline structure. It is seen that there was no mineralogical change in the XRD patterns for the soil stabilised with fly ash only. However, the intensity of the sharp peaks detected at 2θ values of about 12° and 25° in crystalline kaolinite and 2θ value of 9° in illite slightly decreased with increasing the curing time and fly ash content. Additionally, the peaks of quartz

detected at 2θ values of 19° and 52° generally showed small changes with the curing time. Sun and Vollpracht (2018) indicated that the dissolution of minerals would occur under a high pH environment. Therefore, for soils stabilised with fly ash, the dissolution of kaolinite and illite may not be possible due to the neutral pH environment. Moreover, the dissolution of quartz is not expected under normal conditions due to its strong crystalline atomic bonds (Latifi et al, 2016). Thus, the slight decrease in the peak when the kaolinite is mixed with fly ash may be explained by the fact that the minerals become less concentrated due to dilution. The low amount of clay minerals in the peak intensities could support the decrease in the swelling properties of the clay soil (Parhi et al, 2017). The lack of mineralogical change in the XRD patterns for the soil stabilised with fly ash confirmed that no chemical reaction between clay minerals and class F fly ash occurred.

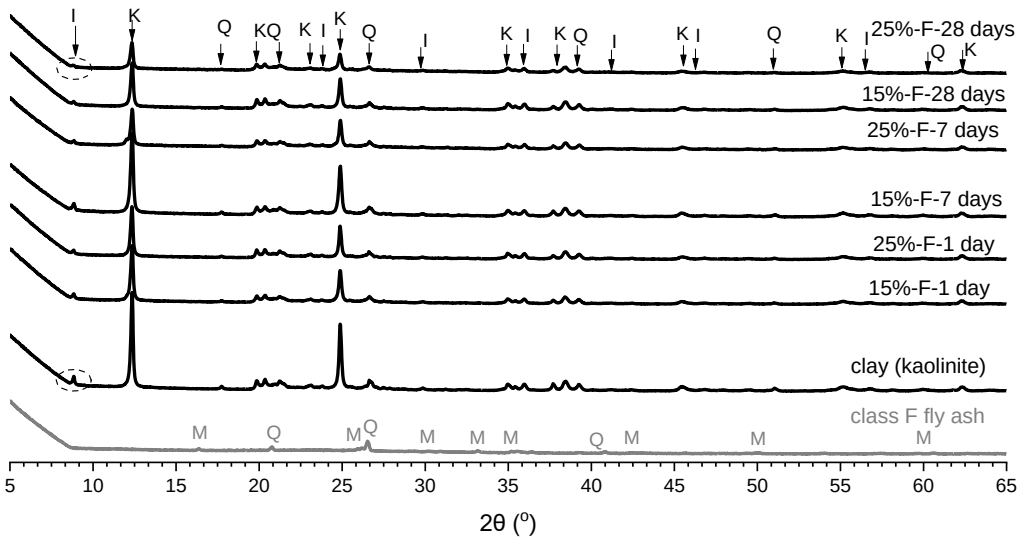

Figure 4.29 XRD patterns of fly ash, clay, and soils stabilised with 15% and 25% of class F fly ash at 1 day, 7 days, and 28 days of curing; I = illite, K = kaolinite, Q = quartz.

Figure 4.30 shows the XRD patterns for fly ash, clay, and soil stabilised with alkali-activated fly ash for M+ of 12% and SM of 1.25 at different curing times. A significant decrease in the peak intensities of kaolinite and illite was observed in

the stabilised soil at each curing time. Essentially, illite detected at 2θ values of 9°, 24°, and 47° was fully dissolved in the soil stabilised with 15% or 25% of alkali-activated fly ash at 28 days of curing. The dissolution of minerals in clay and the dissolution of fly ash lead to the formation of amorphous phase in the stabilised soil. This amorphous phase was observed as a broad hump in the XRD pattern detected at 2θ values of between 12° and 28° at 28 days of curing, as shown in Figure 4.31. This 'featureless hump' indicated the newly precipitated compounds due to the geopolymerisation as described by Duxson et al (2007). The new amorphous geopolymer phase detected at 2θ values of 12–28° indicated the formation of NASH gel (Ye and Radlinska, 2016; Marsh et al, 2018; Zawrah et al, 2018; Khan et al, 2020; Syed et al, 2020). On the other hand, no new crystalline phase was observed in the stabilised soil. Duxson et al (2007) argued that the transition from amorphous to crystalline phases of geopolymers is significantly affected by temperature, aging, and soluble silica amount. Based on their study, no new crystalline phases were observed with curing at 70 °C or 90 °C, whereas curing at 120 °C showed new crystalline phases. In addition, high level of soluble silica in the samples represented more amorphous and featureless humps in XRD analysis (Duxson et al, 2007).

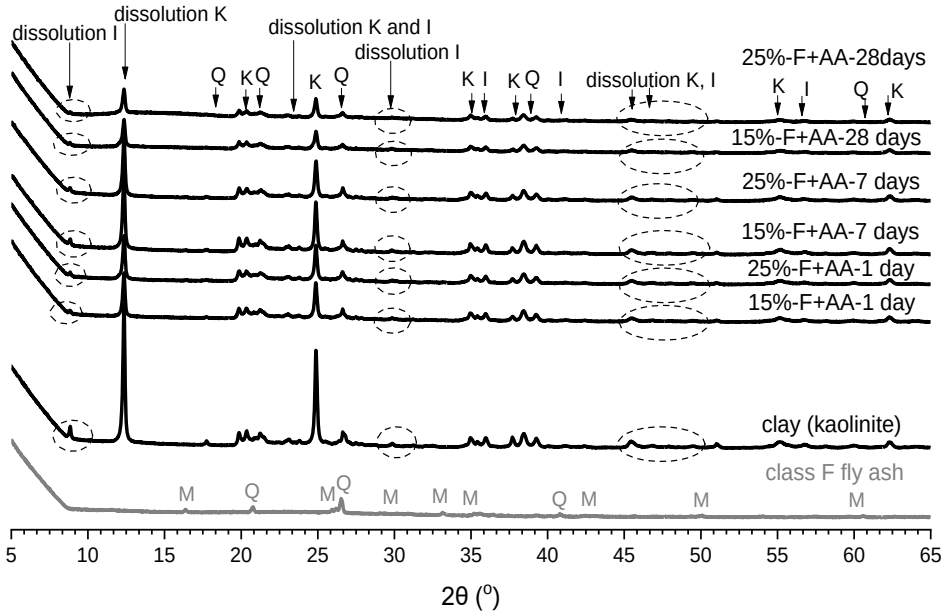

Figure 4.30 XRD patterns of fly ash, clay, and soil stabilised with 15% and 25% of alkali-activated fly ash at 1 day, 7 days, and 28 days of curing; I = illite, K = kaolinite, Q = quartz.

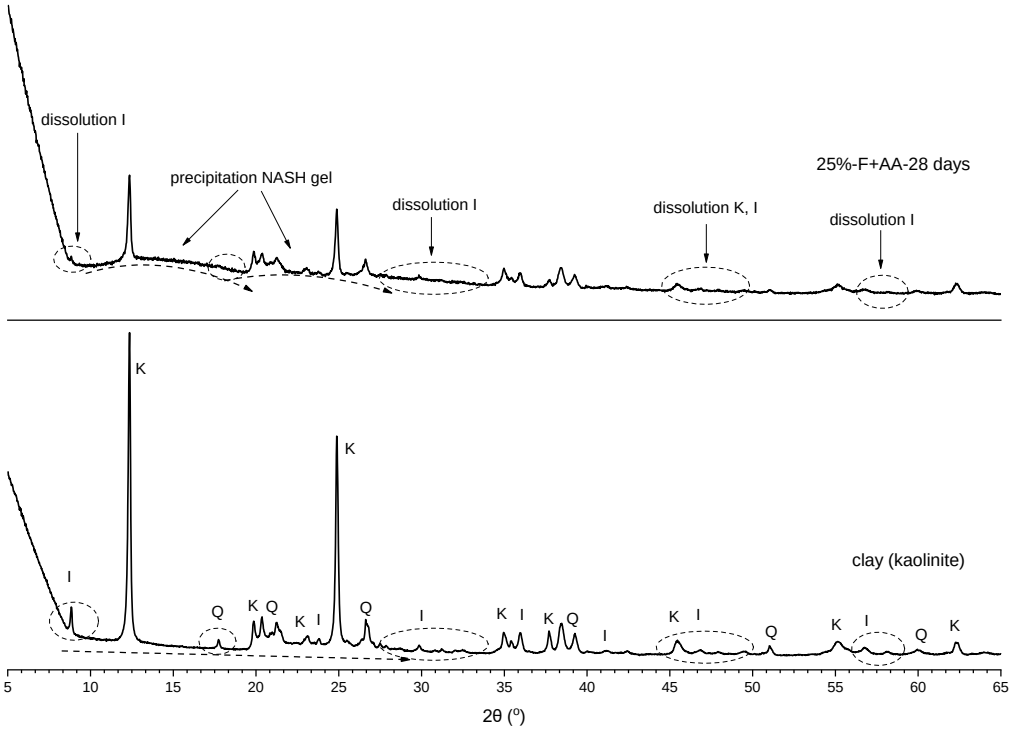

Figure 4.31 XRD patterns of clay and soil stabilised with 25% of alkali-activated fly ash at 28 days of curing; I = illite, K = kaolinite, Q = quartz.

In general, the soil stabilised with fly ash only, presented a slight decrease in the peaks of mainly kaolinite and illite during curing. On the other hand, the soil stabilised with alkali-activated fly ash presented high dissolution starting from 1 day to 28 days of curing. The dissolution of kaolinite and illite, followed by the formation of NASH gel, could correspond to the lower swelling properties and higher UCS in the soil stabilised with alkali-activated fly ash.

4.2.7 Scanning electron microscopy analysis

The microstructures of the soils stabilised with fly ash, and the soils stabilised with alkali-activated fly ash samples (M+ of 12% and SM of 1.25) are shown in Figures 4.32 and 4.33, respectively. Aggregated samples were used to observe the entire microstructure of the soil. The figures show the SEM images that are magnified to 2.00 kx. The microstructure of control sample is indicated in methodology section 3.2. The control sample shows the plate-like particles of the non-stabilised clay that was also reported by Abdullah et al (2020b). Generally, a regular microstructure was observed in the sample morphology.

Figures 4.32(a–f) show the results of the SEM analysis on the soils stabilised with class F fly ash only. Unreacted fly ash particles were observed in the stabilised soils at each curing time. This is because class F fly ash does not react in the absence of a suitable, high pH chemical environment. On the other hand, the presence of reaction products was observed at 7 and 28 days of curing due to the pozzolanic reactions (Figures 4.32(c–f)). Reaction products were observed in the SEM images due to enhanced pozzolanic reactions, similar to those reported by Raj et al (2018). Even though the reaction products observed in the system improved the mechanical properties of stabilised soil, the presence of unreacted

fly ash at 28 days of curing justified the insignificant improvement in the soils stabilised with class F fly ash. Turan et al (2022a) suggested that, due to the low Ca content, class F fly ash has limited cementitious properties; hence, class F fly ash is not able to react with soil in a significant way.

Figures 4.33(a-b) show the results for the soils stabilised with 15% and 25% of alkali-activated fly ash after 1 day of curing. The structure of the samples predominantly consisted of pores, hollow cavities, and unreacted/partially dissolved fly ash cenospheres. This is in agreement with the findings of Jaditager and Sivakugan (2017) and Syed et al (2020), who found pores in the stabilised soil at an early age. NASH cementitious products or geopolymer gels were also observed around the fly ash and clay particles in several parts of the samples; however, more cementitious products were formed with the increase in the fly ash content. Rios et al (2016) and Abdullah et al (2020) argued that aluminosilicate materials from the fly ash leach because of the highly alkaline environment in activators; hence, the spherical shape of some ash particles disappears due to the dissolution process. Thereafter, NASH cementitious products coat clay particles and the remaining fly ash particles. Figures 4.33(c-d) show the results for 7 days of curing for the soil stabilised with 15% and 25% alkali-activated fly ash. The morphologies of the samples were dominated by structured/aggregated clay particles connected by NASH geopolymer gels and unreacted/partially dissolved fly ash particles. Figures 4.33(e-f) show the results for 28 days of curing for the soil stabilised with 15% and 25% of alkali-activated fly ash. The samples were found to have a dense matrix structure. During the curing time, pores and hollow cavities were filled with cementitious products/geopolymer gels and a dense matrix was formed. This finding is in

agreement with those observed in previous studies on soils stabilised with alkali-activated fly ash (Phummiphan et al, 2016; Abdullah et al, 2018; Syed et al, 2020). Lin et al (2022) also indicated that the denser the microstructure, the higher the compressive strength, which is comparable with the findings in Section 4.2.3.

In general, the soils stabilised with fly ash did not present a significant improvement in the soil morphology, whereas by increasing the alkali-activated fly ash dosage and curing time, the samples showed a denser structure and fewer unreacted fly ash particles. The microstructural studies conducted on the soil stabilised with alkali-activated fly ash showed a reinforcement in the clay structure due to the formation of cementitious products during curing, which led to an improvement in compressive strength. In addition, the pores and hollow cavities found at the early curing time were filled with the cementitious products. The UCS results obtained in section 4.2.3 are in good agreement with the SEM analysis findings.

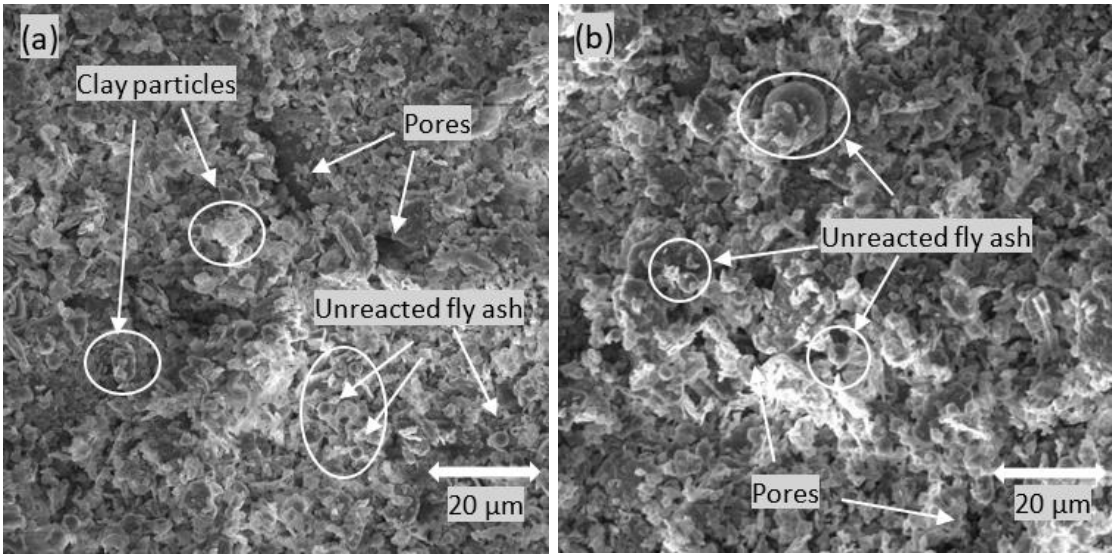

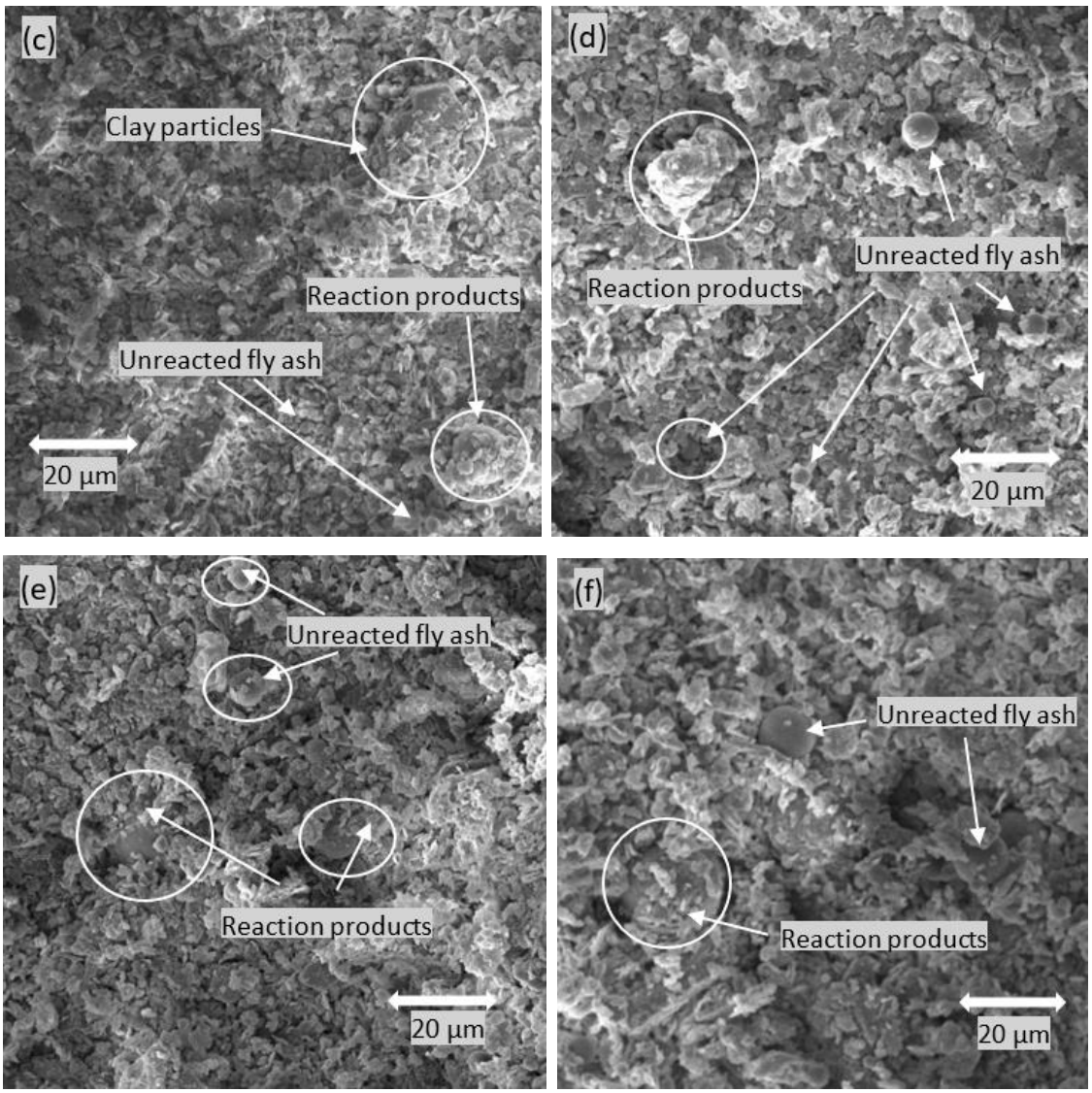

Figure 4.32 SEM images of soils stabilised with (a) 15% fly ash at 1 day of curing; (b) 25% fly ash at 1 day of curing; (c) 15% fly ash at 7 days of curing; (d) 25% fly ash at 7 days of curing; (e) 15% fly ash at 28 days of curing; and (f) 25% fly ash at 28 days of curing at 20 µm.

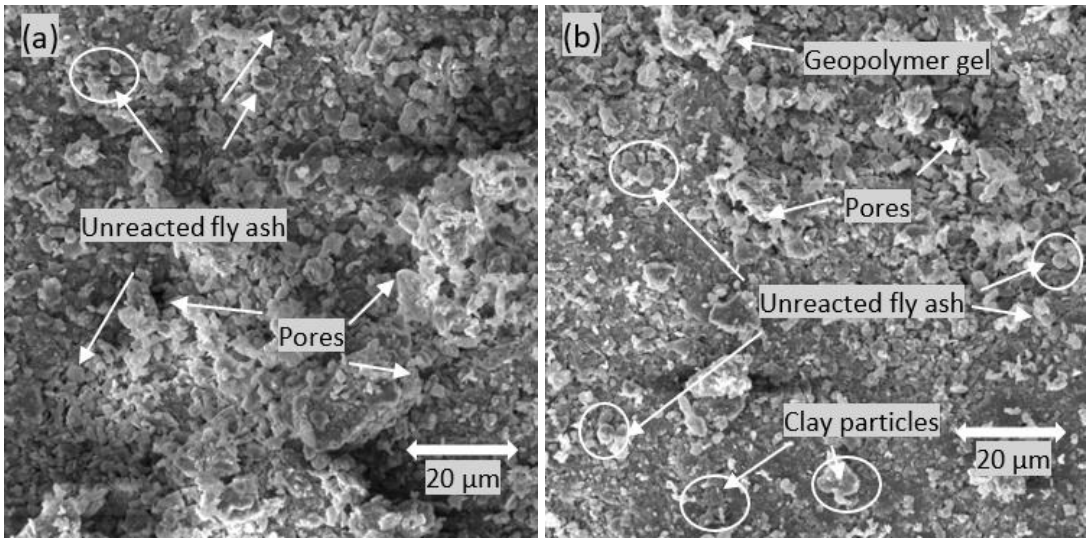

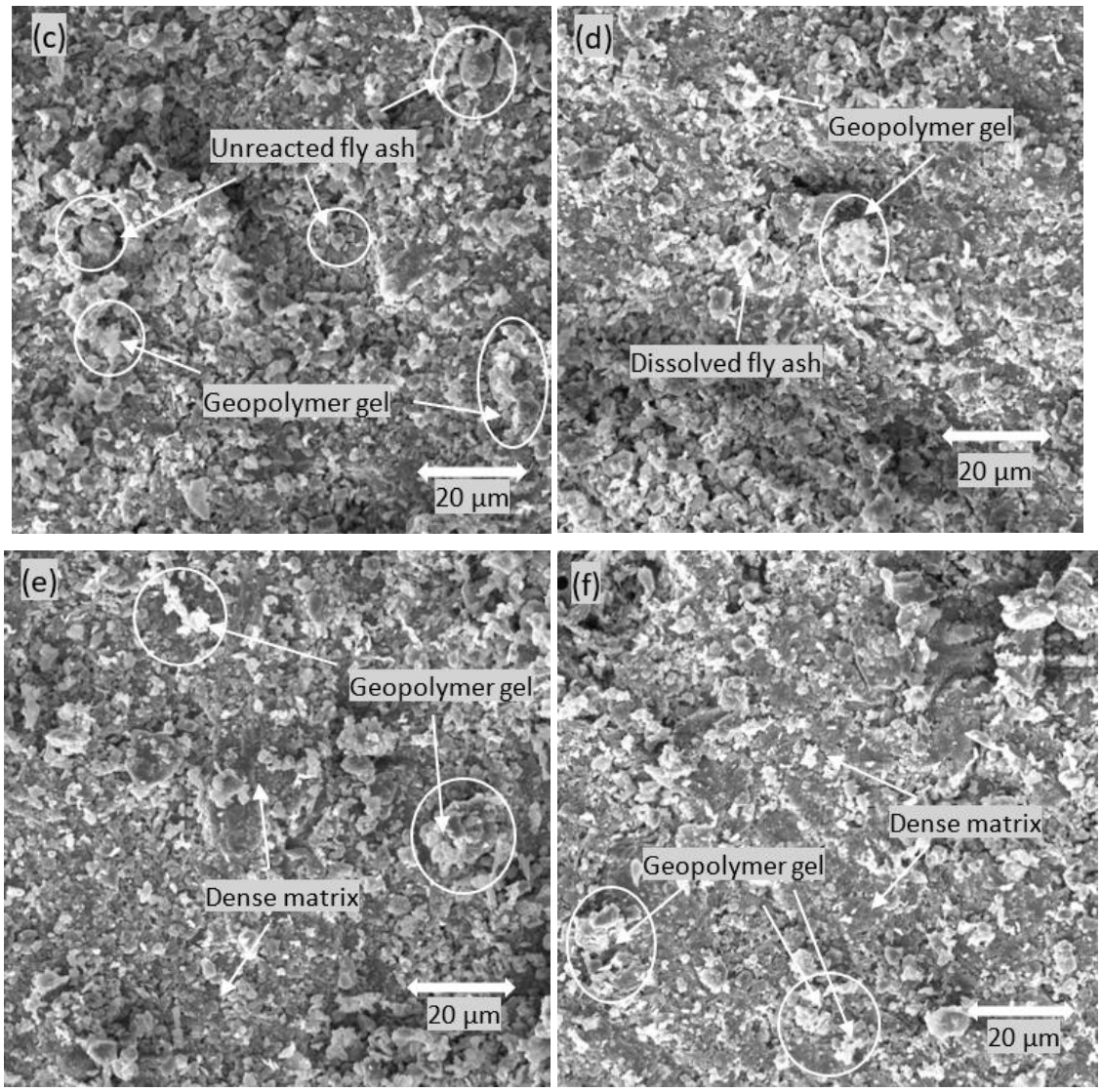

Figure 4.33 SEM images of soils stabilised with (a) 15% of alkali-activated fly ash at 1 day of curing; (b) 25% of alkali-activated fly ash at 1 day of curing; (c) 15% of alkali-activated fly ash at 7 days of curing; (d) 25% of alkali-activated fly ash at 7 days of curing; (e) 15% of alkali-activated fly ash at 28 days of curing; and (f) 25% of alkali-activated fly ash at 28 days of curing at 20 µm.

4.2.8 Summary of the findings

This section investigated the effects of class F fly ash with and without alkali activators (SH and SS) as stabilisation additives on the compaction, consolidation, strength, mineralogical, and microstructural behaviour of clay soil at different curing times. The effects of class F fly ash on the tests were also studied to highlight the effects of alkali activators. The following outcomes can be summarised from the results obtained in this section:

- The control sample had higher MDD and lower OMC than the soil stabilised with fly ash and the soil stabilised with alkali-activated fly ash. The modest increase in MDD ranging from 14.3 to 14.7 kN/m3 and the modest decrease in OMC ranging from 23.8 to 21.6% were observed with the increase in M+ and SM.
- The UCS of the soil increased with the addition of alkali activators, fly ash content, and the curing time. The highest UCS result was found with 25% fly ash content, M+ of 16% and SM of 1.25 at 28 days of curing which can improve the UCS by about 6.3 times over the control sample.
- M+ = 12% was found to be optimal at 1 day of curing, whereas M+ = 16% gave the highest strengths at 7 and 28 days of curing. However, the increase of UCS from M+ of 12% to M+ of 16% was generally found to be marginal; thus M+ = 12% was chosen for further tests.
- SM = 1.25 resulted in the highest strength improvement at 7 and 28 days of curing, and was therefore chosen for further tests.
- The compression index of the soil decreased with the addition of fly ash or alkali activated fly ash and with curing time (except for the soil stabilised by fly ash only, at 1-day curing time). The value of C_c of the soil showed a slight increase with addition of 15% fly ash, and thereafter decreased with 25% fly ash at 1 day curing time.
- The swelling index of the soil decreased with the addition of fly ash or alkali activated fly ash and with curing time due to the non-swelling and pozzolanic characteristics of fly ash.

- The permeability of the soil stabilised with alkali activated fly ash was greater than the control sample at early curing times. However, the value of k decreased as the time progressed and it became less permeable compared to the control sample. The void ratio of the stabilised soil indicated a similar trend to permeability.
- Curing time had a significant effect in improving deviator stress on soils stabilised with alkali activated fly ash, essentially from 7 to 28 days of curing. The increase of curing time and the addition of alkali activated fly ash to the soil increased the maximum deviator stress considerably. On the other hand, in the soils stabilised with class F fly ash only, the increase of maximum deviator stress was found insignificant with the increase of curing time and fly ash content.
- The addition of alkali activated fly ash to the soil modified the stress-strain behaviour from typical ductile to brittle stress-strain response at 28 days of curing. The increase of alkali activated fly ash from 15% and 25% showed much stiffer and sudden post-peak strain-softening response at 28 days of curing, whereas the stress-strain behaviour had ductile response for all samples stabilised with fly ash only. With the increase of confining pressure, the maximum deviator stress and excess pore water pressure increased for soils stabilised with alkali activated fly ash or fly ash only.
- The effective cohesion of soils stabilised with alkali activated fly ash increased significantly with the increase of fly ash content and curing time. This was due to the effects of geopolymerisation bonding. However, the soils stabilised with class F fly ash had lower c’ than the control sample

due to their silty characteristics and low amount calcium contents for cementation bonding. The values of φ' increased with the addition of fly ash or alkali activated fly ash and with the increase of curing time.

- Increasing fly ash or alkali activated fly ash and curing time increased the M parameter. Also, an increase was observed in y-intercept of the CSL for soils stabilised with alkali activated fly ash at 7 and 28 days of curing due to the cementation effects. The values of λ and Γ decreased with increase in alkali activated fly ash content and with curing time. However, for the soil stabilised with class F fly ash, Γ initially increased at 1 day of curing, followed by a decrease at 7 and 28 days of curing.
- The XRD analysis showed that, in the soil stabilised with fly ash, the peak intensities of kaolinite and illite slightly decreased at 28 days of curing, whereas in the soil stabilised with alkali-activated fly ash, the peak intensities of kaolinite and illite significantly decreased at all curing times.
- For the soils stabilised with alkali-activated fly ash, the microstructure of the soil was altered with the addition of alkali-activated fly ash, resulting in pores and hollow cavities at an early age. During the curing, aggregated-coarser particles were observed, leading to a denser fabric. On the other hand, the soils stabilised with fly ash showed insignificant microstructural changes.

In general, it was observed that stabilisation with alkali-activated fly ash had significantly positive effects on the mechanical properties of the clay soil. Therefore, it could replace ordinary Portland cement in soil stabilisation projects. Further studies on the environmental impacts and a durability assessment are

recommended to understand the applicability of soils stabilised with alkali-activated fly ash.

Chapter 5 Conclusions and recommendations for future work

Utilisation of clay soils without any consideration is very risky in geotechnical engineering projects due to their low strength and high compressibility, and it could cause differential settlement. Hence, stabilisation methods are required to improve the clay properties. Chemical stabilisation is one of the common methods that provides enhanced interfacial strength between soil particles and binders (Ghadir and Ranjbar, 2018). OPC and lime are the most commonly used chemical binders to stabilise soils (Turan et al, 2019). However, utilisation of cement or lime as a binder is becoming unsustainable owing to their greenhouse gas emissions like carbon dioxide (CO_2) and nitric oxide (NOx) during their manufacturing process (Murmu et al, 2018; Wong et al, 2019). The manufacture of OPC is estimated to cause approximately 7 - 10% of CO_2 emissions annually (Parhi et al, 2018; Abdullah et al, 2019a; Abdullah et al, 2020b). Therefore, binders with lower environmental impacts have been investigated by many researchers to decrease greenhouse gas emissions and to compete with OPC or lime (Parhi et al, 2018; Wong et al, 2019). Industrial by-products such as fly ash have been used as alternative binders due to their low-emission properties. Although there have been many studies on the behaviour of fly ash stabilised soils using several soil tests, such as, compaction, UCS, and CBR, there is a lack of study mainly on triaxial and consolidation behaviours of soils stabilised with fly ash. Also, there is no available literature to clarify the different effects of class C and class F fly ash on triaxial, consolidation, and microstructural behaviour of stabilised soils. Therefore, the first research area of the thesis included a comparative study of class C and class F fly ash in clay stabilisation. A detailed

experimental programme including compaction, UCS, triaxial, and one-dimensional consolidation tests and SEM analysis was carried out.

According to the results described in section 4.1, class C fly ash is more efficient in improving the mechanical properties of soils in comparison with class F fly ash. Also, in the literature, insufficient mechanical properties have been reported by using only class F fly ash in comparison with cement. Hence, geopolymers, (as synthetic alkali aluminosilicates) (Behnood et al, 2018) were recommended as innovative binders, due to their excellent mechanical properties and the possible reduction of binder-related environmental impacts (Pacheco-Torgal et al, 2007a; Benhood et al, 2018; Parhi et al, 2018; Yaghoubi et al, 2019; Wong et al, 2019). In addition, compared to cement-based binders, geopolymers can have more resistance to chemical attacks such as chloride, sulphate, and acid attacks, hence the durability of geopolymer based materials is high (Rios et al, 2016a). Therefore, the second research area of the thesis (section 4.2) included physical, mechanical, microstructural, and mineralogical behaviour of soils stabilised with alkali activated fly ash. The dosage factors SM and M+ were used to assess the effects of alkali activator concentration on compaction and UCS. After obtaining optimal dosages from the UCS, triaxial and consolidation tests, and SEM and XRD analysis were carried out. Comparison was also made with soils stabilised with class F fly ash to appreciate the effects of alkali activators.

5.1 Conclusions

The aim of the research was to study the behaviour of clay soils when stabilised with class C fly ash, class F fly ash, or alkali activated class F fly ash, through compaction, UCS, triaxial, and consolidation tests as well as SEM and XRD analysis. With respect to this aim, from the results presented in this thesis, the following key conclusions can be drawn regarding the addition of class C and class F fly ash to clay soil (Section 4.1):

- The addition of class C fly ash or class F fly ash to soil leads to decrease in maximum dry density and increase in optimum moisture content.
- UCS of soil increases with the addition of fly ash, however, class C fly ash is more effective in comparison with class F fly ash.
- The increase of curing time has a positive effect on the UCS of soil due to the time-dependent pozzolanic properties of fly ash.
- The optimal fly ash content (based on the weight of dry soil) is found to be 25% for class C fly ash or class F fly ash.
- Class C fly ash increases effective cohesion, whereas class F fly ash decreases the cohesion.
- The angle of shearing resistance of the soil improves with increasing the class C fly ash or class F fly ash content.
- The increase in class C fly ash or class F fly ash leads to an increase in the gradient of the critical state line.
- Curing time improves the shear strength and critical state line parameters.
- Swelling index, compression index, and coefficient of volume compressibility generally decrease with the addition of class C fly ash or class F fly ash, and with the increase of curing time.

- Coefficient of consolidation and permeability increase with the addition of class C fly ash or class F fly ash; both values decrease with the increase of curing time.
- SEM analysis confirms the gradual improvement observed in the mechanical properties of soils stabilised with class C fly ash or class F fly ash with the curing time. However, more reaction products and denser fabric can be observed in soils stabilised with class C fly ash than soils stabilised with class F fly ash.

In general, class C fly ash is more effective in improving the mechanical and microstructural properties of the soil compared to class F fly ash. Therefore, class C fly ash can be used effectively in the stabilisation of clay soils. Class F fly ash can be used with the other additives such as slag, lime or alkali activators to achieve higher mechanical properties in clay soils.

The following key conclusions can be drawn regarding the addition of alkali activated class F fly ash or class F fly ash to soils (Section 4.2):

- A modest increase in maximum dry density and a modest decrease in optimum moisture content is observed with the increase of alkali dosages and silica modulus for soil stabilised with alkali activated fly ash; the control sample has the highest maximum dry density and lowest optimum moisture content.
- Alkali activated fly ash significantly increases UCS of the soil.
- Very high or low alkali dosages and silica modulus are not suitable to maximise the UCS.
- Alkali dosage of 12% and silica modulus of 1.25 can be recommended as optimal dosages of activator concentration.

- Curing time has considerable effect on improving UCS of soils stabilised with alkali activated fly ash.
- Compression index and swelling index of soil decrease with the addition of alkali activated fly ash and with the increase of curing time.
- Permeability and void ratio of stabilised soil are higher than the control sample at an early age, however, the values decrease with the curing time.
- Yield stress of soil increases significantly with the addition of alkali activated fly ash and with curing time.
- Maximum deviator stress, shear strength, and critical state parameters of the soil improve with the increase of alkali activated fly ash and curing time. Essentially, curing time has a significant effect in improving cohesion of alkali activated fly ash stabilised soils.
- Alkali activated fly ash modifies the stress-strain behaviour from ductile to brittle response at 7 and 28 days of curing.
- The increase of alkali activated fly ash and curing time leads to denser soil matrix.
- Alkali activated fly ash significantly decreases the peak intensities of kaolinite and illite in the stabilised soil at all curing times, and leads to full dissolution, precipitation, and formation of NASH products at 28 days of curing. On the other hand, class F fly ash shows marginal decrease in the peak intensities of kaolinite and illite in the stabilised soil.

5.2 Original contributions to the knowledge

The main innovation and original contributions to the knowledge in the field of soil stabilisation with fly ash are presented below:

- The fundamental knowledge of how class C and class F fly ash influence the overall shear, consolidation, and microstructural behaviour of soils was addressed. The lack of study was stated in the literature on soils stabilised with both fly ash types in terms of triaxial and consolidation parameters. A comparison of soils stabilised with class C and class F fly ash was discussed through an experimental programme including triaxial and consolidation tests. The outcome of the results covered the current understanding of the effects of class C and class F fly ash on the triaxial and consolidation behaviour as well as microstructural characteristics of stabilised soils.
- For the soils stabilised with alkali activated fly ash, dosage parameters borrowed from alkali activated cement technology, i.e., alkali dosages (M+) and silica modulus (SM), were used to find optimal parameters in stabilised soils. The previous studies indicated promising results in soils stabilised with alkali activated fly ash. The dosage factors SS/SH and alkali activator solution/fly ash ratios have been traditionally used in the literature to find optimal parameters. However, based on the literature in Section 2.5.2, it was deduced that using SS/SH ratio as dosage factor is insufficient for meaningful comparisons between various investigations. This is because SS and SH solutions produced for the use of alkali activated binders are commercially available with different chemical compositions. The factors M+ and SM described in the geopolymer concrete studies

could bridge this gap, however, no study using these parameters was found in the soil stabilisation field. The effects of dosage factors M+ and SM were discussed using various M+, SM, and fly ash content through compaction and UCS tests, and the optimal dosages of M+ and SM were proposed to achieve desired strength in soil stabilisation.

- The stress-strain behaviour, shear strength, critical state, and consolidation parameters of soils stabilised with alkali activated fly ash were discussed through isotropically consolidated-undrained triaxial and one-dimensional consolidation tests. XRD and SEM analyses were conducted on soils stabilised with alkali activated fly ash to characterise the mineralogical and microstructural properties of stabilised soils. The new optimal dosage factors of the stabilised soils obtained from UCS tests in Section 4.2.3 were used. The literature showed that UCS test was commonly used because of its ease to characterise the strength characteristics of stabilised soils. However, due to the lack of control over drainage conditions, the UCS test has drawback in the accurate prediction of load-deformation responses. Triaxial test simulates the effects of confining pressure and pore water pressure that are important in determining strength parameters. A limited study was found available on the broader mechanical properties of soils stabilised with alkali activated fly ash, such as, stress-strain, undrained shear, and consolidation behaviour. The outcome of the results using the factors of M+ and SM in the analysis of triaxial and consolidation tests covered this knowledge gap.

5.3 Recommendations for future work

This study carried out a comprehensive investigation into the use of waste materials or waste materials with alkali activation as alternative binders in clay soil stabilisation. However, further research areas that need to be covered in future research as recommended below:

- The investigations of the behaviour of soils stabilised with fly ash or alkali activated fly ash were conducted at laboratory scale. Further research is required to carry out large-scale or field tests for a better understanding of the in-situ behaviour of fly ash- or alkali activated fly ash-stabilised soils. In this way, the effects of scale on the behaviour of soil can be evaluated.
- The reuse of fly ash may contribute to some cost savings in many soil stabilisation applications, but cost-benefit analysis of fly ash is found to be limited in the literature. Therefore, cost-benefit analysis of fly ash against traditional construction materials can be recommended to increase the utilisation of fly ash.
- Although many geotechnical characteristics of soils stabilised with alkali activated fly ash were investigated through the extensive experimental programme of this study, the effects of the stabilised soils on other properties, such as, CBR and permeability can be investigated. The review of the literature indicates that there are studies conducting CBR tests on soils stabilised with fly ash. However, there is a lack of studies on CBR tests for soils stabilised with alkali activated fly ash.
- Class C fly ash or alkali activated fly ash were found to be effective binders to stabilise clay soils. Future research is needed to study the use of these binders on other problematic soils, such as fine sand or silty soils, to

analyse how different type of soils affect the geotechnical properties of stabilised soils.

- Geopolymerisation can immobilise the heavy metals in soil matrix. Therefore, no contamination or pollution can be transported to the environment or water systems. Leaching tests can be recommended to verify and support the environmentally friendly aspect of the binders, along with the rigorous assessment of possible environmental impacts through Life Cycle Assessment (LCA) methods.
- In this study, the microstructural properties were analysed by conducting SEM tests. To provide more evidence in terms of observing the types of reaction products, EDS analysis together with SEM can be highly recommended.
- There is a lack of study in the literature on the durability of soils stabilised with alkali activated fly ash. Thus, to understand the applicability of soils stabilised with alkali activated fly ash, studying on wetting-drying and freeze-thaw cycles can be suggested.

References

Abdila, S., Abdullah, M., Ahmad, R., Rahim, S., Rychta, M., Wnuk, I., Nabiałek, M., Muskalski, K., Tahir, M., & Isradi, M., et al. (2021). Evaluation on the Mechanical Properties of Ground Granulated Blast Slag (GGBS) and Fly Ash Stabilized Soil via Geopolymer Process. Materials, 14, 2833. https://doi.org/10.3390/ma14112833.

Abdullah, M. M. A., Hussin, K., Bnhussain, M., Ismail, K. N., & Ibrahim, W. M. W. (2011). Mechanism and Chemical Reaction of Fly Ash Geopolymer Cement—A Review. *International Journal of Pure and Applied Sciences and Technology, 6*, 35–44.

Abdullah, H.H., Shahin, M.A., & Sarker, P. (2018). Use of Fly-Ash Geopolymer Incorporating Ground Granulated Slag for Stabilisation of Kaolin Clay Cured at Ambient Temperature. *Geotechnical and Geological Engineering*, *37*, 721–740. https://doi.org/10.1007/s10706-018-0644-2.

Abdullah, H. H., Shahin, M. A., & Walske, M. L. (2019a). Geo-mechanical behavior of clay soils stabilized at ambient temperature with fly-ash geopolymer-incorporated granulated slag. *Soils and Foundations*, *59*, 1906–1920. https://doi.org/10.1016/j.sandf.2019.08.005.

Abdullah, H. H., Shahin, M. A., Walske, M. L., & Karrech, A. (2019b). Systematic approach to assessing the applicability of fly-ash-based geopolymer for clay stabilization. *Canadian Geotechnical Journal, 57,* 1356-1368. dx.doi.org/10.1139/cgj-2019-0215.

Abdullah, H.H., Shahin, M.A., Walske, M.L., Karrech, A. (2020b). Cyclic behaviour of clay stabilised with fly-ash based geopolymer incorporating ground granulated slag. *Transportation Geotechnics, 26*, 100430. https://doi.org/10.1016/j.trgeo.2020.100430.

Ahmaruzzaman, M. (2010). A review on the utilization of fly ash. *Progress in Energy and Combustion Science,* 36(3), 327-363. https://doi.org/10.1016/j.pecs.2009.11.003.

Al Bakri, A. M., Faheem, T. M., Sandhu, A. V., Alida, A., Salleh, M. A. A. M., & Ruzaidi, C. (2013). Microstructure Studies on Different Types of Geopolymer Materials. *Applied Mechanics and Materials*, *421*, 384–389. https://doi.org/10.4028/www.scientific.net/amm.421.384.

Amiralian, S., Chegenizadeh, A., & Nikraz, H. (2012a, December 18-19). *Laboratory Investigation on the Effect of Fly Ash on the Compressibility of Soil.* International Conference on Civil and Architectural applications, Phuket, Thailand.

Amiralian, S., Chegenizadeh, A., & Nikraz, H. (2012b). A Review on the Lime and Fly ash Application in Soil Stabilization. *International Journal of Biological, Ecological and Environmental Sciences (IJBEES) 1,* 3.

Asokan, P., Saxena, M., & Asolekar, S. R. (2005). Coal combustion residues-environmental implications and recycling potentials. *Resources, Conservations, and Recycling, 43*(3), 239-262. https://doi.org/10.1016/j.resconrec.2004.06.003.

ASTM C618-05, (2005). Standard Specification for Coal Fly Ash and Raw or Calcined Natural Pozzolan for Use in Concrete. ASTM International, West Conshohocken, United States, www.astm.org.

ASTM D2435-11, (2011). Standard Test Methods for One-Dimensional Consolidation Properties of Soils Using Incremental Loading. ASTM International, West Conshohocken, United States.

ASTM D4767-11, (2011). Standard Test Method for Consolidated Undrained Triaxial Compression Test for Soils Cohesive. ASTM International, West Conshohocken, United States.

ASTM D7762-18, (2018). Standard Practice for Design of Stabilization of Soil and Soil-Like Materials with Self-Cementing Fly Ash. ASTM International, West Conshohocken, United States, www.astm.org.

Azimi, E. A., Abdullah, M. M. A. B., Vizureanu, P., Salleh, M. A. A. M., Sandu, A. V., Chaiprapa, J., Yoriya, S., Hussin, K., & Aziz, I. H. (2020). Strength Development and Elemental Distribution of Dolomite/Fly Ash Geopolymer Composite under Elevated Temperature. *Materials*, *13*, 1015. https://doi.org/10.3390/ma13041015.

Barišić, I., Grubeša, I. N., Dokšanović, T., & Marković, B. (2019). Feasibility of Agricultural Biomass Fly Ash Usage for Soil Stabilisation of Road Works. *Materials*, *12*, 1375. https://doi.org/10.3390/ma12091375.

Behnood, A. (2018). Soil and clay stabilization with calcium- and non-calcium-based additives: A state-of-the-art review of challenges, approaches and techniques. *Transportation Geotechnics, 17*, 14-32. https://doi.org/10.1016/j.trgeo.2018.08.002.

Bhatt, A., Priyadarshini, S., Mohanakrishnan, A. A., Abri, A., Sattler, M., & Techapaphawit, S. (2019). Physical, chemical, and geotechnical properties of coal fly ash: A global review. *Case Studies in Construction Materials*, *11*, e00263.

Bhuvaneshwari, S., Robinson, R. G., & Gandhi, S. R. (2005). *Fly Ash Utilization Programme (FAUP)* TIFAC, DST, New Delhi – 110016.

Binal, A. (2016). The Effects of High Alkaline Fly Ash on Strength Behaviour of a Cohesive Soil. *Advances in Materials Science and Engineering, 2016,* 1-11. doi: 10.1155/2016/3048716.

Bin-Shafique, S., Edil, T., Benson, C., & Senol, A. (2004). Incorporating a fly-ash stabilised layer into pavement design. *Proceedings of the Institution of Civil Engineers: Geotechnical Engineering*, *157*(GE4), 239-249. doi: 10.1680/geng.157.4.239.51822.

Bin-Shafique, S., Rahman, K., Yaykiran, M., & Azfar, I. (2009). The long-term performance of two fly ash stabilized fine-grained soil subbases. *Resources, Conservation and Recycling, 54*(10), 666-672. doi: 10.1016/j.resconrec.2009.11.007.

Boral Resources, (2018). *Fly Ash Slides for Investors*. https://flyash.com/.

Bowles, J.E. (1992). *Engineering Properties of Soils and Their Measurement*. McGraw-Hill, New York, NY.

Borm, P. J. A. (1997). Toxicity and occupational health hazards of coal fly ash (CFA). A review of data and comparison to coal mine dust. *The Annals of Occupational Hygiene*, *41*(6), 659-676. https://doi.org/10.1016/S0003-4878(97)00026-4.

Britpave (2017). *Soil improvement and soil stabilization. Definitive industry guide.* https://www.britpave.org.uk/Publications/Soil-Stabilisation/.

Brooks, R. M. (2009). Soil stabilization with Fly ash and Rice Husk Ash. *International Journal of Research and Reviews in Applied Sciences, 1*(3).

Bryson, L. S., Mahmoodabadi, M., Adu-Gyamfi, K. (2017). Prediction of Consolidation and Shear Behavior of Fly Ash–Soil Mixtures Using Mixture Theory. *Journal of Materials in Civil Engineering, 29*(11), 04017222. doi: 10.1061/(asce)mt.1943-5533.0002077.

BS 1377-2, (1990). Methods of Test for Soils for Civil Engineering Purposes. Classification Tests, BSI Standard Publications: London, UK.

BS 1377-4, (1990). Methods of Test for Soils for Civil Engineering Purposes. Compaction-Related Tests, BSI Standard Publications: London, UK.

BS 1377-5, (1990). Methods of Test for Soils for Civil Engineering Purposes. Compressibility, permeability, and durability tests. BSI Standard Publications: London, UK.

BS 1377-7, (1990). Methods of Test for Soils for Civil Engineering Purposes. Shear strength tests (total stress), BSI Standard Publications: London, UK.

BS 1377-8, (1990). Methods of Test for Soils for Civil Engineering Purposes. Shear strength tests (effective stress), BSI Standard Publications: London, UK.

BS EN 16907-4, (2018). Earthworks Part 4: Soil treatment with lime and/or hydraulic binders, British Standard Institution.

BS EN ISO 14688-2, (2018). Geotechnical Investigation and Testing– Identification and Classification of Soil, Part 2: Principles for a Classification. British standard institution: London, UK.

BS ISO 21748, (2017). Guidance for the use of repeatability, reproducibility, and trueness estimates in measurement uncertainty evaluation. British standard institution: London, UK.

Chew, S., Kamruzzaman, A., & Lee, F. (2004). Physicochemical and Engineering Behavior of Cement Treated Clays. *Journal of Geotechnical and Geoenvironmental Engineering, 130*(7), 696-706. doi: 10.1061/(asce)1090-0241(2004)130:7(696).

Chi, M. (2015). Effects of modulus ratio and dosage of alkali-activated solution on the properties and micro-structural characteristics of alkali-activated fly ash mortars. *Construction and Building Materials, 99*, 128–136. https://doi.org/10.1016/j.conbuildmat.2015.09.029.

Çokça, E. (2001). Use of Class C Fly Ashes for the Stabilization of an Expansive Soil. *Journal of Geotechnical and Geoenvironmental Engineering, 128*(11), 966-966. doi: 10.1061/(asce)1090-0241(2002)128:11(966).

Consoli, N. C., Lopes, L. S., Rosa, A. D., & Masuero, J. R. (2012). The strength of soil–industrial by-products–lime blends. *Proceedings of the Institution of Civil Engineers Geotechnical Engineering, GE5*,431-440. http://dx.doi.org/10.1680/geng.10.00130.

Consoli, N. C., Rocha, C. G., & Saldanha, R. B. (2014). Coal fly ash–carbide lime bricks: An environment friendly building product. *Construction and Building Materials, 69*, 301-309. http://dx.doi.org/10.1016/j.conbuildmat.2014.07.067.

Consoli, N. C., Filho, H. C. S., Godoy, V. B., Rosembach, C. M. D. C., & Carraro, A. H. (2018). Durability of reclaimed asphalt pavement–coal fly ash–carbide lime blends under severe environmental conditions. *Road Materials and Pavement Design.* https://doi.org/10.1080/14680629.2018.1506354

Correa-Silva, M., Araujo, N., Cristelo, N., Miranda, T., Gomes, A. T., & Coelho, J. (2018). Improvement of a clayey soil with alkali activated low-calcium fly ash for transport infrastructures applications*. Road Materials and Pavement Design, 20*(8), 1912-1926. https://doi.org/10.1080/14680629.2018.1473286.

Correa-Silva, M., Miranda, T., Rouainia, M., Araujo, N., Glendinning, S., & Cristelo, N. (2020). Geomechanical behaviour of a soft soil stabilised with alkali-activated blast-furnace slags. *Journal of Cleaner Production, 267,* 122017.

Craig, R. F. (2004). *Craig's Soil Mechanics.* Seventh edition. Spon Press-Taylor and Francis Group, London and New York.

Dahale, P., Nagarnaik, P., & Gajbhiye, A. (2017). Engineering Behavior of Remolded Expansive Soil with Lime and Fly ash. *Materials Today: Proceedings 4*(9), 10581-10585. doi: 10.1016/j.matpr.2017.06.423.

Damrongwiriyanupap, N., Srikhamma, T., Plongkrathok, C., Phoo-Ngernkham, T., Sae-Long, W., Hanjitsuwan, S., Sukontasukkul, P., Li, L.-Y., & Chindaprasirt, P. (2022). Assessment of equivalent substrate stiffness and mechanical

properties of sustainable alkali-activated concrete containing recycled concrete aggregate. *Case Studies in Construction Materials 16*, e00982. https://doi.org/10.1016/j.cscm.2022.e00982.

Davidovits, J. (1994). Properties of Geopolymer Cements. *In Proceedings of the First International Conference on Alkaline Cements and Concretes, 1*, 131-149.

de Azevedo, A., Cruz, A., Marvila, M., de Oliveira, L., Monteiro, S., Vieira, C., Fediuk, R., Timokhin, R., Vatin, N., & Daironas, M. (2021). Natural Fibers as an Alternative to Synthetic Fibers in Reinforcement of Geopolymer Matrices: A Comparative Review. *Polymers, 13*, 2493. https://doi.org/10.3390/polym13152493.

Diambra, A. (2010). *Fibre reinforced sands: experiments and constitutive modelling.* Ph.D. thesis. University of Bristol, Bristol, UK.

Dungca, J. R., & Codilla E. E. T. (2018). Fly ash based geopolymer as stabilizer for silty sand embankment materials. *International journal of GEOMATE*, *14*(46), 143-149. https://doi.org/10.21660/2018.46.7181.

Duxson, P., Fernández-Jiménez, A., Provis, J. L., Lukey, G. C., Palomo, A., & van Deventer, J. S. J. (2007). Geopolymer technology: The current state of the art. *Journal of Material Science, 42*, 2917–2933. https://doi.org/10.1007/s10853-006-0637-z.

Edil, T., Acosta, H., & Benson, C. (2006). Stabilizing Soft Fine-Grained Soils with Fly Ash. *Journal of Materials in Civil Engineering, 18*(2), 283-294. doi: 10.1061/(asce)0899-1561(2006)18:2(283).

Efthymiou, S., Anagnostopoulos, A., & Kavvadas, M. (2019). *Effect of fly ash on the behaviour of a high plasticity clay.* Proceedings of the XVII ECSMGE-2019. doi: 10.32075/17ECSMGE-2019-0970.

Estabragh, A. R. & Javadi, A. A. (2008). Critical state for overconsolidated unsaturated silty soil. *Canadian Geotechnical Journal, 45*, 408-420. doi:10.1139/T07-105.

Firdous, R., & Stephan, D. (2019). Effect of silica modulus on the geopolymerization activity of natural pozzolans. *Construction and Building Materials, 219,* 31-43. doi: 10.1016/j.conbuildmat.2019.05.161.

Gado, R. A., Hebda, M., Łach, M., & Mikuła, J. (2020). Alkali Activation of Waste Clay Bricks: Influence of The Silica Modulus, SiO_2/Na_2O, H_2O/Na_2O Molar Ratio, and Liquid/Solid Ratio. *Materials*, *13*, 383. https://doi.org/10.3390/ma13020383.

Ghadir, P., & Ranjbar, N. (2018). Clayey soil stabilization using geopolymer and Portland cement*. Construction and Building Materials, 188,* 361-371. doi: 10.1016/j.conbuildmat.2018.07.207.

González, A., Navia, R., & Moreno, N. (2009). Fly ashes from coal and petroleum coke combustion: current and innovative potential applications. *Waste Management & Research, 27*(10), 976-987. doi: 10.1177/0734242x09103190.

Harris, D., Feuerborn, H-J., & Heidrich, C. (2019, July). *Global Aspects on Coal Combustion Products,* EUROCOALASH conference, Dundee, Scotland.

Head, K. H. & Epps, R. (2014). Manual of Soil Laboratory Testing. Volume 3: Effective Stress Tests. Third Edition. Whittles Publishing, Dunbeath, Scotland, UK.

Hejazi, S. M., Sheikhzadeh, M., Abtahi, S. M., & Zadhoush, A. (2012). A simple review of soil reinforcement by using natural and synthetic fibers. *Construction and Building Materials, 30*, 100-116. doi:10.1016/j.conbuildmat.2011.11.045.

Ho, M. -H., Chan, C. -M., Bakar, I. (2010). One Dimensional Compressibility Characteristics of Clay Stabilised with Cement-Rubber Chips. *International Journal of Sustainable Construction Engineering and Technology, 1*, 91–104.

Horpibulsuk, S., Miura, N., & Bergado, D. T. (2004). Undrained Shear Behavior of Cement Admixed Clay at High Water Content. *Journal of Geotechnical and Geoenvironmental Engineering, 130*(10), 1096-1105. DOI: 10.1061/(ASCE)1090-0241(2004)130:10(1096).

Horpibulsuk, S., Liu, M. D., Liyanapathirana, D. S., & Suebsuk, J. (2010). Behaviour of cemented clay simulated via the theoretical framework of the Structured Cam Clay model. *Computers and Geotechnics, 37*(2010), 1-9. doi:10.1016/j.compgeo.2009.06.007.

Jaditager, M., & Sivakugan, N. (2017). Influence of Fly Ash–Based Geopolymer Binder on the Sedimentation Behavior of Dredged Mud. *Journal of Waterway, Port, Coastal, and Ocean Engineering, 143*, 04017012. https://doi.org/10.1061/(asce)ww.1943-5460.0000390.

Jaditager, M. & Sivakugan, N. (2018). Consolidation Behavior of Fly Ash-Based Geopolymer-Stabilized Dredged Mud. *Journal of Waterway, Port, Coastal, and Ocean Engineering, 144*, 06018003. https://doi.org/10.1061/(asce)ww.1943-5460.0000455.

Ji-ru, Z., & Xing, C. (2002). Stabilization of expansive soil by lime and fly ash. *Journal of Wuhan University of Technology-Mater. Sci. Ed. 17*(4), 73-77. doi: 10.1007/bf02838423.

Jose, J., Jose, A., Kurian, J. M., Francis, K. J., & James, S. K. (2018). Stabilization of expansive soil using fly ash. *International Research Journal of Engineering and Technology, 5*(3), 3075-3078.

Khan, H. A., Castel, A., & Khan, M. (2020). Corrosion investigation of fly ash based geopolymer mortar in natural sewer environment and sulphuric acid solution. *Corrosion Science, 168*, 108586. https://doi.org/10.1016/j.corsci.2020.108586.

Kamruzzaman, A. H. M.; Chew, S. H., & Lee, F.H. (2009). Structuration and Destructuration Behaviour of Cement-Treated Singapore Marine Clay. *Journal of Geotechnical and Geoenvironmental Engineering*, *135*, 573–589.

Karakoç, M. B., Türkmen, I., Maraş, M. M., Kantarci, F., Demirboğa, R., & Toprak, M.U. (2014). Mechanical properties and setting time of ferrochrome slag based geopolymer paste and mortar. *Construction and Building Materials, 72*, 283–292. https://doi.org/10.1016/j.conbuildmat.2014.09.021.

Kasama, K., Zen, K., & Iwataki, K. (2006). Undrained Shear Strength of Cement-treated Soils. *Soils and Foundations, 46*(2), 221-232.

Kassim, K. A., & Chow, S. H. (2000). Consolidation Characteristics of Lime Stabilized Soil. *Malaysian Journal of Civil Engineering, 12*(1), 31-42.

Kate, J. M. (2005, January). Strength and Volume change Behavior of Expansive soils treated with Fly Ash. Geo-Frontiers Congress, Texas, United States. https://doi.org/10.1061/40783(162)19.

Kelly, R. P. (2015, May 5-7) *Parallels and Nonconformities in Worldwide Fly Ash Classification: The Need for a Robust, Universal Classification System for Fly Ash.* World of Coal Ash (WOCA) Conference, Nashville.

Keramatikerman, M., Chegenizadeh, A., Nikraz, H., & Sabbar, A. (2018). Effect of fly ash on liquefaction behaviour of sand-bentonite mixture. *Soils and Foundations, 58*(5), 1288-1296. doi: 10.1016/j.sandf.2018.07.004.

Kichou, Z. (2015). *A study on the effects of lime on the mechanical properties and behaviour of London clay.* Ph.D. Thesis. London South Bank University, London, UK.

Kolay, P., & Ramesh, K. (2016). Reduction of Expansive Index, Swelling and Compression Behavior of Kaolinite and Bentonite Clay with Sand and Class C

Fly Ash. *Geotechnical and Geological Engineering, 34*(1), 87-101. doi: 10.1007/s10706-015-9930-4.

Kolbe, J. L., Lee, L. S., Jafvert, C. T., Murarka, I. P. (May, 2011). *Use of Alkaline Coal Ash for Reclamation of a Former Strip Mine.* World Coal Ash Conference, Denver, CO, USA.

Kolias, S., Kasselouri-Rigopoulou, V., & Karahalios, A. (2005). Stabilisation of clayey soils with high calcium fly ash and cement. *Cement and Concrete Composites, 27*(2), 301-313. doi: 10.1016/j.cemconcomp.2004.02.019.

Kumar, B. R. P., & Sharma, R. S. (2004). Effect of fly ash on engineering properties of expansive soils. *Journal of Geotechnical and Geoenvironmental Engineering, 130*(7), 764-767.

Kumar, S., & Patil, C. (2006). Estimation of resource savings due to fly ash utilization in road construction. *Resources, Conservation and Recycling, 48*(2), 125-140. doi: 10.1016/j.resconrec.2006.01.002.

Latifi, N., Meehan, C.L., & Majid, M. A. (2016). Horpibulsuk, S. Strengthening montmorillonitic and kaolinitic clays using a calcium-based non-traditional additive: A micro-level study. *Applied Clay Science, 132–133*, 182–193. https://doi.org/10.1016/j.clay.2016.06.004.

Leong, H. Y., Ong, D. E. L., Sanjayan, J. G., & Nazari, A. (2018). Strength Development of Soil–Fly Ash Geopolymer: Assessment of Soil, Fly Ash, Alkali Activators, and Water. *Journal of Materials in Civil Engineering, 30*, 04018171. https://doi.org/10.1061/(asce)mt.1943-5533.0002363.

Li, L., Edil, T. B., Benson, & C. H. (2009). Mechanical Performance of Pavement Geomaterials Stabilized with Fly Ash in Field Applications. *Coal Combustion and Gasification Products, 1,* 43-49.

Lin, Y., Xu, D., Ji, W., & Zhao, X. (2022). Experiment on the Properties of Soda Residue-Activated Ground Granulated Blast Furnace Slag Mortars with Different Activators. *Materials*, *15*, 3578. https://doi.org/10.3390/ma15103578.

Luis, A., Deng, L., Shao, L., & Li, H. (2019). Triaxial behaviour and image analysis of Edmonton clay treated with cement and fly ash. *Construction and Building Materials, 197,* 208-219. https://doi.org/10.1016/j.conbuildmat.2018.11.222.

Mackiewicz, S. M., & Ferguson, E. G. (2005). *Stabilizing of Soil with Self-Cementing Coal Ashes.* World of Coal Ash, Kentucky, USA.

Mahvash, S., López-Querol, S., & Bahadori-Jahromi, A. (2018). Effect of fly ash on the bearing capacity of stabilised fine sand. *Proceedings of The Institution of Civil Engineers - Ground Improvement*, *171*(2), 82-95. doi: 10.1680/jgrim.17.00036.

Marsh, A., Heath, A., Patureau, P., Evernden, M., & Walker, P. (2018). Alkali activation behaviour of un-calcined montmorillonite and illite clay minerals. *Applied Clay Science, 166*, 250–261. https://doi.org/10.1016/j.clay.2018.09.011.

Mir, B., & Sridharan, A. (2013). Physical and Compaction Behaviour of Clay Soil–Fly Ash Mixtures. *Geotechnical and Geological Engineering, 31*(4), 1059-1072. doi: 10.1007/s10706-013-9632-8.

Mir, B., & Sridharan, A. (2014). Volume change behavior of clayey soil–fly ash mixtures. *International Journal of Geotechnical Engineering, 8*(1), 72-83. doi: 10.1179/1939787913Y.0000000004.

Mir, B., & Sridharan, A. (2019). Mechanical behaviour of fly-ash-treated expansive soil. *Proceedings of The Institution of Civil Engineers - Ground Improvement, 172*(1), 12-24. doi: 10.1680/jgrim.16.00024.

Moghal, A. A. B. (2017). State-of-the-art Review on the Role of Fly Ashes in Geotechnical and Geoenvironmental Applications. *Journal of Materials in Civil Engineering*, *29*(8), 04017072.

Murmu, A. L., Dhole, N., & Patel, A. (2018). Stabilisation of black cotton soil for subgrade application using fly ash geopolymer. *Road Materials and Pavement Design, 21*, 867–885. https://doi.org/10.1080/14680629.2018.1530131.

Nalbantoğlu, Z. (2004). Effectiveness of Class C fly ash as an expansive soil stabilizer. *Construction and Building Materials 18*(6), 377-381. doi: 10.1016/j.conbuildmat.2004.03.011.

Nath, B., Molla, M., & Sarkar, G. (2017). Study on Strength Behavior of Organic Soil Stabilized with Fly Ash. *International Scholarly Research Notices, 2017*, 1-6. doi: 10.1155/2017/5786541.

Nawaz, I. (2013). Disposal and utilization of fly ash to protect the environment. *International Journal of Innovative Research in Science, Engineering and Technology 2*(10), 5259-5266.

Pacheco-Torgal, F., Castro-Gomes, J., & Jalali, S. (2007a). Alkali-activated binders: A review: Part 2. About materials and binders manufacture. *Construction and Building Materials, 22*, 1315–1322. https://doi.org/10.1016/j.conbuildmat.2007.10.015.

Pacheco-Torgal, F., Castro-Gomes, J., & Jalali, S. (2007b). Alkali-activated binders: A review: Part 1. Historical background, terminology, reaction mechanisms and hydration products. *Construction and Building Materials, 22*, 1305–1314. https://doi.org/10.1016/j.conbuildmat.2007.10.015.

Pal, S., & Ghosh, A. (2014). Volume Change Behavior of Fly Ash–Montmorillonite Clay Mixtures. *International Journal of Geomechanics 14*(1), 59-68. doi: 10.1061/(asce)gm.1943-5622.0000300.

Parhi, P. S., Garanayak, L., Mahamaya, M., & Das S. K. (2018). Stabilization of an expansive soil using alkali activated fly ash based geopolymer. *International congress and exhibition "Sustainable civil infrastructures: innovative infrastructure geotechnology"* Springer, pp 36-50. DOI 10.1007/978-3-319-61931-6_4.

Parsons, R. L., & Kneebone, E. (2005). Field performance of fly ash stabilised subgrades. *Proceedings of The Institution of Civil Engineers - Ground Improvement, 9*(1), 33-38.

Petry, T., & Little, D. (2002). Review of Stabilization of Clays and Expansive Soils in Pavements and Lightly Loaded Structures—History, Practice, and Future. *Journal of Materials in Civil Engineering*, *14*(6), 447-460. doi: 10.1061/(asce)0899-1561(2002)14:6(447).

Phanikumar, B., & Sharma, R. (2007). Volume Change Behavior of Fly Ash-Stabilized Clays. *Journal of Materials in Civil Engineering, 19*(1), 67-74. doi: 10.1061/(asce)0899-1561(2007)19:1(67).

Phanikumar, B. (2009). Effect of lime and fly ash on swell, consolidation and shear strength characteristics of expansive clays: a comparative study. *Geomechanics and Geoengineering, 4*(2), 175-181. doi: 10.1080/17486020902856983.

Phetchuay, C., Horpibulsuk, S., Arulrajah, A., Suksiripattanapong, C., & Udomchai, A. (2016). Strength development in soft marine clay stabilized by fly ash and calcium carbide residue based geopolymer. *Applied Clay Science, 127–128*, 134–142. https://doi.org/10.1016/j.clay.2016.04.005.

Phummiphan, I. Horpibulsuk, S., Sukmak, P., Chinkulkijniwat, A. A., & Shen, S-L. (2016). Stabilisation of marginal lateritic soil using high calcium fly ash-based geopolymer. *Road Materials and Pavement Design, 17*(4), 877-891. https://doi.org/10.1080/14680629.2015.1132632.

Porbaha, A., Shibuya, S., & Kishida, T. (2000). State of the art in deep mixing technology. Part III: geomaterial characterization. *Ground Improvement, 3*, 91-110.

Prabakar, J., Dendorkar, N., & Morchhale, R. (2004). Influence of fly ash on strength behavior of typical soils. *Construction and Building Materials, 18*(4), 263-267. doi: 10.1016/j.conbuildmat.2003.11.003.

Premkumar, S., Piratheepan, J., & Rajeev, P. (2017). Effect of brown coal fly ash on dispersive clayey soils. *Proceedings of The Institution of Civil Engineers - Ground Improvement, 170*(4), 231-244. doi: 10.1680/jgrim.17.00008.

Rafeet, A., Vinai, R., Soutsos, M., & Sha, W. (2017). Guidelines for mix proportioning of fly ash/GGBS based alkali activated concretes. *Construction and Building Materials, 147*, 130–142. https://doi.org/10.1016/j.conbuildmat.2017.04.036.

Raj, S. S., Sharma, A. K., & Anand, K. B. (2018). Performance appraisal of coal ash stabilized rammed earth. *Journal of Building Engineering 18*, 51-57. https://doi.org/10.1016/j.jobe.2018.03.001.

Rajak, T. R., Yadu, L., & Pal, S. K. (2019). Analysis of slope stability of fly ash stabilized soil slope. *Geotechnical Applications 4*, 119-126. https://doi.org/10.1007/978-981-13-0368-5_13.

Rajpura, A. S., Shah, B. R., & Dave, H. K. (2017). Review of Industrial Waste Used in Stabilization of Expansive Soil in Road Subgrade. *International Journal of Advance Research, Ideas, and Innovations in Technology, 3*(2), 1124-1127.

Ramaji, A. E. (2012). A review on the soil stabilization using low-cost methods. Journal of Applied Sciences Research, 8(4), 2193-2196.

Ridtirud, C., Leekongbub, S., & Chindaprasirt, P. (2018). Compressive Strength of Soil Cement Base Mixed with Fly Ash – Based Geopolymer. *International Journal of GEOMATE*, *14*(46), 82-88. doi: 10.21660/2018.46.mat61.

Rios, S., Cristelo, N., da Fonseca, A. V., & Ferreira, C. (2016a). Structural Performance of Alkali-Activated Soil Ash versus Soil Cement. *Journal of Materials in Civil Engineering, 28,* 04015125. https://doi.org/10.1061/(asce)mt.1943-5533.0001398.

Robin, V. (2014) *Analytical and Numerical Modelling of Artificially Structured Soils.* Ph.D. Thesis, University of Exeter, Exeter, UK.

Robin, V., Cuisinier, O., Masrouri, F., & Javadi, A. A. (2014). Chemo-mechanical modelling of lime treated soils. *Applied clay science, 95,* 211-219. http://dx.doi.org/10.1016/j.clay.2014.04.015.

Runci, A. & Serdar, M. (2022). Effect of curing time on the chloride diffusion of alkali-activated slag. *Case Studies in Construction Materials*, *16*, e00927. https://doi.org/10.1016/j.cscm.2022.e00927.

Samidurai, V., Gokulan, Y., & Krishnan, N. (2017). Influence of Fly ash on expansive Soils. *International Journal of Emerging Trends in Science and Technology, 03,* 4998-5003. doi: 10.18535/ijetst/v4i3.03.

Santos, F., Li, L., Li, Y., & Amini, F. (2011, May 9-12). *Geotechnical Properties of Fly Ash and Soil Mixtures for Use in Highway Embankments.* World of Coal Ash (WOCA) Conference in Denver, USA.

Sas, Z., Vandevenne, N., Doherty, R., Vinai, R., Kwasny, J., Russell, M., Sha, W., Soutsos, M., & Schroeyers, W. (2019). Radiological evaluation of industrial residues for construction purposes correlated with their chemical properties. *Science of The Total Environment*, *658*, 141-151.

Savaş, H., Türköz, M., Seyrek, E., & Ünver, E. (2018). Comparison of the effect of using class C and F fly ash on the stabilization of dispersive soils. *Arabian Journal of Geosciences, 11*(20). doi: 10.1007/s12517-018-3976-6.

Schofield, A. & Wroth, P. (1968). *Critical State Soil Mechanics; McGraw-Hill:* London, UK.

Senol, A., Bin-Shafique, M., Edil, T., & Benson, C. (2002, Sep 25-27). *Use of class C fly ash for stabilization of soft subgrade.* Fifth International Congress on Advances in Civil Engineering, Istanbul, Turkey.

Senol, A., Edil, T., Bin-Shafique, M., Acosta, H., & Benson, C. (2006). Soft subgrades' stabilization by using various fly ashes. *Resources, Conservation and Recycling, 46*(4), 365-376.

Seyrek, E. (2016). Engineering behaviour of clay soils stabilized with class C and class F fly ashes. *Science and Engineering of Composite Materials, 25*(2), 273-287. https://doi.org/10.1515/secm-2016-0084.

Sezer, A., İnan, G., Yılmaz, H., & Ramyar, K. (2006). Utilization of a very high lime fly ash for improvement of Izmir clay. *Building and Environment, 41*(2), 150-155. doi: 10.1016/j.buildenv.2004.12.009.

Sharma, L., & Singh, T. (2017). Regression-based models for the prediction of unconfined compressive strength of artificially structured soil. *Engineering with Computers, 34*(1), 175-186. doi: 10.1007/s00366-017-0528-8.

Shi, C., Qu, B., & Provis, J. L. (2019). Recent progress in low-carbon binders. *Cement and Concrete Research*, *122*, 227–250. https://doi.org/10.1016/j.cemconres.2019.05.009.

Shil, S., & Pal, S. K. (2015). Permeability and Volume Change Behaviour of Soil Stabilized with Fly Ash. *International Journal of Engineering Research & Technology (IJERT) 4*(2), 840-846.

Siddiqua, S., & Barreto, P. N. M. (2018). Chemical stabilization of rammed earth using calcium carbide residue and fly ash. *Construction and Building Materials, 169*, 364-371.

Sifton, J. B., & Arato, C. (2019, July). *2020 to 2070 and Beyond: Transitioning from Production to Post-production Coal Ash Use,* EUROCOALASH conference, Dundee, Scotland.

Silitonga, E., Levacher, D., & Mezazigh, S. (2009). Effects of the use of fly ash as a binder on the mechanical behaviour of treated dredged sediments. *Environmental Technology 30*(8), 799-807. https://doi.org/10.1080/09593330902990089.

Soutsos, M., Boyle, A. P., Vinai, R., Hadjierakleous, A., & Barnett, S. (2016). Factors influencing the compressive strength of fly ash based geopolymers. *Construction and Building Materials, 110*, 355–368. https://doi.org/10.1016/j.conbuildmat.2015.11.045.

Striprabu, S., Siti, N. L. T., Norazzlina, M. S., Fauziah, A. (2018). Chemical Stabilization of Sarawak Clay Soil with Class F fly Ash. *Journal of Engineering Science and Technology, 13*(10), 3029-3042.

Subramaniam, P., Sreenadh, M. M., & Banerjee, S. (2015). Critical State Parameters of Dredged Chennai Marine Clay Treated with Low Cement Content. *Marine Georesources and Geotechnology 34*, 603–616. https://doi.org/10.1080/1064119X.2015.1053641.

Sukmak, P., Horpibulsuk, S., Shen, S.-L., Chindaprasirt, P., & Suksiripattanapong, C. (2013). Factors influencing strength development in clay–fly ash geopolymer. *Construction and Building Materials*, *47*, 1125–1136. https://doi.org/10.1016/j.conbuildmat.2013.05.104.

Sun, Z. & Vollpracht, A. (2018). Isothermal calorimetry and in-situ XRD study of the NaOH activated fly ash, metakaolin and slag. *Cement and Concrete Research, 103*, 110–122. https://doi.org/10.1016/j.cemconres.2017.10.004.

Suryawanshi, N. T., Bansode, S. S., & Nemade, P. D. (2012). Use of Eco-friendly Material like Fly Ash in Rigid Pavement Construction & It's Cost Benefit Analysis. *International Journal of Emerging Technology and Advanced Engineering, 2*(12), 795-800.

Syed, M., GuhaRay, A., & Kar, A. (2020). Stabilization of Expansive Clayey Soil with Alkali Activated Binders. *Geotechnical and Geological Engineering, 38*, 6657–6677. https://doi.org/10.1007/s10706-020-01461-9.

Tastan, E. O., Edil, T. B., Benson, C. H., & Aydilek, A. H. (2011). Stabilization of Organic Soils with Fly Ash. *Journal of Geotechnical and Geoenvironmental Engineering, 137*(9). doi: 10.1061/(ASCE)GT.1943-5606.0000502.

Than, S. N., Zaw, T. (2019). Study on Stabilization of Expansive Soil with Fly-ash. *IRE Journals*, *3*(1), 395-399.

Trinh, S. H., & Bui, Q. A. T. (2018). Influencing of Clay and Binder Content on Compression Strength of Soft Soil Stabilized by Geo-polymer Based Fly Ash. *International Journal of Applied Engineering Research, 13*, 7954–7958. http://www.ripublication.com.

Trzebiatowski, B. D., Edil, T. B., & Benson, C. H. (2004, October 19-21). *Case study of subgrade stabilisation using fly ash: State Highway 32, Port Washington, Wisconsin.* Recycled Material in Geotechnics Sessions at ASCE Civil Engineering Conference, Baltimore, Maryland, United States.

Turan, C., Javadi, A., Vinai, R., Cuisinier, O., Russo, G., & Consoli, N. C. (2019, June 10-12) *Mechanical Properties of Calcareous Fly Ash Stabilized Soil*, EUROCOALASH conference, Dundee, Scotland.

Turan, C., Javadi, A., Vinai, R., Shariatmadari, N., & Farmani, R. (2020, October 19-21). *Use of class C fly ash for stabilisation of fine-grained soils.* In proceedings of the EUNSAT conference, Lisbon, Portugal.

Turan, C., Javadi, A.A., & Vinai, R. (2022a). Effects of Class C and Class F Fly Ash on Mechanical and Microstructural Behavior of Clay Soil—A Comparative Study. *Materials*, *15*, 1845. https://doi.org/10.3390/ma15051845.

Turan, C., Javadi, A.A., & Vinai, R. & Russo, G. (2022b). Effects of Fly Ash Inclusion and Alkali Activation on Physical, Mechanical, and Chemical Properties of Clay. *Materials, 15,* 4628. https://doi.org/10.3390/ma15134628.

UKQAA, (2020). *United Kingdom Quality Ash Association*. http://www.ukqaa.org.uk/.

U.S. Environmental Protection Agency Office of Solid Waste (USEPA). (2007). *Human and Ecological Risk Assessment of Coal Combustion Wastes, (Report No. NC 27709)*.

U.S. Federal Highway Administration (FHWA), (2003). *Fly Ash Facts for Highway Engineers.* (Report No. FHWA-IF-03-019).

United States Geological Survey (USGS). (1997). *Radioactive elements in coal and fly ash: Abundance, forms, and environmental significance FS-163-97 Reston VA*. https://pubs.usgs.gov/fs/1997/fs163-97/FS-163-97.html.

Van Deventer, S. J. S. J., Lukey, G. C., & Xu, H. (2006). Effect of curing temperature and silicate concentration on fly ash based geopolymerization. Industrial & Engineering Chemistry Research, *45*, 3559-3568.

van Jaarsveld, J. G. S., van Deventer, J. S. J., & Lukey, G. C. (2003). The characterisation of source materials in fly ash-based geopolymers. *Materials Letters, 57*, 1272–1280. https://doi.org/10.1016/s0167-577x(02)00971-0.

Vindula, S. K., Chavali, R. V. P., & Reddy, P. H. P. (2016). Role of fly ash in control of alkali induced swelling in kaolinitic soils: a microlevel investigation. International *Journal of Geotechnical Engineering 12*(1), 46-52. doi: 10.1080/19386362.2016.1247023.

Vitale, E., Russo, G., & Deneele, D. (2019). Use of Alkali-Activated Fly Ashes for Soil Treatment. *Springer Nature, 40*, 723–733. https://doi.org/10.1007/978-3-030-21359-6_77.

Wang, W., & Noguchi, T. (2020). Alkali-silica reaction (ASR) in the alkali-activated cement (AAC) system: A state-of-the-art review. *Construction and Building Materials*, *252*, 119105. https://doi.org/10.1016/j.conbuildmat.2020.119105.

Wang, D. & Korkiala-Tanttu, L. (2018). 1-D compressibility behaviour of cement-lime stabilized soft clays. *European Journal of Environmental and Civil Engineering, 24*, 1013–1031. https://doi.org/10.1080/19648189.2018.1440633.

Whitlow, R. (1996). *Basic Soil Mechanics*; Longman: Essex, UK,

Wong, B., Wong, K., & Phang, I. (2019). A review on geopolymerisation in soil stabilization. *IOP Conference Series: Materials Science and Engineering*, *495*, 012070. doi: 10.1088/1757-899x/495/1/012070.

World Nuclear Association, (2020). *Naturally Occurring Radioactive Materials (NORM).* https://www.world-nuclear.org/.

WWCCPN. (2020). *World-wide Coal Combustion Products Network-* http://www.wwccpn.com/glossary.html.

Yaghoubi, M., Arulrajah, A., Disfani, M. M., Horpibulsuk, S., Darmawan, S., & Wang, J. (2019). Impact of field conditions on the strength development of a geopolymer stabilized marine clay. Applied clay science, 167, 33.42. https://doi.org/10.1016/j.clay.2018.10.005.

Yao, Z. T., Ji, X. S., Sarker, P. K., Tang, J. H., Ge, L. Q., Xia, M. S., & Xi, Y.Q. (2015). A comprehensive review on the applications of coal fly ash. *Earth-Science Reviews 141*, 105-121.

Ye, H. & Radlińska, A. (2016). Fly ash-slag interaction during alkaline activation: Influence of activators on phase assemblage and microstructure formation. *Construction and Building Materials*, *122*, 594–606. https://doi.org/10.1016/j.conbuildmat.2016.06.099.

Yoobanpot, N., Jamsawang, P., & Horpibulsuk, S. (2017). Strength behavior and microstructural characteristics of soft clay stabilized with cement kiln dust and fly ash residue. *Applied Clay Sciences, 141*, 146–156. https://doi.org/10.1016/j.clay.2017.02.028.

Yoobanpot, N., Jamsawang, P., Poorahong, H., Jongpradist, P., & Likitlersuang, S. (2020). Multiscale laboratory investigation of the mechanical and microstructural properties of dredged sediments stabilized with cement and fly ash. *Engineering Geology, 267*, 105491. https://doi.org/10.1016/j.enggeo.2020.105491.

Yusuf, M. O., Johari, M. A. M., Ahmad, Z. A. & Maslehuddin, M. (2014). Impacts of silica modulus on the early strength of alkaline activated ground slag/ultrafine palm oil fuel ash-based concrete. *Materials and Structure, 48*, 733–741. https://doi.org/10.1617/s11527-014-0318-3.

Zawrah, M. F., Gado, R., & Khattab, R. M. (2018). Optimization of Slag Content and Properties Improvement of Metakaolin-slag Geopolymer Mixes. *The Open Materials Science Journal, 12*, 40–57. https://doi.org/10.2174/1874088x01812010040.

Zha, F., Liu, S., Du, Y., & Cui, K. (2008). Behavior of expansive soils stabilized with fly ash. *Natural Hazards, 47*(3), 509-523. doi: 10.1007/s11069-008-9236-4.

Zhang, M., Guo, H., El-Korchi, T., Zhang, G., & Tao, M. (2013). Experimental feasibility study of geopolymer as the next-generation soil stabilizer. *Construction and Building Materials, 47*, 1468-1478. http://dx.doi.org/10.1016/j.conbuildmat.2013.06.017.

Zhou, S., Zhou, D., Zhang, Y., & Wang, W. (2019). Study on Physical-Mechanical Properties and Microstructure of Expansive Soil Stabilized with Fly Ash and Lime. *Advances in Civil Engineering, 2019*, 1-15. doi: 10.1155/2019/4693757.

Zhuang, X. Y., Chen, L., Komarneni, S., Zhou, C. H., Tong, D. S., Yang, H. M., Yu, W. H., & Wang, H. (2016). Fly ash-based geopolymer: clean production, properties and applications. *Journal of cleaner production, 125*, 253-267. http://dx.doi.org/10.1016/j.jclepro.2016.03.019.

Zuber, S. Z. S., Kamarudin, H., Abdullah Binhussain, M., & Salwa, M. S. S. (2013). Review on Soil Stabilization Techniques. *Australian Journal of Basic and Applied Sciences, 7*(5), 258-265.

Appendix: Experimental procedures and calculations

Compaction test

- ***Sample set-up***

The following detailed procedures were applied in the compaction tests (BS 1377-4, 1990):

- The mould with baseplate was weighed (m_1).
- The moist soil was placed into the mould (enough to fill one-third of the height of the mould).
- A 2.5 kg rammer falling from a height of 300 mm was used to compact the soil in 3 layers in a 1 L compaction mould. 27 blows were applied for each layer.
- After the third layer was compacted, the extension of the mould on the top was removed and the excess soil was removed and flattened.
- The soil and mould with baseplate were weighed (m_2).
- The compacted soil was removed from the mould using hydraulic jack. Small samples were taken from all layers to determine the moisture content.
- At least 5 determinations were applied for each sample. Increment of water content was applied as 2% due to the cohesive nature of the soil.

- ***Calculations***

Compaction calculations were applied based on BS 1377-4, 1990:

The bulk density, ρ, of each compacted sample:

$$\rho = \frac{m_2 - m_1}{V}$$

where m_1 is the mass of mould and baseplate and m_2 is the mass of mould, baseplate, and compacted soil.

The dry density, ρ_d, of each compacted sample:

$$\rho_d = \frac{100\rho}{100 + w}$$

where *w* is the moisture content of the soil.

Unconfined compressive strength test

- ***Calculations***

The axial strain (ε) of each sample:

$$\varepsilon = \frac{\Delta L}{L_0}$$

where ΔL is the change in length of the sample (in mm) and L_0 is the initial length of the sample (in mm).

The axial compressive stress (σ_1) (in kPa):

$$\sigma_1 = \frac{P}{A_0} 1000$$

where P (in N) is the force and A_0 is the initial cross-sectional area of the sample (in mm^2).

One-dimensional consolidation (oedometer) test

- ***Sample set-up***

The tests were carried out based on the procedures of British Standard, BS 1377-5 (1990) as described below:

- The height and inner diameter of the consolidation ring were measured, 3 measurements were taken, and the average was calculated.
- The consolidation ring was weighed and recorded.
- The soil sample was placed into the ring.
- The excess soil was trimmed by using a palette and the top and bottom faces of the samples were smoothed. Also, from the excess soil, a soil sample was taken and used to analyse the initial moisture content.
- The consolidation ring + wet sample was weighed and recorded.
- Before using the porous discs, the surfaces of the discs were cleaned using a nylon brush. Then, both porous discs and filter papers were saturated in distilled water in distilled water for at least 20 minutes.
- Larger porous plate was placed centrally in the bottom of the consolidation cell, after that filter paper, consolidation ring, and filter paper was placed sequentially. Then, the small porous plate and loading cap were finally placed. The consolidation cell was ready to assemble to the load frame.
- After assembling the consolidation cell, calibrated bubble was used to check whether or not the loading arm was horizontal.
- The consolidation cell was filled with water, the first load was placed, and the software was set up to record the time and change in thickness.
- For the loading sequence, in every loading step, the stress was doubled and at least four incremental steps were applied on each sample. The unloading was done in a smaller number of steps as stated in the Standard. For the soils stabilised with class C and class F fly ash, the samples were sequenced to apply vertical stresses of 10, 20, 40, 80, 40, and 10 kPa.

- Due to the high stiffness of the soils stabilised with alkali activated fly ash, vertical stresses of 50, 100, 200, 400, 800, 1600, 800, 400, and 200 kPa were sequenced to analyse pre-consolidation pressures.
- Drainage was allowed from the top and bottom of the samples and each loading or unloading step was applied for 24 hours.
- After completing the unloading process, the consolidation ring was dismantled from the cell.
- The ring + saturated sample was weighed and recorded.
- The soil was removed from the ring and put it in the oven for the analysis of final moisture content.

➢ ***Calculations***

Consolidation parameters of the samples were calculated based on Whitlow (1994):

Void ratio at end of test (e_1): Since S_r=1:

$$e_1 = w_1 G_s$$

where w_1 is the water content at end of test, G_s is the specific gravity of the sample.

The change in void ratio (Δe):

$$\Delta e = \frac{\Delta h}{h_1}(1 + e_1)$$

where Δh is the change in thickness, h_1 is the thickness at end of the stage.

Void ratio at start of the test (e_0):

$$e_0 = e_1 - \Delta e$$

The coefficient of volume compressibility (m_v) describes the amount of change in unit volume resulting from a unit increase in effective stress.

$$m_v = \frac{\Delta e}{\Delta \sigma'} \frac{1}{1 + e_0}$$

where Δσ' is the effective vertical stress increment.

The compression index (C_c) was determined as the slope of the linear portion of the e-log σ' plot. The approximate slope of the swelling/recompression curve was defined as swelling index (C_s).

$$C_c \; or \; C_s = \frac{e_0 - e_1}{\log \left({\sigma'_1}/{\sigma'_0} \right)}$$

For the determination of coefficient of consolidation (c_v), the square root time method (Taylor's method) was used.

$$c_v = \frac{0.848 d^2}{t_{90}}$$

where d is the length of drainage path:

d = (the thickness of the sample at end of the stage + (total change in thickness during increment/2)),

t_{90} is the time required to achieve 90% of primary consolidation.

Permeability (k) of the samples was calculated as:

$$k = c_v m_v \gamma_w$$

where γ_w is the unit weight of water.

Consolidated – undrained triaxial tests

- ***Sample set-up***

- The pressure controllers (cell pressure and back pressure) were filled with an appropriate amount of de-aired water using manual controls.
- All pipes were flushed with water to remove any air in the pipes since it might affect the readings and processes. For instance, air within the pore pressure pipe might cause wrong pore pressure transducer reading.
- The cylindrical soil sample was prepared for installation on the triaxial apparatus using filter papers, porous discs, O rings, water-proof membrane, and membrane stretcher. The porous discs were saturated in distilled water. Filter papers were used to prevent the filtration of small soil particles from the porous discs. The sample was initially placed in a water-proof membrane with the help of a membrane stretcher. Then, filter papers and porous discs were placed on both sides of the sample. The sample was finally assembled between the base plate and top cap and was sealed with the O rings to create an isolated environment for the sample.
- The triaxial cell was placed and fixed with screws.
- The triaxial cell was filled with de-aired water from the delivery tank. After ensuring all air was removed from the cell, the air valves were closed.
- The delivery pipes were attached from the pressure controllers to the appropriate valves on the triaxial apparatus.
- The GDS software was set up, all appropriate data values were zeroed on both pressure pumps and management system in the software.
- A cell pressure of 20 kPa was manually set up. This was done to check if there was any leak between the sample and the cell.

- The cell and back pressure valves were finally opened to start the first stage (saturation stage) of the experiment.

➢ ***Calculations***

Calculations were made at the end of the triaxial tests based on GDS help sheet notes, BS 1377-8 (1990), and Craig (2004).

Average cross-sectional area (corrected area) (A):

$$A = A_0 \frac{1 - \varepsilon_v}{1 - \varepsilon_a}$$

where A_0 is the initial area of the sample, ε_v is the volumetric strain, ε_a is the axial strain.

Axial strain (ε_a):

$$\varepsilon_a = \frac{\Delta L}{L_0}$$

where ΔL is the change in height of the sample, L_0 is the initial height of the sample.

Deviator stress (q):

$$q = \sigma_1 - \sigma_3$$

where σ_1 is the major principal stress, σ_3 is the minor principal stress.

Deviator stress (q):

$$q = \frac{P}{A}$$

where P is the axial load and A is the average cross-sectional area.

Effective major principal stress (σ'_1):

$$\sigma'_1 = \sigma_1 - u$$

where u is the pore water pressure.

Effective minor principal stress (σ'_3):

$$\sigma'_3 = \sigma_3 - u$$

The average effective principal stress (p'):

$$p' = \frac{1}{3}(\sigma'_1 + 2\sigma'_3)$$

Mohr-Coulomb failure criterion:

$$\tau_f = c' + \sigma'_f tan\varphi'$$

where σ'_f is the effective stress at failure, c and φ are the shear strength parameters, τ_f is the shear strength.

Equation of the critical state line in q-p' space:

$$q' = Mp'$$

where M is the slope of CSL.

Equation of the critical state line in v-lnp' space:

$$v = \Gamma - \lambda \ln(p')$$

Where Γ is the value of v on the CSL at p' = 1 kPa and λ is the gradient of the CSL.